ALY (S.M.)

Ph.D.

(Physics)

1948.

III

A B S T R A C T.

The object of this work was first to investigate, by the ionization method the dependence on the wall material of the ionization produced within chambers by high voltage radiations of wave lengths from 0.013 A.U. to 0.5 A.U. The ionization chambers were pressed from mixtures of bakelite powder and graphite powder either with vanadium or cerium oxide. Secondly to investigate the possibility of measuring the quality of radiation by means of the ratio of ionizations in two chambers one of them is air walled and the other of higher atomic number. A study was also made of the validity of Gray's theory for culculating the ratio of ionization in such small chambers.

The results of these investigations have shown that:

I- Chambers moulded from the above mentioned mixtures are satisfactory electrical conductors and behave consistently in their interactions with the radiations used.

2- The method may be useful in examining the quality of the scattered radiations from harder beams of X-rays generated at say between 400 and 1000 KV. The ratio of ionization calculated according to Gray's theory agrees with the experimental one up to a wave lengh of 0.08.A.U.

3- The effective wave lengths of the X-ray beams were obtained from the complete spectral distribution of the energy and from measurement of the half value layers of the beams . It was found that in most cases it is sufficiently accurate, when considering the calculation of the ratio of ionizations in two chambers, to regard the beam as having that effective wave length corresponding to its half value layer.

A STUDY OF THE DEPENDENCE ON WALL MATERIAL OF THE IONIZATION PRODUCED WITHIN A CAVITY BY HIGH VOLTAGE RADIATIONS

AND

AN INVESTIGATION OF A POSSIBLE METHOD OF MEASURING THE RADIATION QUALITY

A Thesis submitted to the University of London
for the Degree of Ph. D. in Physics
by

Samira M. Aly.

CONTENTS

Page

INTRODUCTION

The method whereby the ratio of the ionizations in two chambers (one air walled and the other with walls of higher atomic number) is used as an index of quality, has been applied by many observers for the study of the quality of the total radiations within media irradiated by X and γ-rays. Mayneord [1] measured the ratios of ionization in thin walled chambers of different materials and found they disagreed with his theoretical calculation. Clarkson and Mayneord [2] used small ionaization chambers of carbon (as an air wall material) and copper in their investigations. They obtained results for the ionization in the two chambers which were appreciably lower than the values calculated from the theory of Bragg [3] or Gray [4]. Because they used chambers of Acheson graphite electroplated from the inside by layers of copper of thickness 8 μ, they attributed the discrepancy partly to the insufficient thickness of copper plating to give full equilibrium electronic emission over the short wave region. Wilson [5] using small chambers of carbon and electron metal or copper for investigating the quality of the radiation used in radium γ-ray therapy (5-209 X.U.) calculated the ratio

of the ionization and found it deviated considerably from Mayneord's [1] experimental results. This is partly due to the fact that, in this case, the chambers could not be regarded as thin. In one case the chamber was of magnesium 4 mm. thick and in the other of copper 1 mm. thick. Clarkson,[6] in his attempts to measure by the ionization method, the real energy absorption in different gases for x radiation of wave length 0.208 A.U. , arrived at a similar result i.e. the experimental values for the ionization deviated considerably from the theoretical ones. He suggested that the deviation might possibly be due to contamination on the inner surface of the ionization chamber. All these investigations were made with chambers constructed from materials consisting of a single element.

In recent years conducting, thermo-setting resins have been used for the large scale production of ionization chambers and it seemed likely that by suitably adjusting the material proportions in the resins, wall materials of various effective atomic numbers could easily be made. It seemed possible therefore, to press small condenser ionization chambers, identical except for effective atomic numbers of the walls. Pairs of them (if one was air-walled)

appeared likely to be of use for simultaneous measurement of "depth-dose" and "depth quality". In particular, since it is possible easily to mould very small chambers, such pairs appeared suitable for the study of the quality of the scattered radiation generated in a medium irradiated by x-rays [7]. Before this stage could be arrived at, however, it seemed necessary to investigate the behaviour of such pressed ionization chambers in order to examine:-

1. Whether the pressed material made of such different mixtures could be relied upon to produce a specific interaction with x-rays i.e. an interaction which is the same from sample to sample.
2. Over what range of wavelengths it might be satisfactory to use the method for quality determinations and in this respect whether a mixture of one particular atomic number might be better than another.
3. How the experimentally observed ratios compare with those calculated from the theory and whether this comparison leads to any new information concerning the ionization in a walled chamber.

An instrument for measuring directly the ratio of the

ionization currents was used as being the most appropriate[8]. The radiations (x γ) available, enabled us to take measurements over a wide range of qualities from 0.013 A.U. to 0.4 A.U. For the latter the following sources were used.

1. A radium unit[9] of 4 gm. content was used to obtain radiation of 0.013 A.U.
2. The Metropolitan Vickers constant potential, continuously-evacuated million volts tube at St. Bartholomew's Hospital[10] was used for obtaining wave lengths 0.041 and 0.06 A.U.
3. A Victor Maximar tube having electrodes designed such that it operates almost as a constant potential x-ray generator, the exciting voltage being nearly the peak kilovoltage. With 220 kVp and suitable filters, x-rays of effective wavelengths from about 0.1 A.U. to 0.082 A.U. were obtained.
4. A Westinghouse tube with Villard circuit was used for measurements in the region of 0.10 - 0.30 A.U.
5. A Siemen's tube for measurement in the medium kilovoltage region (60 - 110 kVp) was used for obtaining qualities in the range 0.3 to 0.6 A.U.

II

DETERMINATION OF THE QUALITY OF X-RAYS

(a) Consideration of the Different Methods Used for the Determination of the Quality.

. . . . . .

The quality of x-rays has been the subject of investigation since the time of its discovery by Roentgen, who studied the quality by observing the penetration through a "Platinum Aluminium window".

This was followed by several other attempts[11,12,13,14,15] based on the same principle of absorption or on others. A variety of methods were used, but for a long time no satisfactory conclusions were reached;

Radiation quality for a monochromatic beam can be specified by stating the wavelength of the radiation, which gives an accurate physical picture of the beam and its behaviour upon interaction with matter. On the other hand, radiation quality for beams of x-rays such as those dealt with in the following investigation cannot be so easily specified by such a simple statement as "the wavelength" used in the case of homogeneous rays. This is because of its heterogeneous nature, i.e. it is composed of

a mixture of wavelengths, the minimum being defined by the voltage, while the total composition depends on the generator waveform, the x-ray target, the tube wall, the filters, etc. Therefore no single parameter of the voltage applied to the tube or the wavelength describes it completely.

The following are the methods most commonly used in the specification of x-ray quality.

(i) The spectrometer method:

The spectrometer can be used for mapping the x-ray spectra in the same way as it is used for ordinary light. But as the wave lengths involved in the beam are usually shorter than those of ordinary light, a large crystal replaces the grating and the rays are reflected from the different atoms and recorded photographically or by means of a current in an ionization chamber.

Seeman[16] made a spectrometer for measuring the minimum wavelength of the beam as an indication of the quality. But, as the spectrum of the beam is a function of the waveform and the latter is exceedingly varied, it follows that the minimum wavelength cannot satisfactorily

describe the quality.

Mayneord and Roberts[17] used the Seeman spectrometer in studying the problem of filters and concluded that it is too complicated to be applied for therapeutic purposes.

It necessitates a great refinement of the experimental technique and takes a long time. Also if the spectrograph is used instead of the ionization spectrometer, a simple density curve of the photographic plate may be misleading because of the many factors one has to deal with such as the photographic halation due to scattering and the complexity of the emulsion response to radiation.

(ii) The Half value layer:

One of the earliest methods of measuring the quality was the method of the "Half Value layer" which was introduced by Cristen[13] in 1912. He claimed that it gave desired information for the specification of the quality. The half value layer is the amount of a specified material which, when the x-ray beam passes through it, reduces its intensity to half its original value. Therefore the more penetrating the radiation, the greater the half value layer "H.V.L.".

Holthusen and Gollwitzer[18] arrived at the conclusion that the determination of the H.V.L. in copper of filtered radiation is a more exact method of expressing the penetrating power of an x-ray beam.

Phole and Bernes[19] following Mayer[20] obtained the H.V.L. in Aluminium and copper photographically but concluded that the photographic estimation was not reliable.

Other observers[21,22,23,24,25] used the method of determination of the half value layer in copper for specifying the quality and they agree fairly well amongst themselves when using constant high potential.

Mayneord and Roberts[17] investigated this problem thoroughly. They introduced a series of filters of a suitable material of increasing thicknesses and measured the intensity in each case, then constructed absorption curves from which they obtained the half value layer.

They also investigated the question of the most suitable metal for measuring the H.V.L. of high voltage radiation and suggested that tin is the most suitable material in that case. They also recommended the measurement of a second H.V.L; the ratio of the first to the

second H.V.L. indicated the heterogenity and gave a more complete idea of the quality of the rays.

Although the H.V.L. method seems to be the most convenient and the least open to criticism, it does not give all the information required for the specification of the quality. But nevertheless it can be used in many cases satisfactorily and it is one of the best methods of expressing the quality by a single parameter which represents a physical picture of the quality. Provided the general well known precautions are taken into account, there are no serious difficulties in obtaining it.

As the x-ray beam generally consists of a wide range of wavelengths it has been found that one material could not be used in the whole range of exciting kilovoltages. For example, aluminium is suitable for longer wavelengths while for shorter ones a great thickness is needed to cut down the intensity into half its value and this, besides its inconvenience, produces scattered radiation which increases the ionization above its real value. So it was agreed at the fifth international congress of Radiology that:

For medical purposes it is sufficient to specify the

quality of the x-radiation by the H.V.L. in suitable materials which are:

For x-rays up to 20 kilovolts peak value (kVp) cellophane or cellone is used as an absorber.

Between 20 and 120 kVp: Aluminium

From 120 to 400 kVp : Copper

Above 400 kVp : Tin or Lead.

Mayneord and Roberts[15] found that Tin is more sensitive at high potentials and found it was superior to Lead.

For a more definite specification of the quality a complete absorption curve is preferable.

(iii) The effective wavelength

This method was suggested by Duane [26,27] in 1922 in an effort to express the quality of an x-ray beam by a single quantity.

When a layer of material is introduced in the path of the x-rays a certain amount of the radiation is absorbed and a reduction is noticed in the final intensity of the beam after leaving the absorber. The wavelength of the monochromatic radiation which would be absorbed in the

same layer by the same amount as the heterogeneous x-ray beam in question is called the "Effective wave length λ_e ".

In the case of monochromatic radiation the following equation describes the phenomenon taking place:

$$I_x = I_o e^{-\mu_\lambda x} \qquad (1)$$

where Io and Ix are the intensities of the radiation before and after passing through a thickness x of the absorber. μ_λ is the total linear absorption coefficient of the material of the absorber for a specified wavelength "λ" .

In the case of the heterogeneous radiation the equation will be:

$$I_x = I_o e^{-\mu_{\lambda e} x} \qquad (2)$$

μ in this case is a composite absorption coefficient corresponding to the effective wavelength " λ_e " defined as previously stated.

The equation

$$I_x = I_o e^{-\mu x} \qquad (3)$$

is actually used to represent the absorption of a beam of heterogeneous radiation bearing in mind the meaning of the different symbols as they are defined in equation (2)

To obtain λ_e Duane measured the intensity of the beam before and after passing through a standard sheet of copper 1 mm. in thickness. Using equation (3) and Richtmeyer's [28] formula or tables he obtained the corresponding "λ_e"

He modified this method by constructing a standard absorption curve representing the percentage transmission in .25 mm. copper against the wavelength. He then measured the percentage transmission in .25 mm. copper of the beam in question and read the corresponding λ_e directly from the standard curve.

Duane's method has the advantage that it needs only one intensity measurement beside the original one and a reference to a standard curve. It gives a physical description of the quality and is more convenient and simple than other methods. This simplicity is outweighed by the indefiniteness of the results. The λ_e obtained depends on the thickness of the copper used as a standard. Therefore a statement of the thickness used should be expressed. As the specification of the quality required small thicknesses (as 1 mm. or .25 mm.) to be used, the measurements of these small thicknesses

are liable to be in error. Any slight error in the thickness may result in considerable error in λ_e . Also the standard used as an absorber should be carefully chosen for what is suitable for soft rays is not so for hard ones.

(iv) The true effective wavelengths

Another way of applying absorption data to specify the quality was suggested by Taylor [29]. He expressed the quality in what he called the "true λ_e " which he obtained from absorption curves by drawing a tangent at the required point, the slope of the absorption curve at this point gave the absorption coefficient. From tables for monochromatic radiation, the true effective wavelength was obtained.

This method is less practical than Duane's method, for it needs a series of measurements for filters of different thicknesses while Duane's method needs only two. The drawing of a tangent at the point in question is not easy and any slight error in this process leads to an appreciable error in the value of the absorption coefficient and hence in the determination of λ_e . This is outweighed by the

claim of the author that drawing a complete absorption curve will average out the error in the measurement of the thickness of filters.

An advantage in this method is that a statement of the thickness used is not included in the expression for the quality; the standard material used as filter must, of course, be specified.

(v) The average wavelength method

The term "average wavelength" was proposed by Mutscheller.(30) Its determination consisted in observing the percentage transmission through an increasing thickness of a metal and plotting these values against the corresponding thicknesses on a semilogarithmic paper. He observed that for greater thickness (above .5 mm. copper) the curve became a straight line indicating a homogeneity in the radiation. He accordingly divided his curve into two parts:

1. The portion from zero filtration to the stage where it became a straight line. In this part he determined his average wavelength at any point by drawing a tangent at that point and determined μ and λ_e. In this case the average wavelength coincides with the 50 called true λ_e of Taylor, having its advantages

disadvantages.

2. The straight portion of the curve. In this case he measured the slope of the line which gave μ and consequently the average wavelength was read off from tables. This method is not sound from the theoretical point of view for the plotting of log $\frac{Ix}{Io}$ against x does not give a straingt line; after a certain amount of filtration, the quality of the beam changes very little with the increase of thickness of filter and the curve approaches linearity but does not become exactly linear.

(vi) The complete absorption curve method

As it was the aim of the different investigators to express the quality by as few parameters as possible provided the main requirements are fulfilled, Taylor[31] approached this aim from a rather different angle.

An x-ray spectrum is a function of the potential applied to the tube. If a constant potential is applied, a simple spectrum results. This simple spectrum is reproduceable and is a function of the value of the exciting voltage and the target material. On the contrary, when a fluctuating potential is applied (as it is usually the case) to the tube, a "composite spectrum" is obtained. Hence the

absorption curve of a constant potential x-ray beam can be used as a standard of reference.

The method adopted was therefore that an absorption curve of the beam in question was plotted on a transparent paper. This paper was moved on the set of standard curves of reference and a standard absorption curve was found which fitted - as regards general character as slope and curvature - the curve under investigation for the same absorber. Then the physical properties of the given beam were similar to those of the beam obtained with a constant potential generator. Hence Taylor described the quality of the beam by two quantities:

1. The constant potential which gives a similar absorption curve as the one in question. He called it "The equivalent constant potential".
2. The initial filtration.

This method of representing the quality seems to be justifiable for, besides giving a physical picture, it includes information of x-ray tube target, tube wall and primary filtration.

(b) Determination of the effective wavelength from the x-ray energy distribution curve.

. . . . . .

In view of the above discussion one can see that the most reliable and accurate method for specifying the quality (besides the spectrometer method which, as previously stated, is not easily applicable in the therapeutic use of x-rays, is the construction of a complete absorption curve[32] using the appropriate material for each range of kilovoltages used. The difference between the various methods arises in the way the data included in the absorption curve are utilized to obtain a significant picture of the quality of radiation.

We shall describe the method adopted for obtaining λ_e from the energy distribution curve based on absorption data.

The method of obtaining the intensity distribution of an x-ray beam theoretically from absorption data was first examined by Silberstein[33]. He gave an approximate method of solving the problem.

He showed that one intensity distribution curve can be derived theoretically from a certain complete absorption curve and applied his method in analysing beams excited by

different kilovolts up to 100 kV. and found it to be fairly satisfactory for practical purposes.

i. The Theory of the Method

In a heterogeneous beam of radiation, the total intensity is given by:

$$I_o = \int_o^\infty f(\lambda)\, d\lambda \qquad (1)$$

where $f(\lambda) \equiv I_\lambda$ is the average intensity for the range of wavelengths from λ to $\lambda + d\lambda$.

If the form of $f(\lambda)$ is known then I_o can be calculated. When the beam passes through a filter of thickness x cm., its intensity is given by:

$$I_x \equiv \int_o^\infty e^{-\mu_\lambda x} f(\lambda)\, d\lambda \qquad (2)$$

where μ_λ is the absorption coefficient of the wavelengths ranging between λ and $\lambda + d\lambda$. The solution of (2) gives the required intensity distribution of a continuous x-ray beam.

For changing the variables put:

$$f(\lambda)\, d\lambda = \phi(\mu)\, d\mu \qquad (3)$$

and denoting $\mu(0)=\mu_0$ and $\mu(\infty)=\infty$, (2) becomes:

$$I_x = \int_{\mu_0}^{\infty} e^{-\mu x}\, \phi(\mu)\, d\mu \qquad (4)$$

An integral equation for unknown function $\phi(\mu)$.

Silberstein found that an equation of the following type

$$I_x = I_0\, e^{-Ax - B\sqrt{x}} \qquad (5)$$

where A and B are constants, generally fits the experimental data in copper and aluminium fairly well and in some cases with great accuracy.

From (4) and (5)

$$\int_{\mu_0}^{\infty} e^{-\mu x}\, \phi(\mu)\, d\mu = I_0\, e^{-Ax - B\sqrt{x}} \qquad (6)$$

A solution of this equation can be obtained from a certain integral evaluated by Laplace:

$$\phi(\mu) = 0 \quad \text{For } \mu \leq A$$

$$\phi(\mu) = \frac{B}{2\sqrt{\pi}} (\mu - A)^{-\frac{3}{2}}\, e^{-\frac{B^2}{4(\mu - A)}} \quad \text{For } \mu \geq A \qquad (7)$$

Using (3) we can return to $f(\lambda)$ thus

$$I_\lambda \equiv f(\lambda) = \frac{B}{2\sqrt{\pi}} (\mu - A)^{-\frac{3}{2}} e^{-\frac{B^2}{4(\mu - A)}} \frac{d\mu}{d\lambda} \qquad (8)$$

which is characterized by the coefficients A and B.

Equation (8) gives the complete spectral distribution of a continuous x-ray beam whose absorption curve is given by (5).

The spectrum is sharply bounded on the short wavelength side by the limiting wavelength $\lambda_0 = 12.35/V_{in\ KV_p}$ (Duane & Hunt) the value of which is governed only by the peak kilovolts applied to the tube. From monochromatic absorption tables the value of μ_0 corresponding to λ_0 is taken and hence A, which was found (34) identical with μ_0.

Jones (35) modified Silberstein's method in the following way:

Equation (5) can be written in the form:

$$\frac{x}{y} = \frac{y}{B^2} \qquad (9)$$

where $y = -\left[\log \frac{I_x}{I_o} + Ax\right]$

If, as Silberstein proposed, equation (5) represents the absorption data given by a beam, then the plot of $\frac{x}{y}$ against y should yield a straight line passing through the origin as suggested by equation (9). This was not found to be the case. Whenever one can obtain a straight line from the plotting of $(\frac{x}{y}, y)$, with a reasonable percentage accuracy, from transmission data, the line does not pass through the origin but gives an intercept on the $(\frac{x}{y})$ axis. The fact suggests that (9) should be modified to the form:

$$\frac{x}{y} = \frac{y}{B^2} + C \qquad (10)$$

in order to represent the experimental data.
The solution of (10) for y is:

$$y = B\left[-\sqrt{d} + \sqrt{x+d}\right] \quad \text{where} \quad d = \frac{B^2C^2}{4}$$

Consequently (5) no longer represents the transmission data. It should be modified to the form:

$$I_x = I_o e^{-Ax - B\left[\sqrt{x+d} - \sqrt{d}\right]} \qquad (11)$$

Therefore equation (8) would become:

$$f(\lambda) \equiv I_\lambda = \frac{B\, e^{B\sqrt{d}}}{2\sqrt{\pi}} \cdot \frac{e^{-(\mu-A)d - \frac{B^2}{4(\mu-A)}}}{(\mu-A)^{\frac{3}{2}}} \cdot \frac{d\mu}{d\lambda} \qquad (12)$$

This equation was found [35] to give the continuous spectral distribution of beams of the kind in x-ray therapy provided the plot of ($\frac{x}{y}$, y) yielded a straight line. In this case the amount of characteristic radiation is negligible (equation (12) allows only one maximum for the intensity).

If, however, characteristic radiation is present in an appreciable amount then the plot of ($\frac{x}{y}$, y) will not give a straight line.

Recently, Greening [36] has extended the Silberstein-Jones formula to cover beams having a certain percentage of characteristic radiation. Applying this extension in some of our cases, where we fail to obtain a straight line, we find that by allowing for an amount of characteristic radiation to be present, we can eliminate the curvature of the line.

ii. Correction for characteristic Radiation

If it is assumed that a certain amount of characteristic radiation is present and correction for this produces a straight line when plotting ($\frac{x}{y}$, y), then for the beams used we can safely say that the continuous spectral distribution given by (12) together with the above amount of characteristic radiation gives a satisfactory description of the total radiation in the beams used, for:- (36)

Let p be the fraction of the total radiation attributed to characteristic radiation

and q be the fraction of characteristic radiation due to K_β line

I_0 and I_x have the previous meanings.

I_0' and I_x' are the corresponding quantities for the continuous radiation only.

Then

$$I_0' = I_0 - pI_0 = I_0(1-p)$$

and

$$I_x' = I_x - pI_0\left[(1-q)e^{-\mu_\alpha x} + qe^{-\mu_\beta x}\right],$$

where μ_α and μ_β are the absorption coefficients of the characteristic lines.

Figure (I)

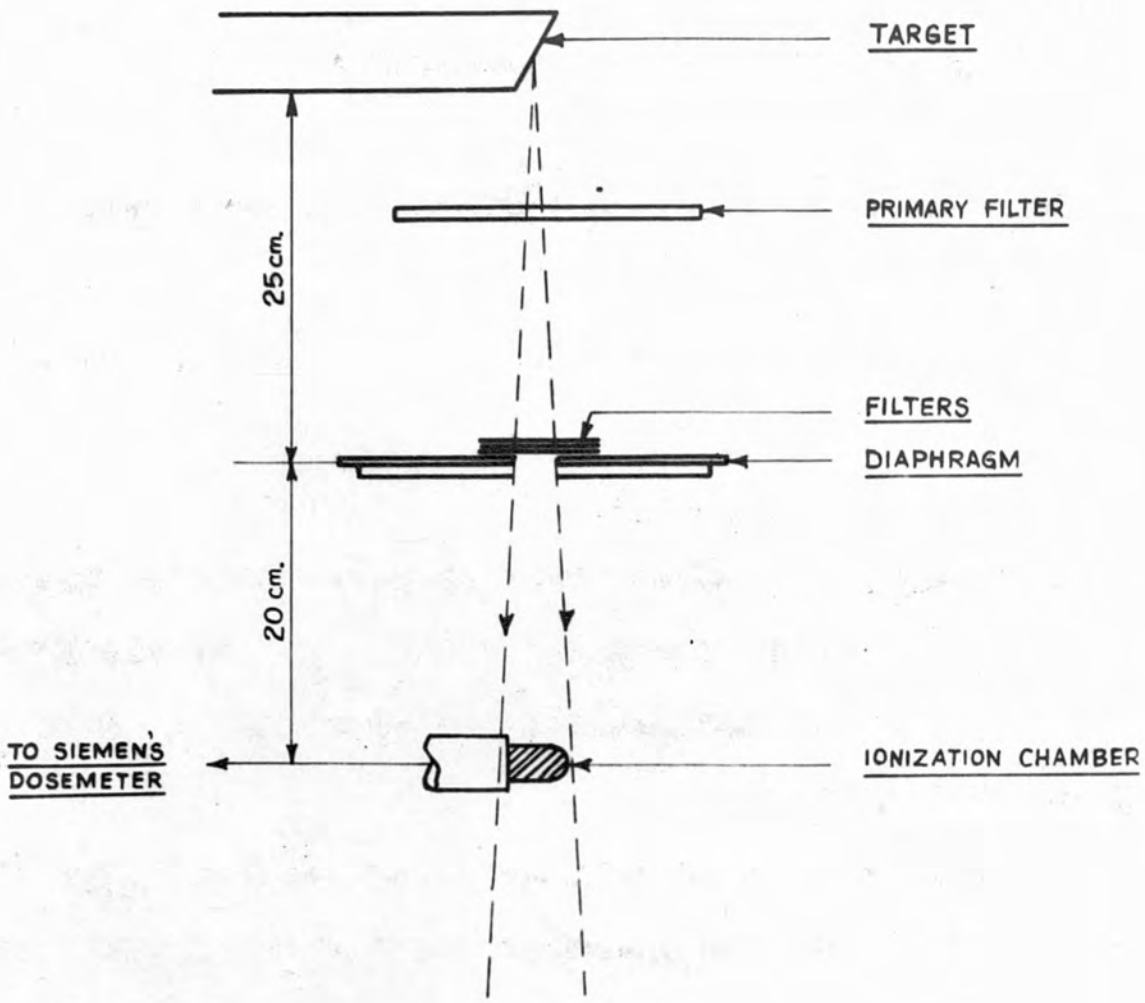

— EXPERIMENTAL ARRANGEMENT FOR MEASUREMENT —
OF THE ABSORPTION CURVES

We have from Jones' analysis

$$y = -\log \frac{I_x}{I_o} - Ax$$

Thus for the continuous radiation in this case

$$y' = -\log \frac{I_x}{I_o} - Ax$$

Substituting the values of I_x' and I_o' we get

$$y = -\log \left[\frac{1}{1-P} \left\{ \frac{I_x}{I_o} - P\left[(1-q) e^{-\mu_\alpha x} + q e^{-\mu_\beta x} \right] \right\} \right] - Ax \quad \ldots (13)$$

The value of p which when inserted in (13) gives a straight line of the plots of $(\frac{x}{y'}, y')$ is the fraction of the characteristic radiation present in the beam. p can be found by trial.

In the above treatment it is supposed that the relative intensities of the characteristic lines present are known.

iii. Experimental Method *

The experimental arrangements are shown in the figure (1). A diaphragm about 0.5 cm. thickness of lead and 1 cm. thickness of aluminium with a hole at the centre having a diameter just large enough to ensure that the whole

* This method was adopted before the apparatus fig.(34) was ready for use.

ionization chamber was totally irradiated (about 1.8 cm. in diameter). The filters used were sheets of pure copper and tin supplied by Messrs. Johnson-Matthey. The thickness of the filters was determined by weighing. Also it was checked by measuring the thickness of several sheets together and calculating the thickness of each. The aluminium filters were standard filters provided with the x-ray tube and their thicknesses were known.

Siemen's ionization chamber was used in some of the investigations. It is built up from pressed material which is electrically conducting, and is wavelength independent over a wide range corresponding to peak values from 80 to 400 kV. This was assured by the makers and has been confirmed by Eddy[37]. The intensity (which is proportional to the dosage rate read on the scale) was measured by the Siemen's Momentum direct reading dosemeter. The ionization current set up in the ionization chamber when it is irradiated is passed through a resistance connected with the central electrode. The drop of potential across the high resistance caused by the ionization current is measured by an electrometer. The reading of the instrument was noted before the insertion of any filters to represent I_o

and then I_x was read for various filters to construct an absorption curve for each kilovoltage applied to the tube.

iv. Evaluation of the constants

The values of I_x / I_o were obtained experimentally together with the corresponding thickness in cm. (x) of the filters used. A smooth curve was drawn between $\log_{10}\left(\frac{I_x}{I_o} \times 100\right)$ and x from which the values of y and $\frac{x}{y}$ were calculated. The value of $\frac{x}{y}$ was plotted against y. In the case of a straight line the intercept was taken to be the value of the constant c . The slope was evaluated and is a measure of $1/\beta^2$ (equation 10).

d was evaluated from the relation

$$d = \frac{\beta^2 c^2}{4}$$

The value of $A \equiv \mu_o$ was obtained from a knowledge of the kilovoltage used and the relation

$$\lambda_o = \frac{12.35}{V} \qquad V \text{ in Kilovolts}$$

The corresponding value of μ_o for λ_o for the material

used as absorber was taken from the following sources as stated above each table.

(1) Lamerton's[38] unpublished work.

(2) Greening's[36] table.

The values of the constants, B, C, d, A, μ and $\frac{d\mu}{d\lambda}$ were all inserted in equation (12) and the value of I_λ was calculated for values of λ covering a range within the area under the curve plotted between I_λ and λ .

In the case where no straight line was obtained from the plot of ($\frac{x}{y}$, y) equation (13) was applied.

The ratio of the intensities[39],[40] $\frac{K_\alpha}{K_\beta} = 3$ with no primary filter but, if the radiation has passed through an added filter this ratio is changed according to the material and the thickness of the filter. When using a filter (.5 mm. Cu + 1 mm. Al) $\frac{K_\alpha}{K_\beta} = \frac{7}{3}$ and hence $q = .03$.

The value of $q = 0.3$ was inserted in (13) then y' was evaluated for each of the filter thicknesses (x) used, with p having arbitrary values 25%, 30% and 40% as shown in the tables. The value of p which reduced the plot of ($\frac{x}{y}$, y) to a straight line (in this case 30%) was the amount of characteristic radiation present. From the

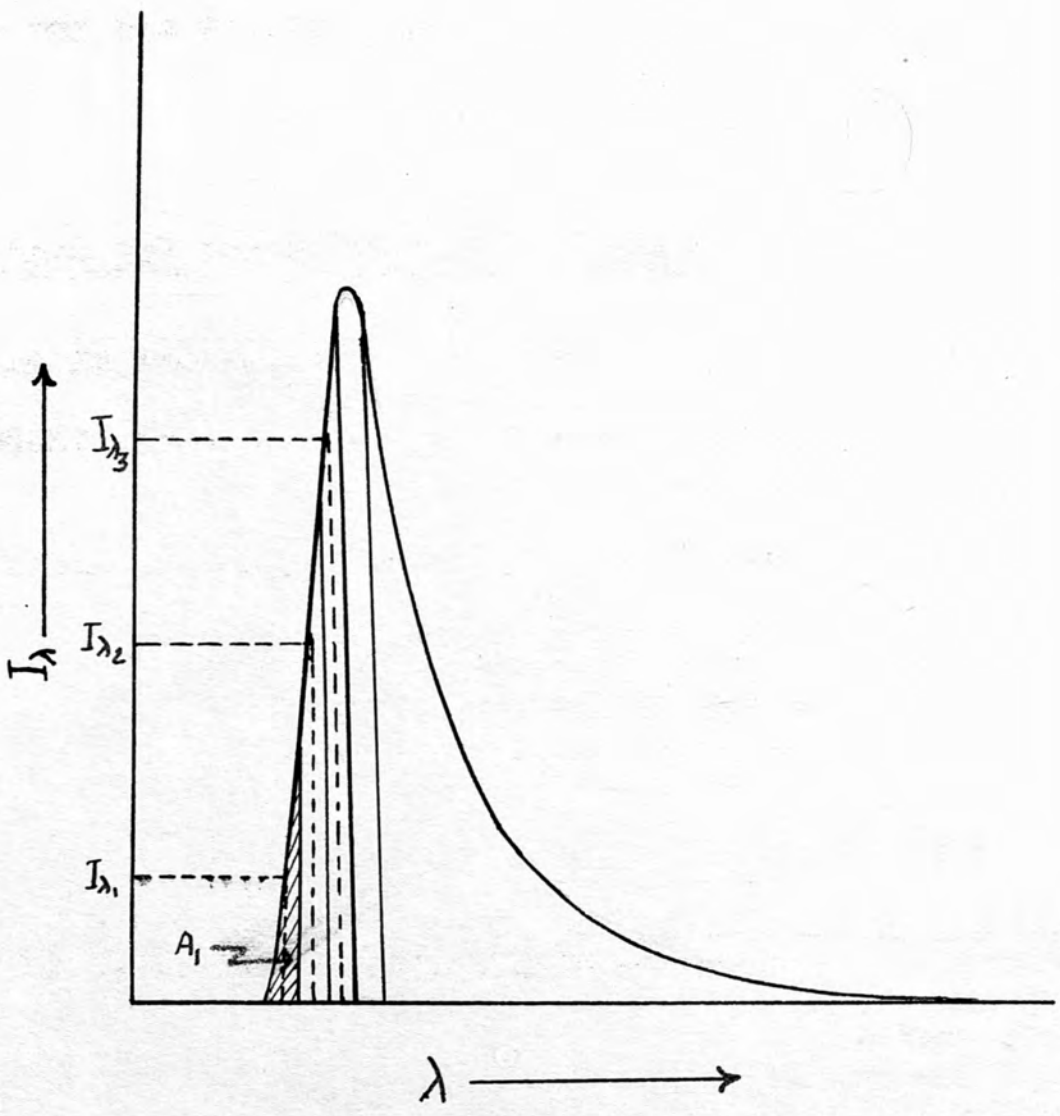

Figure (2)

resulting straight line the values of the constants B, C and d were obtained as previously stated and the evaluation of (13) was carried out.

v. To obtain λ_e from the intensity distribution curve

The area under each (I_λ, λ) curve was divided into strips (fig. (2)) of areas $A_1, A_2, A_3 \ldots\ldots$ etc. where

$$A_1 = I_{\lambda_1} d\lambda_1 \quad , \quad A_2 = I_{\lambda_2} d\lambda_2 \quad \ldots\ldots$$

Thus the total area under the curve

$$A = \Sigma A_1$$

and

$$\lambda_e = \frac{\Sigma A_1 \lambda_1}{\Sigma A_1}$$

where λ_1 is the mean wavelength in the strip of area A_1, etc....

vi. Experimental results

The following tables contain the observations and results obtained with the conditions stated at the top of each one of them.

Figs. (3,4,5,6&7) represent the data in the tables.

Figure(5)

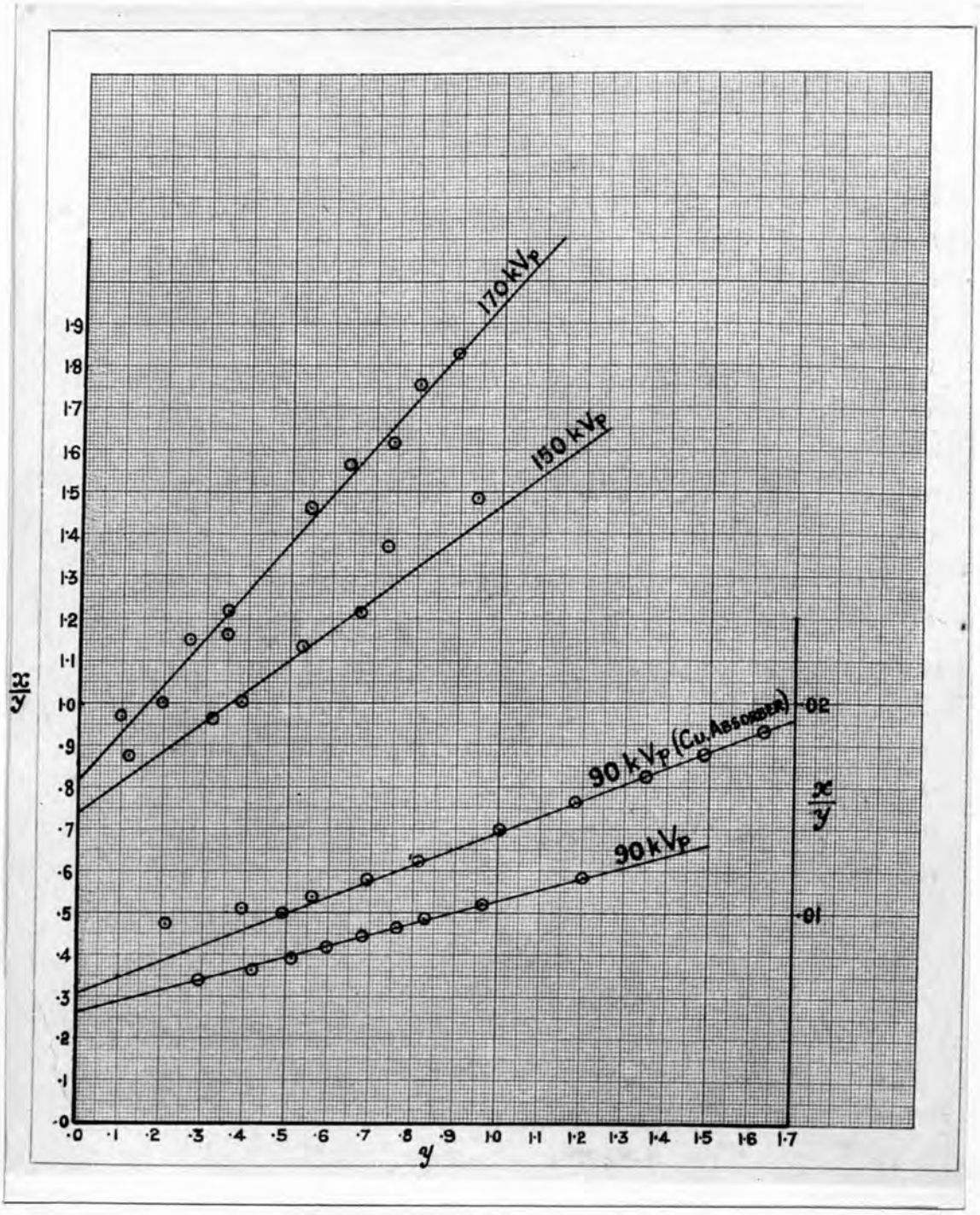
170 kVp
150 kVp
90 kVp (Cu. Absorber)
90 kVp
x/y
y
0·0 0·1 0·2 0·3 0·4 0·5 0·6 0·7 0·8 0·9 1·0 1·1 1·2 1·3 1·4 1·5 1·6 1·7
·1 ·2 ·3 ·4 ·5 ·6 ·7 ·8 ·9 1·0 1·1 1·2 1·3 1·4 1·5 1·6 1·7 1·8 1·9
·02
·01

The exciting voltage = 90kVp.

Added filter = 2 mm. of aluminium

$$\lambda_0 = \frac{12.35}{90} = 0.137 \text{ A.U.}$$

$\mu_0 = .497$ cm^{-1} (from Greening's table[36])

$A = .497$

x in cm. Al	$\log_{10}\left(\frac{I_x}{I_0}\times 100\right)$	$\log_e \frac{I_x}{I_0}$	Ax	y	$\frac{x}{y}$
.05	1.922	-.179	.25	.154	.325
.1	1.85	-.345	.05	.295	.340
.15	1.78_7	-.490	.075	.415	.362
.2	1.73_5	-.610	.099	.511	.391
.25	1.68_5	-.722	.125	.597	.419
.3	1.64	-.827	.149	.678	.443
.35	1.59_7	-.927	.174	.763	.465
.4	1.55_5	-1.022	$.19_9$	.823	$.48_6$
.5	1.47_4	-1.210	$.24_9$	$.96_1$	$.52_1$
.6	1.39_8	-1.38_7	$.29_8$	1.08_9	$.55_1$
.7	1.32_5	-1.55_3	$.34_8$	1.20_5	$.58_1$

Two lines are shown in fig.(3) for 90 KVp :one of them for Al. absorber (corresp0nding to the above data in the table) and the other for Cu. absorber.

In the following table $f(\lambda)$ corresponding to Al. and Cu. absorbers were calculated and the mean was taken. The energy distribution curve was drawn between $f(\lambda)_{mean}$ and λ as shown in fig.(4) number(I).

The corresponding absorption curves are shown in fig.(I0) curve(2).

Figure (4)

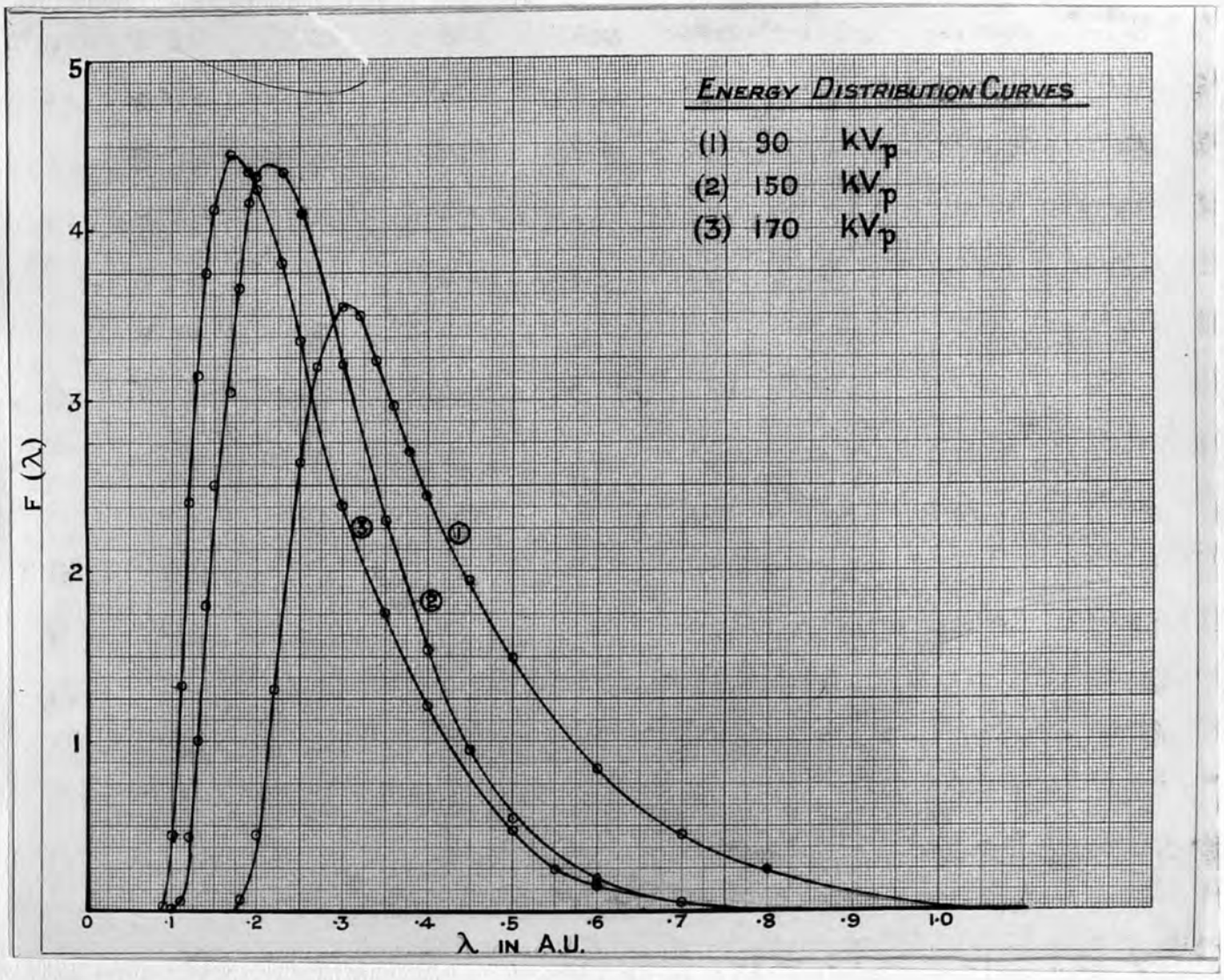
ENERGY DISTRIBUTION CURVES
(1) 90 KVp
(2) 150 KVp
(3) 170 KVp
F (λ)
λ IN A.U.
0
·1
·2
·3
·4
·5
·6
·7
·8
·9
1·0
1
2
3
4
5

Evaluation of $f(\lambda) \equiv I_\lambda$ for 90 kVp /fig.(4) No.1/

Constants for Al. absorber: c = .264, B = 1.94 & d = .063
and for Cu. absorber: c = .0077, B = 1.22 & d = .009

λ in A.U.	μ	$\mu - A$	$(\mu-A)d$	$B^2/4(\mu-A)$	$(\mu-A)d+\frac{B^2}{4(\mu-A)}$	$e^{-[\ ]}$	$(\mu-A)^{\frac{3}{2}}$	$\frac{d\mu}{d\lambda}$	$f(\lambda)_{Al.}$	$f(\lambda)_{Cu.}$	$f(\lambda)_{mean}$
.18	.637	.140	.009	6.72	6.73	.0012	.0624	3.64	.07	.06	.065
.20	.713	.216	.014	4.35	4.36	.0128	.100	4.04	.46	.49	.475
.22	.81	.310	.020	3.04	3.06	.0468	.172	5.40	1.31	1.30	1.305
.25	1.00	.50	.032	1.88	1.91	.148	.353	7.40	2.76	2.50	2.63
.27	1.16	.66	.042	1.43	1.47	.230	.536	8.70	3.32	3.06	3.19
.30	1.45	.95	.061	1.99	1.05	.350	.927	10.60	3.57	3.55	3.56
.32	1.68	1.18	.075	.797	.872	.418	1.285	11.90	3.45	3.55	3.50
.34	1.94	1.44	.091	.653	.744	.475	1.73	13.20	3.23	3.24	3.23_5
.36	2.20	1.70	.108	.554	.662	.516	2.22	14.70	3.05	2.90	2.97_5
.38	2.51	2.01	.127	.468	.595	.551	2.86	16.30	2.80	2.60	2.70
.40	2.85	2.35	.149	.400	.549	.576	3.60	18.00	2.57	2.33	2.45
.45	3.89	3.39	.215	.278	.493	.611	6.23	23.00	2.01	1.88	1.94_5
.50	5.17	4.67	.296	.202	.498	.608	10.10	27.80	1.49	1.50	1.49_5
.60	8.60	8.10	.513	.116	.629	.533	23.10	40.60	.835	.84	.84
.70	13.50	13.0	.823	.072	.895	.408	47.00	55.60	.43	.48	$.45_5$
.80	19.9	19.4	1.23	.048	1.27_8	.278	85.00	70.50	.206	.30	$.25_5$

Effective wavelength for 90 kVp

λ_{mean}	$I_{\lambda_{mean}}$	$d\lambda$	$A_i = I_{\lambda_i} d\lambda_i$	$\lambda_{mean} A_i$
$.187_5$	.15	.025	.0037	.0007
$.212_5$	.775	.025	.0194	.004
$.237_5$	2.10	.025	$.052_5$	.0125
$.262_5$	3.00	.025	.075	.0197
$.287_5$	3.46_8	.025	$.086_8$	.025
$.312_5$	3.52_5	.025	$.088_2$	.0276
.3375	3.30	.025	$.082_5$	.0278
$.362_5$	2.90	.025	$.072_5$	.0262
$.387_5$	2.57_5	.025	$.064_4$	.025
$.412_5$	2.28_8	.025	$.057_3$	.0236
$.437_5$	2.025	.025	$.050_6$	.022
$.462_5$	1.78	.025	$.044_7$	.0207
$.487_5$	1.58_8	.025	$.039_4$	.0192
.575	.975	.15	$.146_2$	.084
.75	.34	.20	.068	.051
.95	.07	.20	.014	.0133

The total area under the curve $A = \Sigma A_i = .9652$

$$\Sigma \lambda_{mean} A_i = .403$$

$$\lambda_e = \frac{.403}{.9652} = .417_5 \text{ A.U.}$$

The exciting voltage = 150 kVp

Added filter = 0

Applicator used (6 x 8 cm. F.S.d 50)

$$\lambda_o = \frac{12.35}{150} = .0823 \text{ A.U.}$$

$A = \mu_o = .405 \text{ cm}^{-1}$ (From Jone's table)

Thickness x in cm. Al.	0	.1	.2	.3	.4	.6	.8	1.0	1.4
Dosage rate in r/min	58.5	50.1	43.1	38	33.9	27.1	22.0	18.9	13.0
I_x / I_o	1	.856	.737	.65	.579	.463	0.376	0.323	.222
$\log_{10}\left(\frac{I_x}{I_o} \times 100\right)$	2	1.93	1.88	1.81	1.76	1.67	1.57	1.51	1.35
$-\log_e \frac{I_x}{I_o}$	0	.155	.305	.431	.546	.769	.978	1.130	1.504
Ax	0	.040	.080	.121	.161	.241	.322	.402	.563
y	0	.115	.225	.311	.385	.528	.657	.728	.941
x/y	0	.88	.89	.96	1.04	1.14	1.22	1.37	1.49

These data are represented in fig. (3) by the straight line specified by 150 kVp.
Absorption curve fig. (10).

Evaluation of $f(\lambda)$ for 150 kVp (fig.(4) No. 2)

$c = .74$ $B = 1.83$ and $d = 1.92$

λ in A.U.	μ cm^{-1}	$(\mu-A)$	$(\mu-A)d$	$B^2/4(\mu-A)$	$\bar{e}[\ ]$	$\frac{d\mu}{d\lambda}$	$\bar{e}[\ ]\frac{d\mu}{d\lambda}$	$(\mu-A)^{\frac{3}{2}}$	$\frac{\bar{e}[\ ]}{(\mu-A)^2}\cdot\frac{d\mu}{d\lambda}$	$f(\lambda)$
.1	.435	.030	.0058	11.67	.00008	1.81	.00014	.0052	.028	.0156
.11	.454	.049	.0094	7.14	.0006	1.98	.0012	.0109	.109	.061
.12	.475	.070	.013	5.0	.0067	2.16	.0145	.019	.78	.44
.13	.498	.093	.018	3.76	.024	2.36	.056	.28	1.95	1.092
.14	.523	.118	.023	2.97	.050	2.58	.1298	.040	3.21	1.80
.15	.550	.145	.028	2.41	.087	2.83	.246	.055	4.47	2.51
.17	.612	.207	.040	1.69	.177	3.40	.603	.095	6.35	3.56
.18	.650	.245	.047	1.43	.228	3.72	.845	.121	6.97	3.91
.19	.690	.285	.055	1.23	.278	4.08	.434	.152	7.44	4.17
.20	.733	.328	.063	1.067	.323	4.48	1.45	.188	7.715	4.32
.23	.878	.473	.091	.74	.436	5.76	2.51	.326	7.725	4.33
285	1.00	.595	.114	.588	.495	6.74	3.33	.459	7.275	4.08
.30	1.40	.995	.191	.352	.581	9.80	5.69	.992	5.74	3.22
.35	2.01	1.60	.309	.218	.590	14.40	8.50	2.033	4.08	2.29
.40	2.87	2.46	.474	.142	.540	19.60	10.59	3.87	2.74	1.53
.45	3.96	3.55	.682	.098	.458	24.70	11.30	6.70	1.69	.95
.50	5.37	4.965	.954	.070	.359	29.70	10.67	11.08	.963	.54
.60	8.79	8.38	1.61	.041	.191	41.80	8.02	24.25	.331	.185
.70	13.6	13.19	2.53	.026	.077	56.10	4.34	47.90	.091	.051

Effective wavelength λ_e for 150 kVp

λ_{mean}	$f(\lambda)$	$d\lambda$	$A_1 = I_\lambda d\lambda$	$A_1 \lambda_{mean}$
.115	.125	.02	$.002_5$	.0004
$.137_5$	1.55	.025	$.038_8$	$.005_3$
$.162_5$	3.17_5	$.02_5$	$.079_4$	$.012_7$
$.187_5$	4.07_5	$.02_5$	.102	$.019_1$
$.212_5$	4.39	$.02_5$	$.109_7$	$.023_3$
$.237_5$	4.32	$.02_5$	.108	$.025_6$
.270	3.78_6	.04	$.151_4$	$.040_8$
.315	2.92_5	.05	$.146_3$	$.046_1$
.370	0.20	.06	.12	$.044_4$
.450	.95	.1	.095	$.042_7$
.575	.25	.15	$.037_5$	$.021_6$
.750	.025	.2	.005	$.003_8$

The total area under the curve $A = \Sigma A_1 = .995_5$

$\Sigma \lambda_{mean} A_1 = .285_8$

$\lambda_e = \frac{.2858}{.9955} = 0.287$ A.U.

The exciting voltage = 170 kVp

added filter = 0

$\lambda_0 = \frac{12.35}{170} = 0.0726$ A.U.

$\mu_0 = .392$ cm^{-1} from Jones' tables

$A = .392$

x in cm.	Dosage rate in r/min.	$\frac{I_x}{I_0}$	$\log_{10}\left(\frac{I_x}{I_0}\times 100\right)$	$-\log_e \frac{I_x}{I_0}$	Ax	y	$\frac{x}{y}$
0	70.9	1.0	2.0	0.0	0.0.	0.0	0.0
0.1	61.5	0.868	1.93_8	0;142	0.039	0.103	0.971
0.2	53.8	0.759	1.88	0.275_8	0.078	0.197	1.01
0.3	48.6	0.686	183_6	0.377_7	0.116	0.260	1.15
0.4	43.0	0.607	1.78_3	0.499_9	0.155	0.343	1.17
0.6	35.5	0.501	1.70	0.691_8	0.233	0.457	1.31
0.8	30.0.	0.423	1.62_7	0.859_9	0.310	0.546	1.46_5
1.0	25.3	0.357	1.55_3	1.030	0.392	0.638	1.57
1.2	21.1	0.298	1.47_4	1.210	0.466	0.741	1.62
1.4.	18.9	0.267	1.42_6	1.347	0.543	0.798	1.75

The straight line between (y, $\frac{x}{y}$) for 170 kVp is shown in fig.(3)

Absorption curve fig. (10)

Evaluation of $f(\lambda)$ for 170 kVp (fig:(4) No.3)

$c = 0.82$ $B = 0.94$ and $d = 0.148$

λ in A.U.	μ	$\mu - A$	$(\mu - A)d$	$B^2/4(\mu-A)$	$e^{-[\ ]}$	$\frac{d\mu}{d\lambda}$	$e^{-[\ ]}\frac{d\mu}{d\lambda}$	$(\mu-A)^{\frac{3}{2}}$	$\frac{e^{-[\ ]}}{(\mu-A)^{\frac{3}{2}}}\cdot\frac{d\mu}{d\lambda}$	$f(\lambda)$
.09	.418	.026	.004	8.50	.0002	1.65	.0004	.004	0.079	0.03
.1	.435	.043	.006	5.15	.006	1.81	.010	.009	1.18	0.45
.11	.454	.062	.009	3.57	.027	1.98	.054	.015	3.51	1.34
.12	.475	.083	.012	2.67	.068	2.16	.148	.024	6.28	2.40
.13	.498	.106	.016	2.87	.122	2.36	.286	.035	8.30	3.15
.14	.523	.131	.019	1.69	.181	2.58	.467	.047	9.85	3.75
.15	.550	.158	.023	1.40	.241	2.83	.682	.063	10.82	4.12
.17	.612	.220	.033	1.01	.354	3.40	1.21	.103	11.68	4.45
.19	.690	.298	.044	.743	.455	4.08	1.86	.165	11.47	4.36
.20	.733	.341	.051	.648	.497	4.48	2.23	.199	11.18	4.25
.23	.878	.486	.072	.455	.591	5.76	3.41	.339	10.05	3.82
.25	1.00	.608	.090	.363	.636	6.74	4.28	.475	8.80	3.35
.30	1.40	1.01	.149	.22	.692	9.80	6.77	1.01	6.67	2.38
.35	2.01	1.62	.239	.137	.686	14.4	9.87	2.10	4.70	1.78
.40	2.87	2.478	.366	.089	.634	19.6	12.40	3.90	3.18	1.21
.45	3.96	3.57	.528	.417	.388	24.7	9.60	6.28	1.10	.775
.50	5.37	4.97	.735	.302	.354	29.7	10.54	11.08	.95	.475
.55	6.99	6.60	.975	.227	.301	35.7	10.74	16.90	.635	.242
.60	8.79	8.40	1.24	.178	.242	41.8	10.10	24.20	.417	.159
.70	13.60	12.20	1.96	.113	.126	56.1	7.05	48.00	.147	.056

λ_e for 170 kVp

λ_{mean}	I_λ	$d\lambda$	$A_1 = I_{\lambda_1} d\lambda_1$	$\lambda_{mean} A_1$
$.097_5$	.35	.015	.0053	.0005
.115	1.75	.02	.035	.004
.135	3.42_5	.02	.069	.0093
.155	4.25	.02	.085	$.013_2$
.175	4.44	.02	.089	$.015_5$
.205	4.18_8	.04	.168	$.034_3$
.245	3.52_5	.04	.141	$.034_6$
.285	2.62_5	.04	.105	$.029_9$
.330	1.96_3	.05	.098	.032
.445	.85	.08	.068	.030
.575	.262	.18	.047	.027
.750	.025	.17	.0043	.0032

The total area under the curve $A = \Sigma A_1 = .914$

$\Sigma \lambda_{mean} A_1 = .234$

$\lambda_e = \frac{.234}{.914} = 0.256$ A.U.

Absorption Curves in Cu.& Sn.

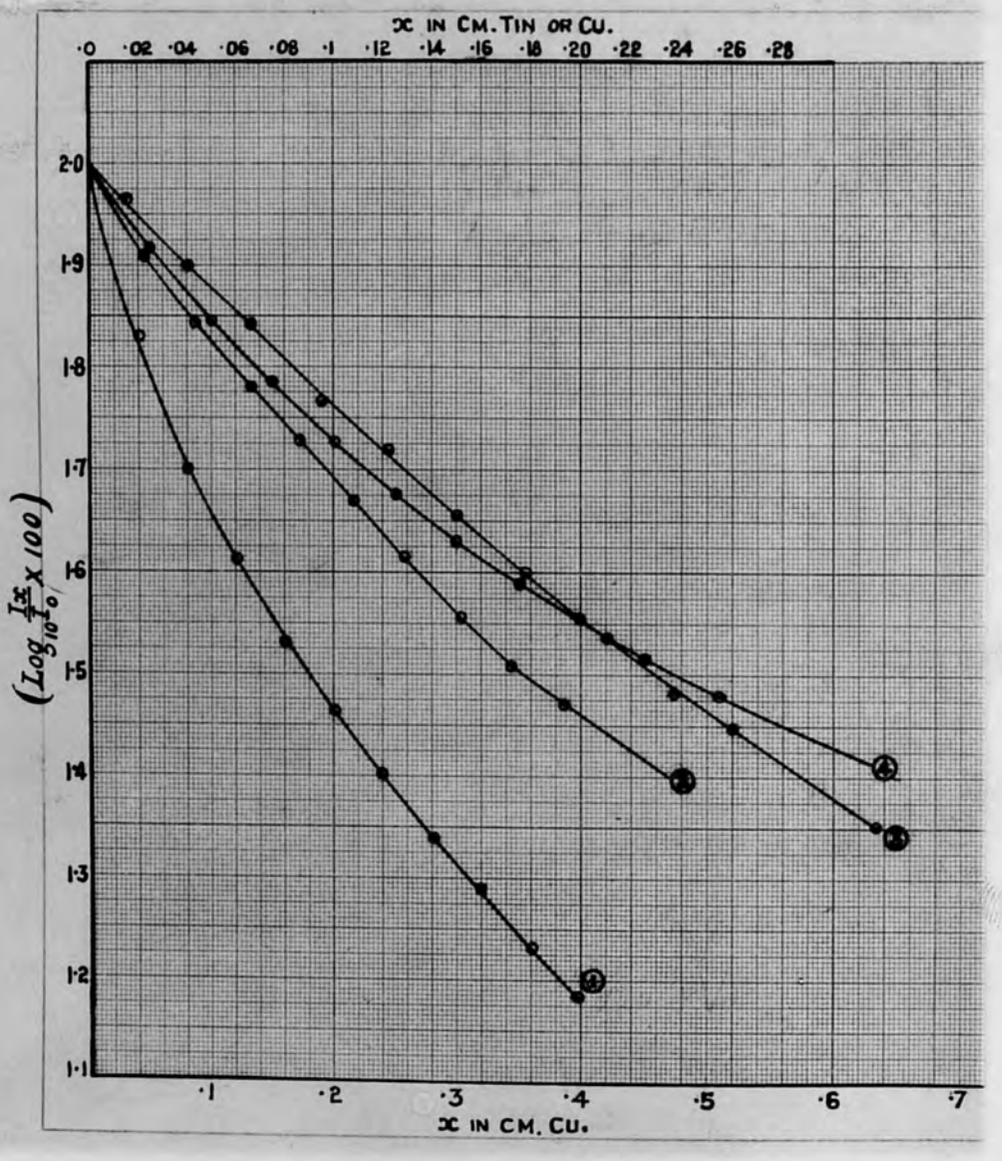

Figure(5)

The exciting voltage = 220 kVp

Added filter = .5 mm. Cu + 1 mm. Al

$\lambda_0 = \frac{12.35}{220}$ .0614 A.U.

$\mu_0 = 1.3$ cm^{-1} (from Greening's table)

$A = 1.3$

The absorption curves are shown in fig. (5) curve (4) for Cu filters, & (1) for tin filters.

x in cm. Cu.	$\frac{I_x}{I_0}$	$\log_{10}\left(\frac{I_x}{I_0} \times 100\right)$	y	x/y
.025	.828	1.918	.157	.159
.05	.703	1.847	.288	.174
.075	.610	1.785	.398	.189
.100	.533	1.727	.500	.200
.125	.475	1.677	.582	.215
.150	.428	1.631	.655	.229
.175	.388	1.589	.720	.243
.200	.356	1.551	.775	.238
.225	.327	1.514	.829	.271
.250	.301	1.479	.878	.285

cont.

P = 25%

$.25\left((1-q)e^{-\mu x}+q\,e^{-\mu\beta x}\right)$	$\left[\frac{I_x}{I_o}-.15(\ )\right]$	$\frac{1}{.75}\left\{\frac{I_x}{I_o}-.15(\ )\right\}$	$\log\frac{1}{.75}\{\ \}$	Ax	$y_{.25}$	$\frac{x}{y_{.25}}$
.179	.649	.866	.144	.0325	.112	.223
.129	.574	.767	.267	.065	.203	.246
.093	.517	.689	.373	.0976	.276	.272
.067	.466	.621	.477	.13	.348	.288
.049	.426	.568	.567	$.162_5$	.406	.308
.035	.393	.524	.647	.195	.453	.331
.026	.362	.483	.728	$.227_6$	.502	.349
.019	.337	.449	.802	.26	.544	.368
.014	.313	.417	.875	$.292_5$	.585	.385
.01	.291	.388	.247	.325	.625	.400

cont.

$P = 40\%$

$.4\left((1-\gamma)e^{-\mu_\alpha x} + \gamma e^{-\mu_\beta x}\right)$	$\frac{I_x}{I_0} - .4(\ )$	$\frac{1}{.6}\left\{\frac{I_x}{I_0} - \cdots\right\}$	$-\log\frac{1}{e}\{\ \}$	$y.4$	$\frac{x}{y.4}$
.286	.542	.903	.101	.069	.362
.206	.497	.829	$.186_5$	$.122_5$	.408
.149	.461	.768	.264	.167	.449
.107	.426	.711	.340	.211	.474
.078	.397	.662	.412	.251	.497
.056	.372	.620	.479	.285	.526
.041	.347	.579	.545	.319	.549
.030	.326	.544	.607	.349	.573
.022	.305	.508	.677	.387	.581
.016	.285	.475	.744	.422	.593

Figure (6)

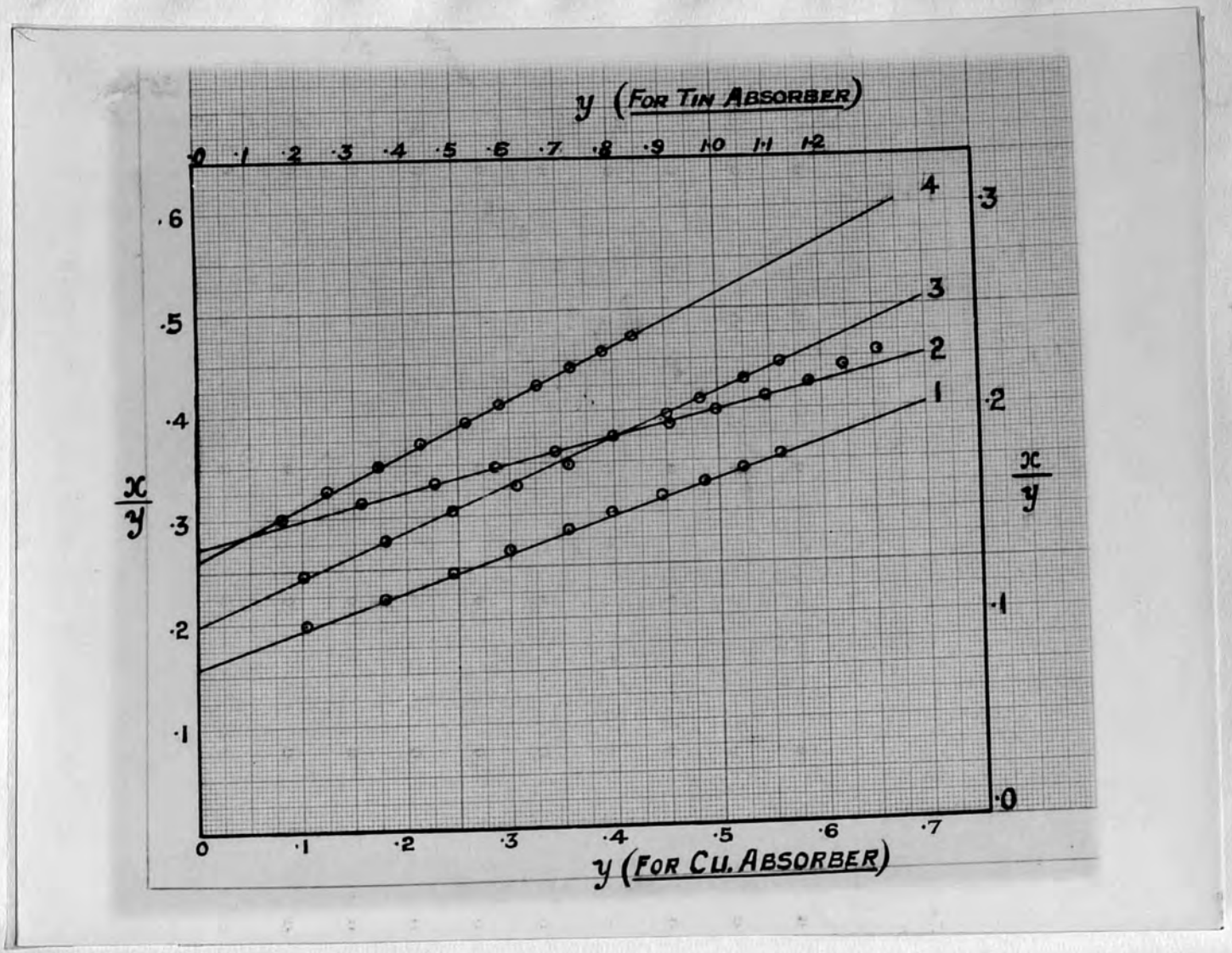
y (For Tin Absorber)
0 ·1 ·2 ·3 ·4 ·5 ·6 ·7 ·8 ·9 1·0 1·1 1·2
·6
·5
·4
·3
·2
·1
x/y
4
3
2
1
·3
·2
·1
·0
x/y
0 ·1 ·2 ·3 ·4 ·5 ·6 ·7
y (For Cu. Absorber)

cont.

P = 30%

$.3((1-q)e^{\mu_\alpha x} + q\,e^{\mu_\beta x})$	$\frac{I_x}{I_o} - .3(\ )$	$\frac{1}{.7}\left\{\frac{I_x}{I_o} - \ldots\right\}$	$-\log_e \frac{1}{.7}\left\{\frac{I_x}{I_o} - \ldots\right\}$	$y_{.3}$	$\frac{x}{y_{.3}}$
.215	.613	.875	$.133_5$	$.101_5$	.246
.155	.548	.783	.244	.180	.278
.112	.498	.711	.341	.244	.307
.080	.453	.647	.435	.306	.327
.059	.416	.594	.521	.360	.347
.042	.386	.551	.596	.402	.373
.031	.357	.510	.672	.446	.392
.023	.333	.476	.742	.484	.413
.017	.310	.443	.815	.525	.430
.012	.289	.413	.884	.562	.445

fig (6): line (3) for Cu absorbers corresponding to the above table and line (1) when tin absorber was used.

Figure(7)

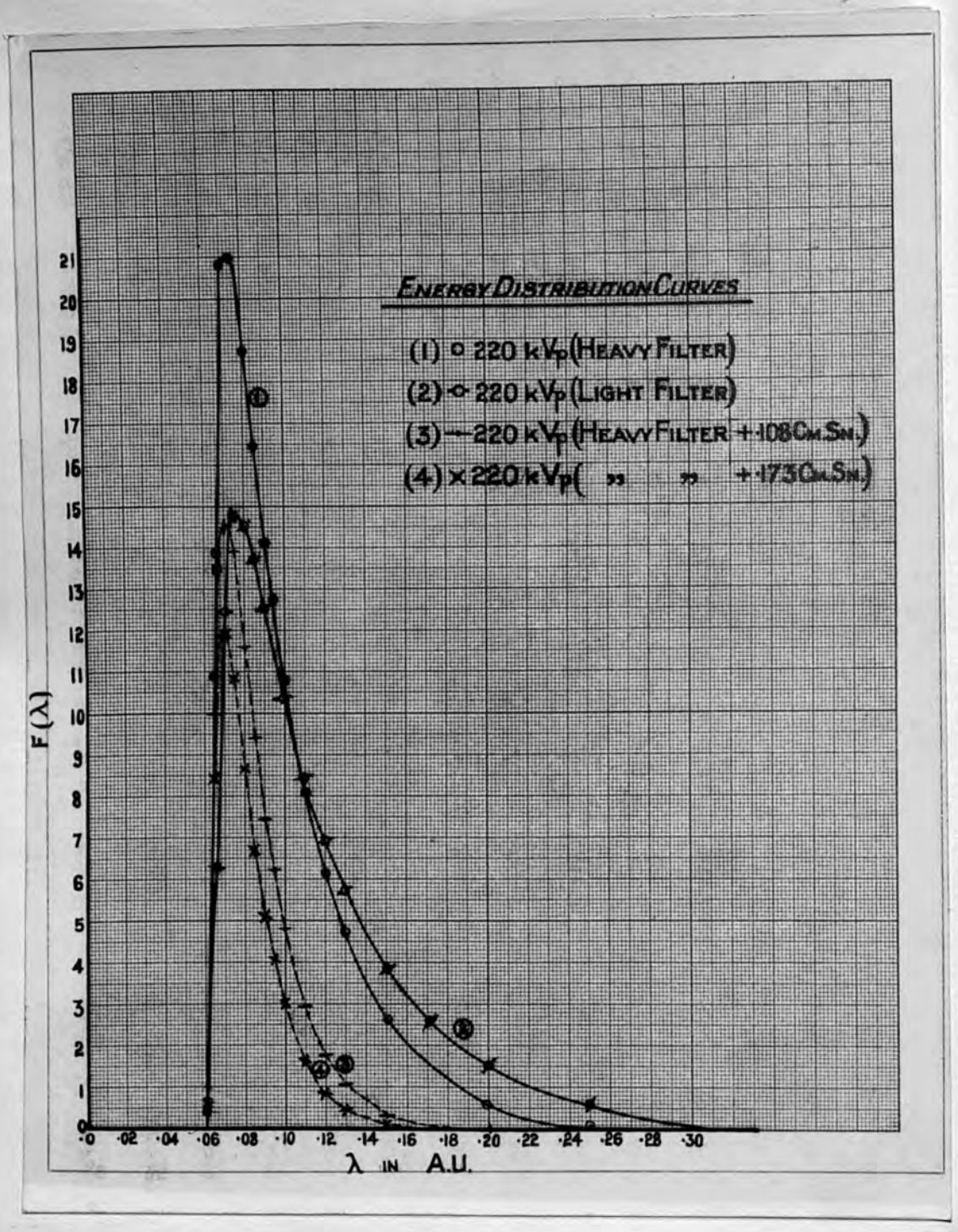
ENERGY DISTRIBUTION CURVES
(1) ○ 220 kVp (HEAVY FILTER)
(2) ○ 220 kVp (LIGHT FILTER)
(3) — 220 kVp (HEAVY FILTER + 108 CM. SN.)
(4) × 220 kVp (» » + 173 CM. SN.)
F(λ)
λ IN A.U.
0 1 2 3 4 5 6 7 8 9 10 11 12 13 14 15 16 17 18 19 20 21
·0 ·02 ·04 ·06 ·08 ·10 ·12 ·14 ·16 ·18 ·20 ·22 ·24 ·26 ·28 ·30

Evaluation of $f(\lambda)$ for 220 kVp with light filter (Fig.(7)No.2.)

Constants for Cu: c=0.20 B)=1.36 d= .026
and for tin: c= .088 B -3.41 d= .019

λ in A.U.	μ	$\mu - A$	$(\mu-A)d$	$B^2/4(\mu-A)$	$\frac{B^2}{4(\mu-A)}+(\mu-A)_2$	$e^{[\ ]}$	$(\mu-A)^{\frac{3}{2}}$	$\frac{d\mu}{d\lambda}$	$f(\lambda)_{Cu.}$	$f(\lambda)_{tin}$	$f(\lambda)_{mean}$
.06	1.38	.08	—	7.20	7.20	.0007	.0226	23.1	—	—	0.38
.065	1.5	.20	.005	2.89	2.90	.055	.0898	25.5	8.40	4.09	6.25
.07	1.63	.33	.008	1.75	1.76	.172	.190	27.8	13.60	11.30	12.42
.075	1.77	.47	.011	1.23	1.24	.289	.322	30.7	0.85	14.7	14.78
.08	1.94	.64	.015	.904	.919	.399	.511	33.7	0.20	14.9	14.56
.085	2.11	.81	.019	.714	.733	.481	.729	37.0	0.20	14.3	13.77
.09	2.31	1.01	.023	.572	.595	.551	1.015	40.4	11.85	13.17	12.51
.10	2.74	1.44	.033	.402	.435	.647	1.73	48.20	9.70	11.08	10.39
.11	3.30	2.00	.046	.289	.335	.715	2.83	57.00	7.80	9.16	8.48
.12	3.90	2.60	.060	.222	.282	.754	4.20	67.00	6.50	7.40	6.95
.13	4.62	3.32	.076	.174	.250	.779	6.03	77.00	5.40	6.16	5.78
.15	6.50	5.20	.120	.111	.231	.794	11.85	99.00	3.60	4.15	3.87
.17	8.80	7.5	.172	.077	.249	.780	20.50	123.0	2.50	2.68	2.59
.20	12.90	11.6	.267	.050	.317	.729	39.40	164.0	1.60	1.43	1.53
.25	23.00	21.7	.498	.027	.525	.592	100.4	250.0	0.80	0.46	0.63

λe for 220 kVp with light filter

λ in A.U.	$f(\lambda)$	$d\lambda$	$A_1 = f(\lambda)_1 d\lambda_1$	$\lambda_{mean} A_1$
.0635	4.4	.009	$.039_6$	.0025
.072	13.8	.008	$.110_4$	.0079
.08	14.52	.008	.1162	.0093
.088	13.15	.008	$.105_2$	.0093
.096	11.2	.008	.09	.0086
.104	9.5	.008	.076	.0079
.112	8.1	.008	.0648	.0073
.122	6.74	.012	.0809	.0091
.134	5.3	.012	.0636	,0085
.148	4.02	.016	.0643	.0095
.166	2.8	.02	.056	.0093
.183 K_β	—	—	.1259	.023
.188	1.9	.024	.0456	.0086
.21 K_α	—	—	$.293_4$	.0616
.214	1.22	.028	.0341	.0073
.244	.7	.037	$.022_4$	.0055
.284	.2	.05	.01	.0028

Total area under the curve $A = \Sigma A_1 =$ 1.398

$\Sigma \lambda_{mean} A_1 =$ .198

$\lambda e = .198/1.398 =$ .142 A.U.

Exciting voltage = 220 kV p.

Primary filter = (0.5 Cu. + .66 Sn. + 1 mm. Al.)

$$\lambda_0 = \frac{12.35}{220} = .0562 \text{ A.U.}$$

$$A = \mu_0 = 1.30 \text{ cm}^{-1}$$ (from Greening's tables)

Fig. (5) shows the absorption curves.
Curve (2) for tin filters and (3) for cu. filters.

x in cm. Cu.	$\frac{I_x}{I_0}$	$\log \frac{I_x}{I_0} \times 100$
.0287	.920	1.964
.080	.790	1.898
.132	.688	1.838
.191	.582	1.765
.243	$.522_5$	1.718
.306	.452	1.655
.358	.396	1.598
.421	.343	1.535
.473	.304	1.483
.519	.281	1.449
.634	.225	1.352

cont.

The following values of I_x / I_o and x are taken from the transmission curve after smoothing.

x cm. Cu.	μx	$\log_e I_x/I_o$	y	x/y
.05	.65	-.145	.080	.625
.10	.130	-.288	.158	.632
.15	.195	-.421	.226	.663
.20	.260	-.548	.288	.694
.25	.325	-.671	.346	.723
.30	.390	-.791	.401	.747
.35	.455	-.908	.453	.772
.40	.520	-1.021	.501	.798
.45	.585	-1.131	.546	.824
.50	.650	-1.233	.583	.856
.55	.715	-1.337	.622	.884
.60	.780	-1.435	.655	.915

Fig (6): shows line (2) for Cu absorber corresponding to the above table and line (4) when tin absorbers are used.

Evaluation of $f(\lambda) \equiv I_\lambda$ for 220 kVp Heavy filter (fig.(7)No.1)

Constants for Cu: c= 0.546 B=1.43 and d=0.157
and for Tin: c= 0.130 B=2.82 and d=0.034

λ in A.U.	μ	$\mu - A$	$(\mu - A)d$	$B^2/4(\mu - A)$	$\frac{B^2}{4(\mu-A)} + (\mu - A)d$	$e^{[\ ]}$	$(\mu - A)^{\frac{3}{2}}$	$\frac{d\mu}{d\lambda}$	$f(\lambda)_{Cu.}$	$f(\lambda)_{tin}$	$f(\lambda)_{mea}$
.06	1.38	.08	.010	6.39	6.40	.0017	.0226	23.1	1.24	.56	0.90
.065	1.50	.20	.030	2.56	2.59	.075	.090	25.5	15.2	13.6	13.9
.07	1.63	.33	.050	1.55	1.60	.202	.190	27.8	21.1	20.6	20.85
.075	1.77	.47	.070	1.09	1.16	.313	.322	30.7	21.3	20.7	21
.08	1.94	.64	.100	.799	.899	.407	.511	33.7	19.15	18.4	18.77
.085	2.11	.81	.127	.631	.758	.469	.729	37.0	16.95	15.95	16.45
.09	2.31	1.01	.158	.506	.664	.515	1.015	40.4	14.6	13.65	14.12
.095	2.51	1.21	.190	.422	.612	.542	1.33	44.2	12.8	12.80	12.80
.10	2.74	1.44	.226	.355	.581	.559	1.73	48.2	11.1	10.50	10.80
.11	3.30	2.00	.314	.256	.570	.566	2.83	57.0	8.1	8.10	8.10
.12	3.90	2.60	.407	.1965	.604	.547	4.2	67.0	6.21	6.15	6.18
.13	4.62	3.32	.521	.154	.675	.509	6.07	77.0	4.6	4.85	4.72
.15	6.50	5.2	.815	.098	.913	.401	11.85	99.0	2.38	2.9	2.64
.2	12.9	11.6	1.82	.044	1.86	.156	39.40	164.0	0.46	0.70	0.58
.25	23.0	21.7	3.40	.024	3.42	.0328	100.4	250.0	0.06	1.3	0.095

λe for 220 kVp with heavy filter

λ in A.U.	$f(\lambda)$	$d\lambda$	$A_1 = f(\lambda)d\lambda$	$\lambda_{mean} A_1$
.064	9.20	.008	.0736	.0047
.072	21.05	.008	$.168_4$	.0127
.08	18.80	.008	.150	.0121
.088	14.90	.008	$.119_2$	.0105
.096	11.70	.008	.0936	.009
.104	9.30	.008	$.074_4$	$.007_8$
.114	7.25	.012	.087	$.009_9$
.128	4.80	.016	$.076_8$	.0098
.146	3.00	.020	.060	.0088
.168	1.75	.024	.042	.0071
.196	.75	.032	.024	.0047
.24	.10	.056	$.005_6$	.0013

Total area under the curve $A = \Sigma A_1 = .975$

$$\Sigma \lambda_{mean} A_1 = .0984$$

$$= \frac{.0984}{.975} = 0.101$$

The following tables give the data deduced from the table on page (47) when extra thicknesses of tin were added to the primary filter. Each $f(\lambda)$ will be reduced to

$$f(\lambda)\, e^{-\mu' x'} = f'(\lambda)$$

where μ' is the absorption coefficient of tin and x' is the thickness of tin added to the primary filter.

Energy distribution curves were drawn for $f'(\lambda)$ against λ . From those curves and in the same manner as described before on page (28) λ_e was calculated.

Fig.(7). Curves (3) & (4)

λ in A.U.	μ'_{tin}	$f(\lambda)$	$\mu' x' = .108\mu'$	$e^{-.108\mu'}$	$f(\lambda') = f(\lambda) e^{-.108\mu'}$	$\mu' x' = .173\mu'$	$e^{-.173\mu'}$	$f'(\lambda) = f(\lambda) e^{-.173\mu'}$
.06	2.27	0.9	.245	.783	.704	.392	.675	.608
.065	2.71	13.5	.293	.746	10.09	.468	.626	8.45
.07	3.21	20.85	.346	.707	14.75	.555	.574	11.97
.075	3.81	21.00	.411	.663	13.92	.658	.518	10.87
.08	4.46	18.77	.481	.618	11.61	.770	.463	8.68
.085	5.16	16.45	.557	.573	9.42	.892	.410	6.73
.09	5.91	14.12	.638	.528	7.46	1.02	.361	5.10
.095	6.66	12.80	.719	.487	6.24	1.15	.316	4.05
.10	7.42	10.80	.81	.445	4.8	1.28	.277	3.00
.11	9.35	8.10	1.01	.364	2.95	1.62	.199	1.61
.12	11.6	6.18	1.25	.286	1.77	2.005	.135	.833
.13	14.0	4.73	1.51	.221	1.045	2,42	.089	.419
.15	20.1	2.64	2.17	.114	3.02	3.47	.031	.082
.20	42.0	0.58	4.54	.0111	.0064	7.26	.0007	.00041
.25	77.0	0.095	8.31	.0002	.00019	13.30	—	—

λ_e for 220 kVp

Primary filter = (.5 mm.Cu + .66 mm.Sn + 1 mm.Al) + .108 cm Sn

λ_{mean}	$f(\lambda)_{mean}$	$d\lambda$	$A_1 = f(\lambda)_1 d\lambda_1$	$\lambda_{mean} A_1$
.062	7.6	.004	$.018_4$	.0011
.066	10.9	.004	$.043_6$	.0029
.07	14.76	.004	.0590	.0041
.075	13.92	.004	$.055_7$	.0042
.08	11.61	.008	$.092_9$	.0074
.088	8.2	.008	$.065_6$	.0058
.097	5.5	.01	.055	.0053
.107	3.4	.01	.034	.0036
.117	2.08	.01	$.020_8$	.0024
.127	1.24	.01	$.012_4$	.0016
.138	.62	.012	.007	$.0010_3$
.152	.24	.016	.0038	$.0005_8$
.17	.12	.02	.002	.00041
.08	.195	.03	.0058	.00047

$$\lambda_e = \frac{\Sigma \lambda_{mean} A_1}{\Sigma A_1}$$

$$= \frac{.041}{.4769} = .086$$

λ_e for 220 kVp

Primary filter = (.5 mm.Cu + .66 mm.Sn + 1 mm. Al + .173 Cm.Sn)

λ_{mean}	$f(\lambda)_{mean}$	$d\lambda$	$A_1 = f(\lambda_1) d\lambda_1$	$\lambda_{mean} A_1$
.062	4.75	.004	.019	.00118
.066	9.45	.004	.0378	.0025
.07	11.97	.004	.0479	.00335
.074	11.25	.004	.0450	.00333
.078	9.4	.004	.0376	.00293
.084	7.05	.008	.0564	.00474
.093	4.5	.01	.045	.00418
.104	2.33	.012	.028	.0029
.117	1.02	.014	.0143	.00167
.132	0.38	.016	.0061	.0008
.16	0.05	.040	.002	.0003

$$\lambda_e = \frac{.02789}{.3391} = .0822_5$$

The following table summarizes the results obtained in the above tables.

kVp	Added filter	H.V.L.	λ_e from H.V.L.	λ_e from energy distribution curve
90	2 mm. Al.	.075 mm. Cu.	.405	.417
150	zero	5.0 mm. Al.	.288	.287
170	zero	6.0 mm. Al.	.269	.256
220	.5 mm. Cu. + 1 mm. Al.	1.14 mm. Cu.	.143	.142
220	.5 mm. Cu. + 66 mm. Sn. + 1 mm. Al.	2.59 mm. Cu.	.098	.101
220	.5 mm. Cu. + 1.74 mm. Sn. + 1mm. Al.	3.085 mm. Cu.	.088	.086
220	.5 mm. Cu. + 2.39 mm. Sn. + 1mm. Al.	—	—	.082

C - Measurement of the Half Value Layer (H.V.L.) and Determination of the Corresponding Effective Wavelength

As a result of the previous calculations (table p. 53) it was seen to be sufficiently accurate for our purpose to use the value of λe determined from the measurement of the H.V.L. of the beam.

The H.V.L.'s of a number of beams covering a comparatively wide range of wavelengths were measured. From these beams the qualities required for these investigations were chosen.

i. Experimental method

The method adopted consists in the direct measurement of the ratio of the intensity of the beam before and after it passes through each filter.

The apparatus described later on page (116) fig. (34) was also used for the measurement of the H.V.L.s; indeed it is eminently suitable for this purpose.

Two of the "air wall" chambers which had been tested for wavelength independence were mounted on the apparatus and set up in the beam. A thick lead diaphragm with two circular holes was used to define the beams falling on the

Figure(8)

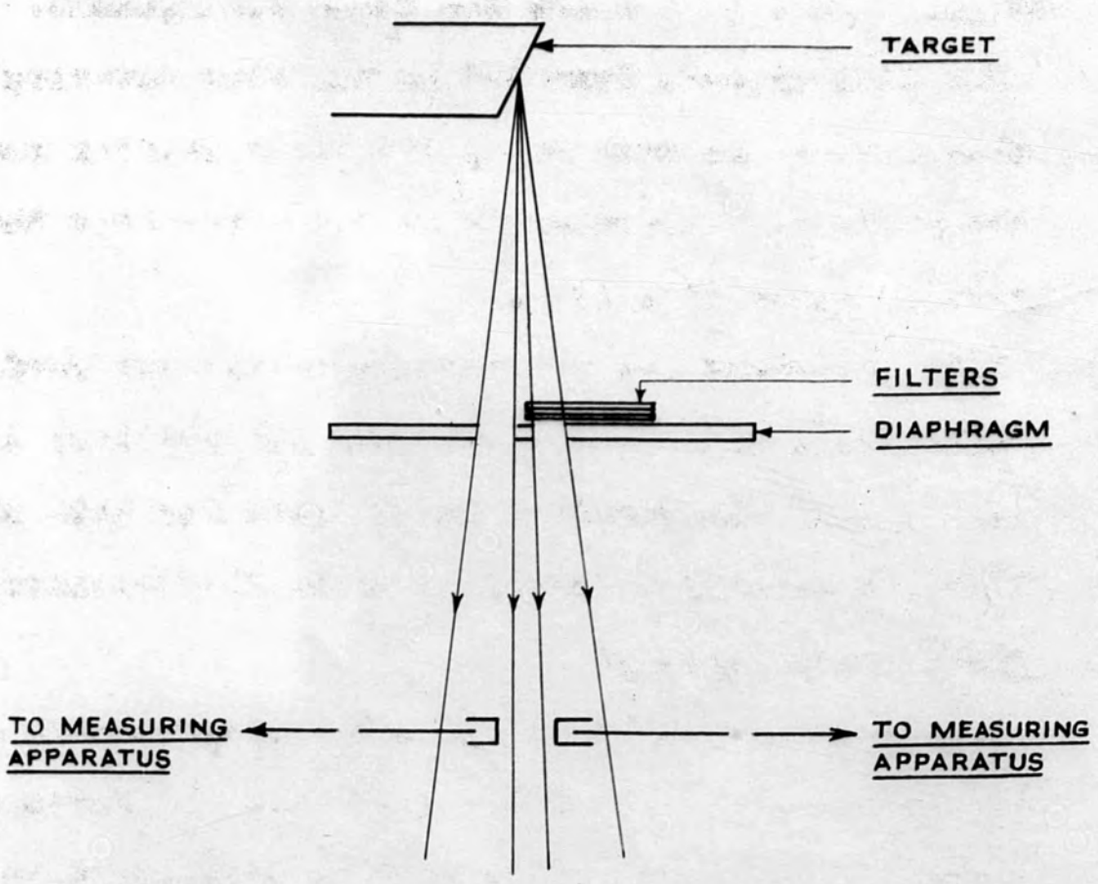

EXPERIMENTAL ARRANGEMENT FOR MEASUREMENT OF THE H. V. L's

chambers. Fig. (8) shows the whole arrangement.

The filters were inserted in the beam covering one of the chambers and in each case, the scale reading was noted and the ratio corresponding to it was taken from the calibration curve fig. (40).

This procedure has the advantage that the reading of the scale (i.e. the ratio of the two intensities) is not affected by any fluctuations in the beam for both the chambers are equally affected by these fluctuations.

ii. Experimental results

The following tables contain the observations and the results obtained. Figs. (9) and (11) show the ratio against thickness of filter and marks on them correspond to the number of table they represent. Figs. (10) and (12) are the absorption curves for tables from 1 to 11.

The ratio of the intensities at the two chambers before the insertion of any filters is taken as unity and the other values are expressed in terms of this.

Intensity Ratio Curves in AL.

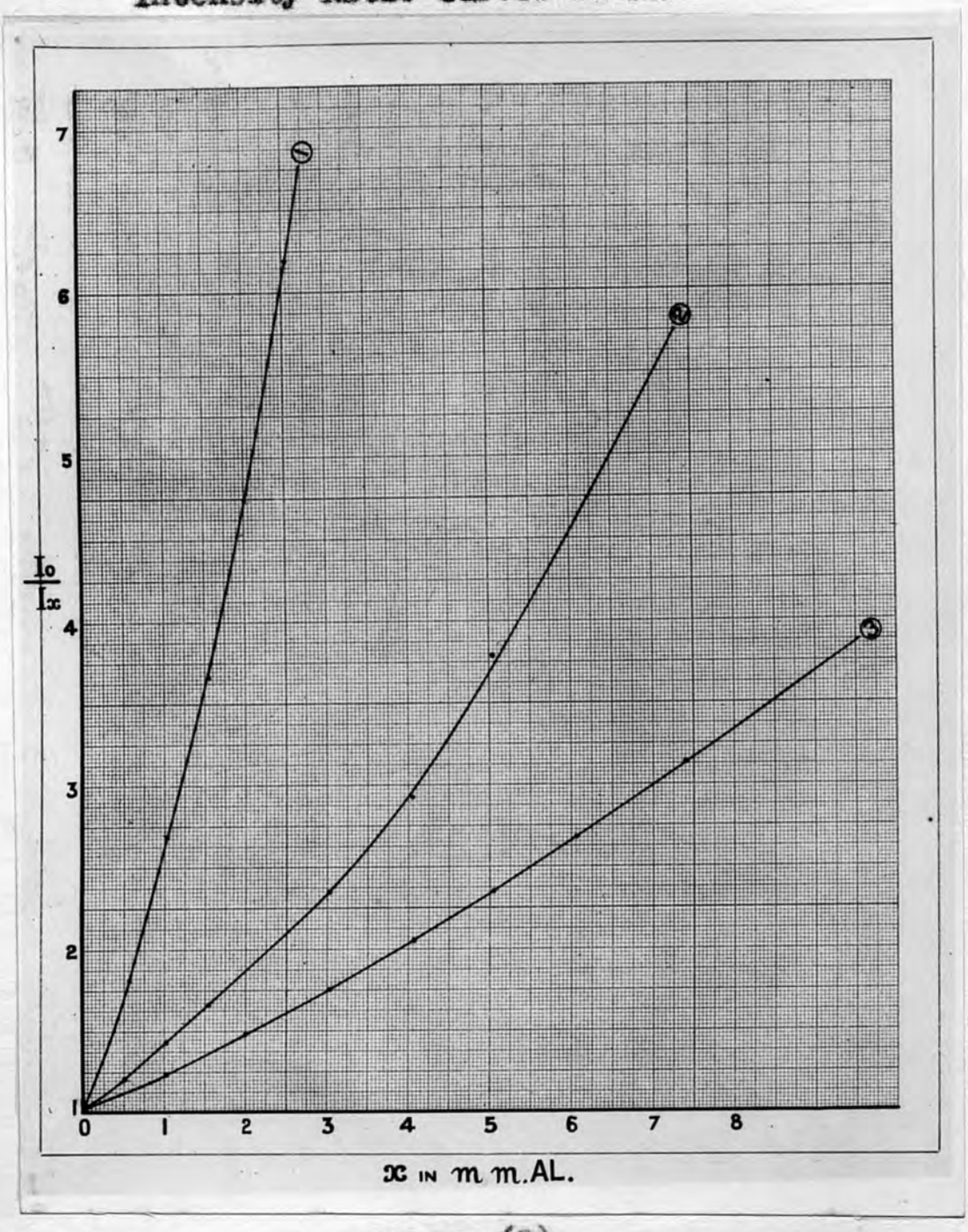

Figure(9)

Beams from the medium voltage machine (60 - 110 kVp)

1. The exciting voltage = 60 kVp (no added filter)

Thickness x in mm. Al.	0	.515	1.025	1.540	2.005	2.53
Ratio $\frac{I_o}{I_x}$	1.02	1.82	2.73	3.668	4.74	6.20
$\frac{I_x}{I_o}$	1	.567	.374	.278	.215	.165
$\log_{10}\left(\frac{I_x}{I_o} \times 100\right)$	2	1.753	1.573	1.444	1.332	1.216

2. The exciting voltage = 90 kVp primary filter 2mm. Al.

Thickness x in mm. Al.	0	.515	1.025	1.540	3.035	4.060	5.040	7.310
$\frac{I_o}{I_x}$	1.026	1.200	1.426	1.660	2.346	2.927	3.796	5.750
$\frac{I_x}{I_o}$	1	.855	.719	.618	.437	.350	.270	.178
$\log_{10}\left(\frac{I_x}{I_o} \times 100\right)$	2	1.932	1.857	1.791	1.641	1.544	1.431	1.251

Absorption Curves in AL.

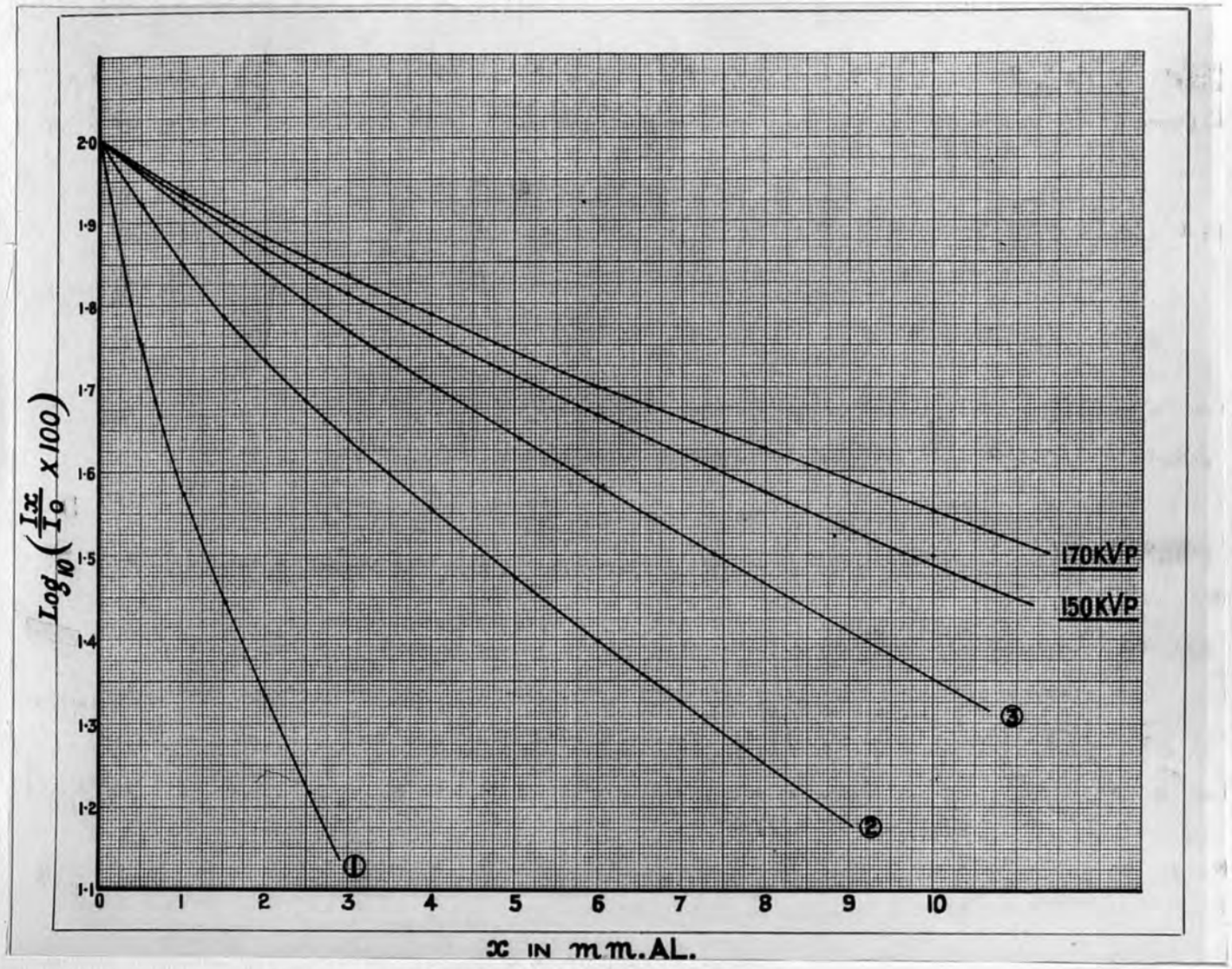

Figure (IO)

3. The exciting voltage = 106.8 kVp Primary filter 4mm. Al.

Thickness x in mm. Al.	0	1.025	2.005	3.035	4.061	5.040	6.065	7.410
$\frac{I_o}{I_x}$	1.026	1.236	1.485	1.755	2.050	2.350	2.670	3.130
$\frac{I_x}{I_o}$	1	.830	.690	.584	.500	.436	.384	.328
$\log_{10}\left(\frac{I_x}{I_o}\times 100\right)$	2	1.919	1.839	1.766	1.699	1.640	1.584	1.515

Beams from the Westinghouse set

4. The exciting voltage = 120 kVp Primary filter (.11 mm.Cu+1mm. Al)

Thickness x in mm. Cu	0	$.143_5$	.287	$.430_5$	.574	$.717_5$	.861	
$\frac{I_o}{I_x}$	1.05	1.475	1.886	2.265	2.750	3.320	3.750	

Intensity Ratio Curves in Cu.

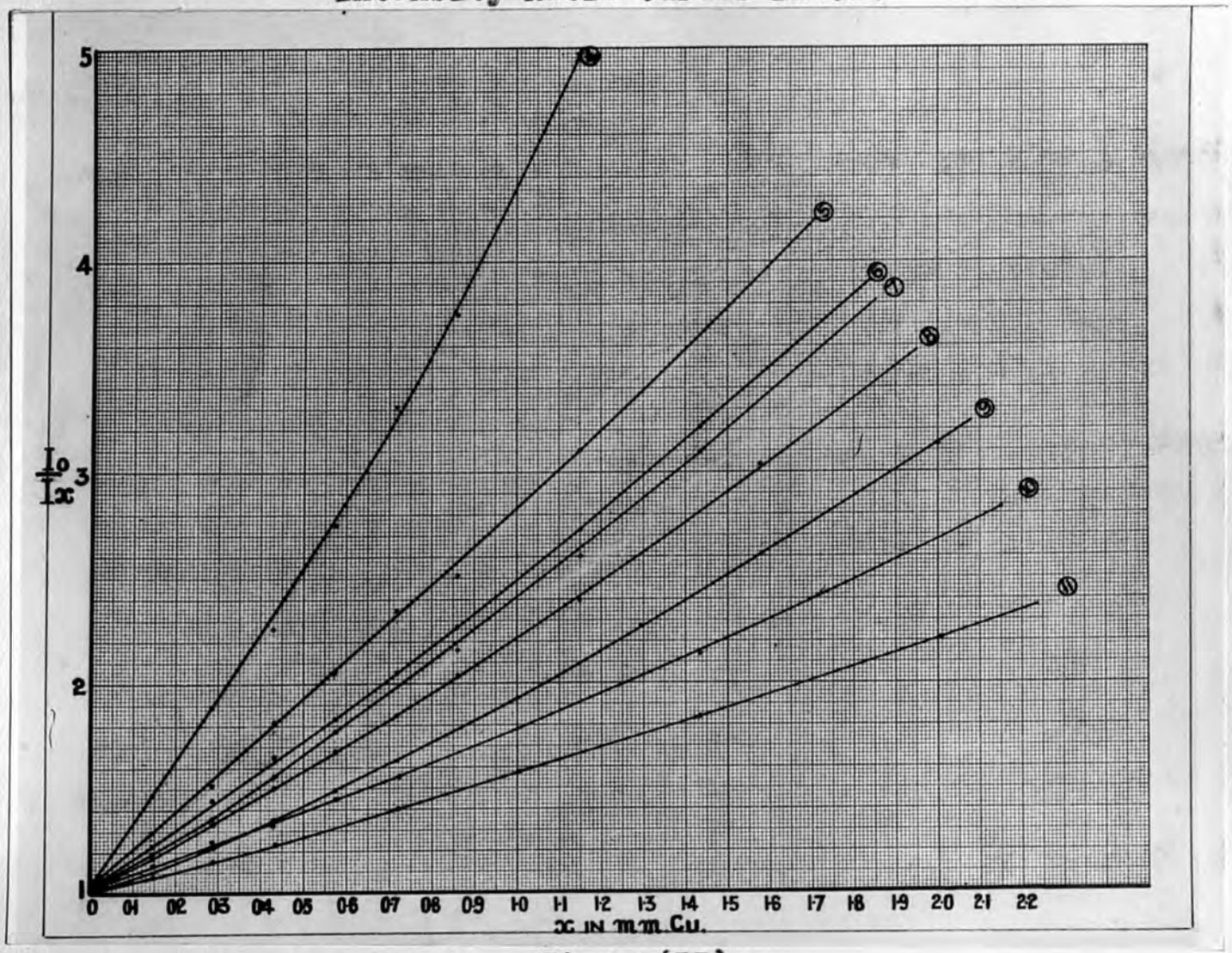

Figure (II)

The following values of x ψ $\frac{I_o}{I_x}$ are taken from the smooth curve

x in mm. Cu.	0	0.1	0.2	0.3	0.4	0.5	0.6	0.7	0.9
$\frac{I_o}{I_x}$	1.05	1.34	1.63	1.93	2.23	2.54	2.86	3.19	3.95
$\frac{I_x}{I_o}$	1	.783	.644	.544	.471	.413	$.366_6$	.329	.266
$\log_{10}\left(\frac{I_x}{I_o}\times 100\right)$	2	1.894	1.809	1.736	1.673	1.616	1.564	1.517	1.425

5. The exciting voltage = 120 kVp Primary filter (.5mm.Cu+1mm. Al.)

Thickness in mm.Cu.	0	0.143_5	.287	$.430_5$	.547	$.717_5$	.861	1.14_8
$\frac{I_o}{I_x}$	1.05	1.294	1.51	1.81_5	2.05	2.35	2.51	3.1

The following values of x ψ $\frac{I_o}{I_x}$ are taken from the smooth curve

x in mm Cu.	0	0.1	0.2	0.3	0.4	0.5	0.6	0.7	0.8	1.0	1.15
I_o/I_x	1.05	1.21_5	1.39_2	1.57	1.75	1.93_2	2.11_9	2.29_2	2.47	2.82	3.1
I_x/I_o	1	.865	.754	.668	.60	.543	.496	.458	.425	.372	.339
$\log_{10}\left(\frac{I_x}{I_o}\times 100\right)$	2	1.937	1.877	1.825	1.778	1.735	1.696	1.661	1.628	1.571	1.53

6. The exciting voltage = 180 kVp Primary Filter (.214 mm. Cu+1 mm. Al.)

Thickness in mm. Cu.	0	.143$_5$	.287	.430$_5$	.574	.717$_5$	.861	1.148	1.435
	1.02	1.225	1.44$_5$	1.65	1.83$_3$	2.06	2.27$_3$	2.72	3.22

The following values of x & $\frac{I_o}{I_x}$ are taken from the smooth curve

x mm.Cu.	0.0	0.1	0.2	0.3	0.4	0.5	0.6	0.7	0.9	1.10	1.40
$\frac{I_o}{I_x}$	1.02	1.16	1.3	1.43$_1$	1.57$_5$	1.72	1.865	2.013	2.33	2.64$_5$	3.15
$\frac{I_x}{I_o}$	1	.879	.785	.713	.648	.593	.547	.507	.438	.386	.324
$\log_{10}\left(\frac{I_x}{I_o}\times 100\right)$	2	1.944	1.895	1.853	1.812	1.773	1.738	1.705	1.641	1.587	1.51

7. The exciting voltage = 150 kVp Primary filter (.5 mm. Cu+1 mm. Al;)

Thickness x in mm. Cu	0	.143$_5$	.287	.430$_5$	.574	.861	1.148	1.435
Ratio $\frac{I_o}{I_x}$	1.04	1.19	1.36	1.56	1.78	2.16	2.60	3.096

Absorption Curves in Cu.

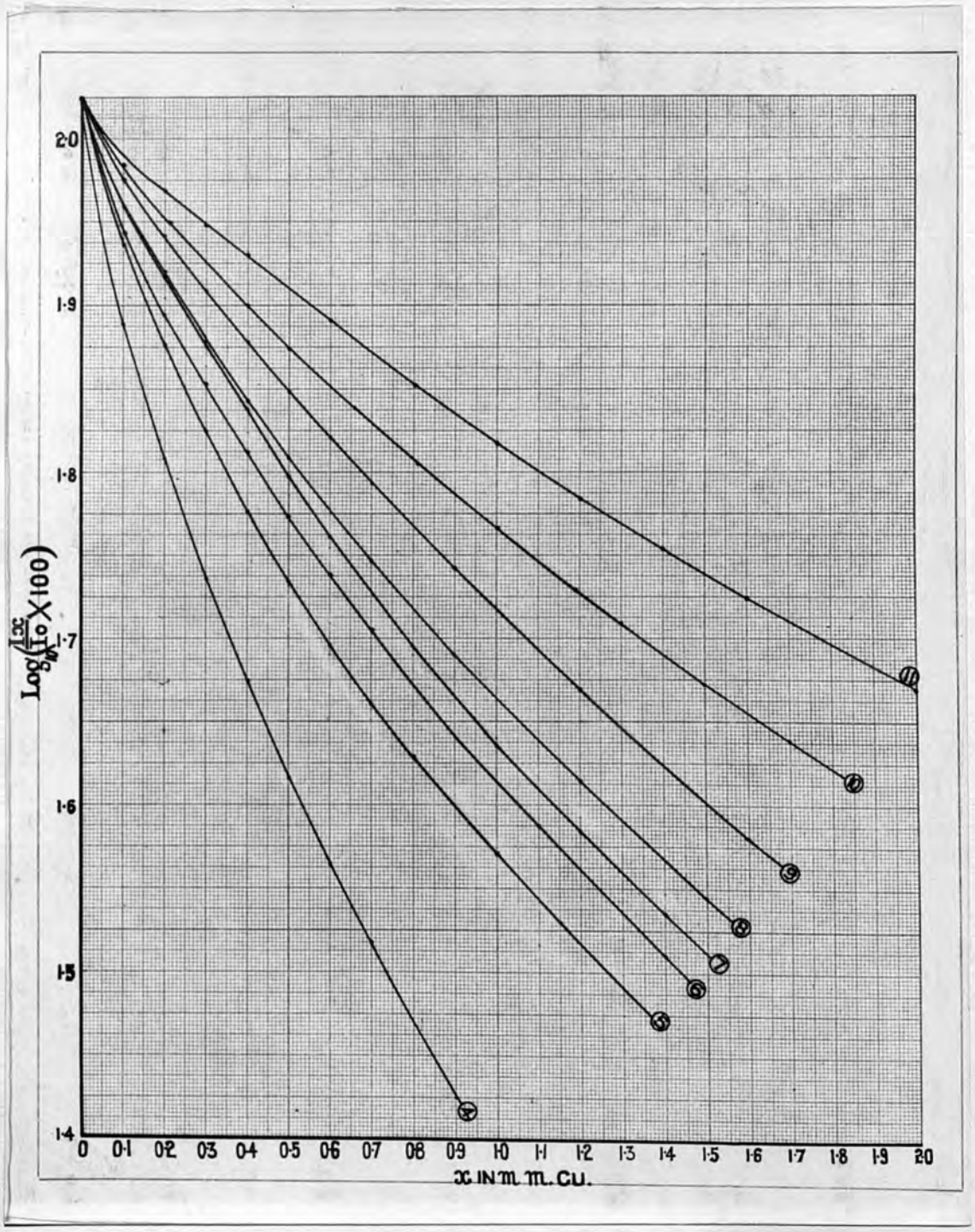

Figure(12)

The following values of x vs $\frac{I_o}{I_x}$ are taken from the smooth curve

x in mm Cu.	0	0.1	0.2	0.3	0.4	0.5	0.6	0.8	1.0	1.2	1.4
I_o/I_x	1.04	1.14	1.25	1.37	1.51	1.66	1.805	2.10	2.406	2.71	3.032
I_x/I_o	1	.912	.832	.756	.689	.626	.577	.495	.432	.384	.343
$\log_{10}\left(\frac{I_x}{I_o}\times 100\right)$	2	1.960	1.920	1.879	1.838	1.797	1.761	1.695	1.636	1.584	1.535

8. The exciting voltage = 170 kVp Primary filter (.5 mm.Cu 1mm.Al..)

Thickness x in mm. Cu	0	.143	.287	.430	.574	.717	.861	1.148	1.58
I_o/I_x	1.02	1.18	1.34	1.50	1.68	1.84	2.04	2.39	3.04

The following values of x vs $\frac{I_o}{I_x}$ are taken from the smooth curve

x in cm.	0	0.1	0.2	0.3	0.4	0.5	0.7	0.9	1.2	1.5
I_o/I_x	1.02	1.126	1.23	1.35	1.46	1.59	1.825	2.08	2.48	2.905
I_x/I_o	1	.907	.826	.756	.627	.642	.5587	.49	.411	.351
$\log_{10}\left(\frac{I_x}{I_o}\times 100\right)$	2	1.958	1.917	1.879	1.843	1.808	1.747	1.690	1.614	1.545

9. The exciting voltage = 200 kVp Primary filter (.5 mm. Cu+1 mm. Al.)

Thickness in mm. Cu x	0	.143	.287	.430	.574	.717	1.00	1.292	1.579	2.009
Ratio I_o/I_x	1.	1.07	1.22	1.325	1.496	1.63	1.93	2.20	2.61	3.13

The following values of x are taken from the smooth curve

x in mm. Cu.	0	0.10	0.2	0.3	0.4	0.5	0.6	0.7	0.9	1.2	1.6
I_o/I_x	1	1.065	1.146	1.234	1.32	1.42	1.51	1.61	1.812	2.15	2.632
I_x/I_o	1.	.94	.874	.81	.755	.704	.662	.6215	.552	.465	.38
$\log_{10}\left(\frac{I_x}{I_o}\times 100\right)$	2	1.973	1.942	1.909	1.878	1.848	1.821	1.793	1.742	1.668	1.58

10. The exciting voltage=180 kVp Primary filter (1.5 mm.Cu+1 mm. Al.)

Thickness x in mm. Cu	0	.143	.287	.430	.574	.717	1.005	1.43	1.722	2.152
I_o/I_x	1.04	1.15	1.256	1.35	1.453	1.56	1.78	2.13	2.42	2.82

The following values of x taken from the smooth curve

x in mm. Cu.	0	0.1	0.21	0.4	0.5	0.66	0.81	1.0	1.19	1.3	1.5	1.7
I_o/I_x	1.04	1.092	1.17	1.31	1.39	1.51	1.63	1.78	1.942	2.035	2.212	2.395
I_x/I_o	1	.952	.889	.794	.748	.6887	.638	.5834	.535	.512	.47	.434
$\log_{10}\left(\frac{I_x}{I_o}\times 100\right)$	2	1.979	1.949	1.9	1.874	1.838	1.805	1.766	1.728	1.709	1.672	1.638

11. The exciting voltage = 200kVp Primary filter (1.5 mm.Cu + 1mm.Al.)

Thickness x in mm. Cu	0	.143	.287	.430	.717	1.005	1.435	2.009
I_o/I_x	1.03	1.09	1.16	1.237	1.40	1.585	1.834	2.21

The following values of x are taken from the smooth curve

x in mm. Cu.	0	0.1	0.2	0.3	0.4	0.6	0.8	1.0	1.2	1.4	1.6	2.0
I_o/I_x	1.03	1.06	1.107	1.16	1.207	1.326	1.45	1.57	1.69	1.82	1.946	2.20
I_x/I_o	1	.967	.93	.888	.854	.777	.71	.656	.61	.566	.53	.466
$\log_{10}\left(\frac{I_x}{I_o}\times 100\right)$	2	1.985	1.969	1.948	1.932	1.891	1.851	1.817	1.785	1.753	1.724	1.668

H.V.L. in Cu.

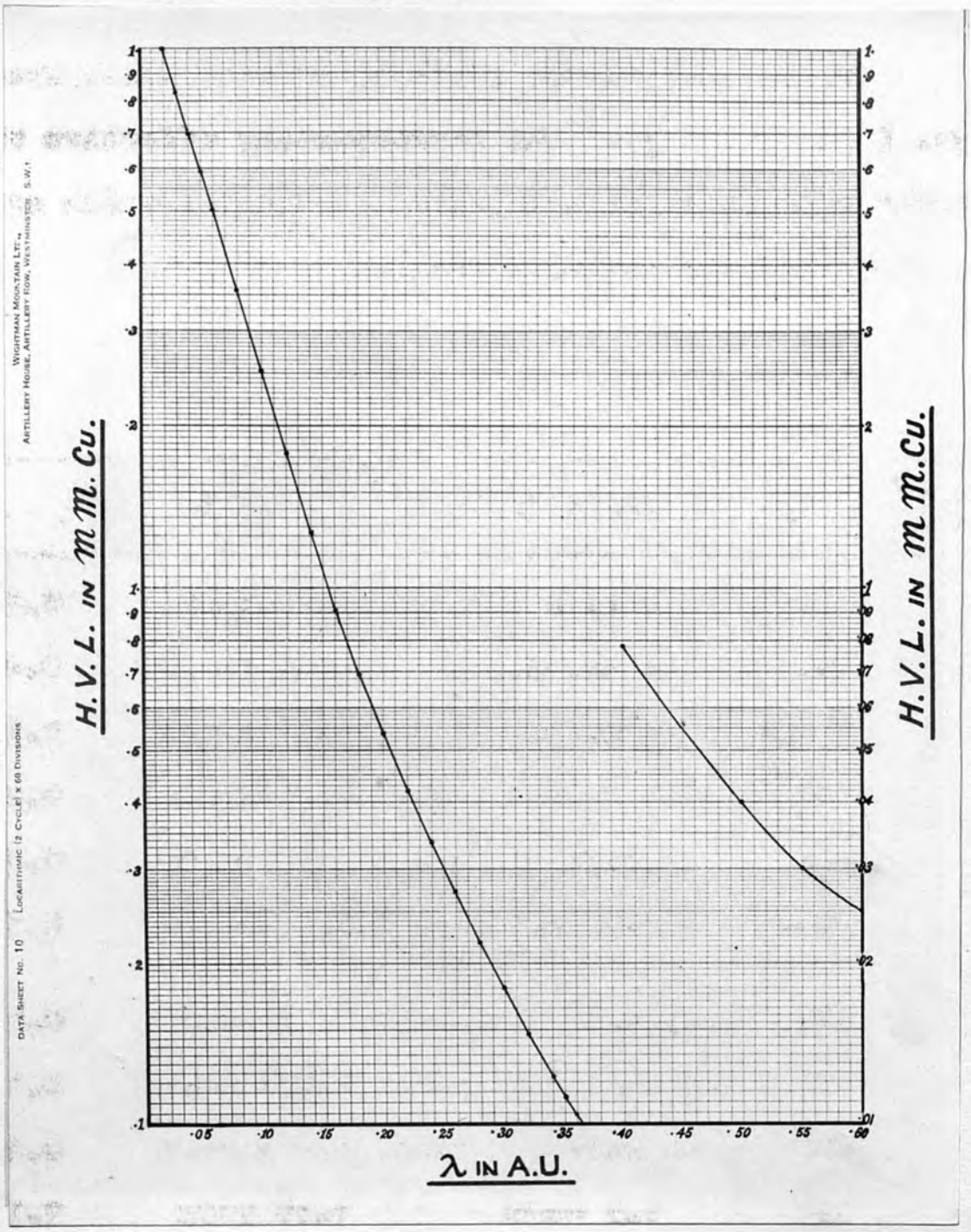

Figure (I4)

The H.V.L.'s of the above beams were taken from figs. (10 & 12) . The corresponding effective wavelengths were taken from figs. (13 & 14) which are calculated from Greening's tables.

No. of table	kVp	Added filter	H.V.L	λ_e in A.U.
1	60	zero	0.7 mm.Al.	0.630
2.	90	2 mm. Al.	2.4 mm.Al.	0.402
3	106.8	4 mm.Al.	4.06 mm.Al.	0.322
4	120	.11 mmCu + 1 mmAl.	0.356mm.Cu.	0.236
5	120	.5 mmCu + 1 mmAl.	0.591mm.Cu.	0.192
6	180	+ .214 mmCu + 1 mm.Al	0.716mm.Cu.	0.177
7	150	.5 mmCu + 1 mmAl.	0.78 mmCu.	0.172
8	170	.5 mmCu + 1 mmAl.	0.875 mmCu.	0.163
9	200	.5 mmCu + 1 mmAl.	1.072 mmCu.	0.150
10	180	1.5 mmCu. + + 1.mm. Al.	1.35 mmCu.	0.137
11	200	1.5 mmCu + 1 mm.Al.	1.77 mmCu.	0.120

III

THEORETICAL DETERMINATION OF THE RATIO OF THE IONIZATION CURRENTS IN CHAMBER PAIRS OF DIFFERENT MATERIALS ACCORDING TO THE THEORY OF BRAGG AND GRAY.

(a) Introduction

The theory of the ionization produced by x-rays in an air filled cavity was first studied by Bragg.(3) In the course of this study of the problem he arrived at the result that the total length of the tracks of the β-particles in matter depends only on the nature i.e. atomic number of the substance, and not on the density. In other words he defined the range of the β-particles in terms of the amount of matter traversed and not the distance travelled. Therefore if we introduce a completely empty cavity in the medium, we should not expect the range and the number of β-particles traversing the cavity to be altered. If the cavity is filled with air it will make no difference to the β-ray density within it unless the atomic number of the medium differs very much from that of air or unless the pressure of the air is too great so that a big fraction of the β-ray energy is used in passing through the cavity. To avoid this, either the cavity should be small or the pressure reduced.

(b) The Theory

Gray[41], in proving that the introduction of a small air filled cavity into a solid meium does not disturb the electronic atmosphere as regards direction and velocity, established his principle of equivalence, which is:

"The energy lost per unit volume by β-particles in the cavity is $1/\rho$ times the energy lost by γ-rays per unit volume of the solid." ρ is the ratio of the energy lost by an electron in traversing a certain distance (a small fraction of its range) in the two media, (air and solid). In this consideration the volume of the chamber is assumed to be very small so that the ionization produced directly in the air itself is negligible.

The energy required for the ionization of air has been thoroughly investigated experimentally and theoretically.[42] The results of these investigations can be summarised:-[42]

1. The average energy lost by the production of an ion-pair in air is $W = 33$ e-volts.
2. W is independent of the speed of the paricles i.e. is the same for all particles having energies between a 10^3 and 10^6 volts.

From (1) the energy lost by secondary electrons in crossing

the cavity per unit vol. $= W \times J$ where J is the number of ion-pairs produced per c.c. i.e. the ionization per unit volume.

From (2) we find that the constant for converting from ionization to energy is the same over a wide range of energy of the secondary electrons and hence for all types of radiation from the softest x-rays to the hardest γ-rays.

Thus the total energy, E, of secondary electrons generated in unit volume of the medium is given by

$$E = \rho W J$$

or

$$J = \frac{E}{\rho W} \quad \ldots\ldots\ldots\ldots\ldots\ldots (1)$$

is proportional to the elctron density, since the rate at which charged particles lose energy is due to encountering the elctrons of the medium through which they pass.

$$\rho = \frac{n_1}{n_a} \cdot \frac{S_1}{S} \quad \ldots\ldots\ldots\ldots\ldots\ldots (2)$$

where n_1 and n_a are the electron densities of the medium and the air respectively and S_1 and S are the electronic stopping power in the medium and the air respectively.

Inserting the value of ρ in (1) we get,

$$J = \frac{E}{\frac{n_1 \cdot s_1}{n_a \cdot s} \cdot W} \qquad \ldots\ldots (3)$$

$$E = n_1 (e\sigma_a + e\tau_1) I \qquad \ldots\ldots (4)$$

$e\sigma_a$ and $e\tau$ are the absorption scattering and photoelectric absorption coefficients respectively. I is the intensity of radiation falling on the material and is considered constant throughout the volume.

From (3) and (4)

$$J = \frac{n_1 (e\sigma_a + e\tau_1) I}{\frac{n_1 \cdot s_1}{n_a \cdot s} \cdot W}$$

$$= (e\sigma_a + e\tau_1) \frac{s}{s_1} \cdot n_a \cdot \frac{I}{W} \qquad \ldots\ldots (5)$$

Equation (5) represents the ionization per unit volume in a chamber specified by the different coefficients in the right hand side.

Similarly for an ionization chamber of another material, the ionization J_2 per unit volume is given by:

$$J_2 = (e\sigma_a + e\tau_2) \cdot \frac{s}{s_2} \cdot \frac{I}{W} \qquad \ldots\ldots (6)$$

∴ The ratio F of the ionization currents in the two chambers will be:

$$F = \frac{J_2}{J_1}$$

$$= \frac{e\sigma_a + e\tau_2}{e\sigma_a + e\tau_1} \qquad \ldots\ldots (7)$$

This equation is true when no reduction of intensity due to absorption in the walls of the chambers takes place. To allow for the absorption in the walls (7) becomes:

$$F' = \frac{e\sigma_a + e\tau_2}{e\sigma_a + e\tau_1} \cdot \frac{S_1}{S_2} \cdot \frac{\bar{e}^{\mu_2' x}}{\bar{e}^{\mu_1' x}} \qquad \ldots (8)$$

if absorption to be allowed for is true absorption only.

or

$$F'' = \frac{e\sigma_a + e\tau_2}{e\sigma_a + e\tau_1} \cdot \frac{S_1}{S_2} \cdot \frac{\bar{e}^{\mu_2 x}}{\bar{e}^{\mu_1 x}} \qquad \ldots (9)$$

if absorption to be allowed for is total absorption.

where x is the thickness of the walls in cm.

$$\mu_2' = (e\sigma_a + e\tau_2) \quad \& \quad \mu_1' = (e\sigma_a + e\tau_1)\, n_1$$

and

$$\mu_2 = (e\sigma_a + e\sigma_s + e\tau_2) \quad \& \quad \mu_1 = (e\sigma_a + e\sigma_s + e\tau_1)\, n_1$$

Expressions (8) and (9) hold when the thickness traversed by the beam is constant and equals x cm.

In our experiments, however, the chambers were mounted in such a way that the leads were outside the field of radiation in order to minimize the radiation reaching them, i.e. the axes of the chambers were $\perp^r$ to the direction of the beam [see fig. (15)]. Therefore the thickness of the wall material through which the beam passes is not always the same. Correction for absorption was carried out as follows. See fig. (16).

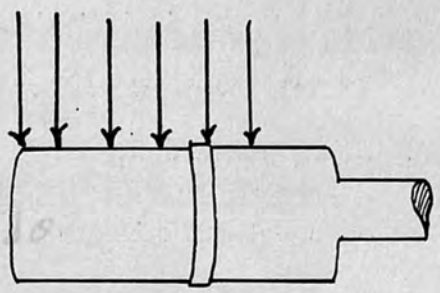

fig. (15)

The amount of radiation incident in an arc of length $r\,d\theta = I r_1\, d\theta \cos\theta$

The amount transmitted $= I r_1\, d\theta \cos\theta\, e^{-\mu c}$

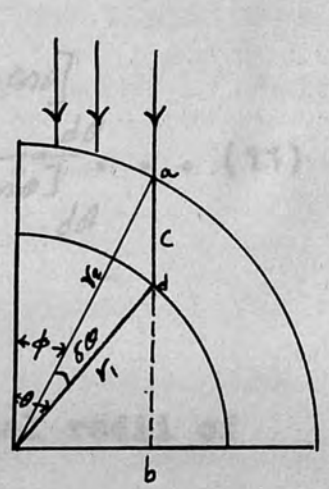

fig. (16)

$$c = r_2 \cos\phi - r_1 \cos\theta$$

$$r_2 \sin\phi = r_1 \sin\theta$$

$$1 - \cos^2\phi = \frac{r_1^2}{r_2^2} \sin^2\theta$$

$$\therefore \quad \cos\phi = \sqrt{1 - \frac{r_1^2}{r_2^2}\sin^2\theta}$$

$$\text{Thus} \qquad C = r_2\left[\sqrt{\frac{r_2^2}{r_1^2} - \sin^2\theta} - \cos\theta\right]$$

The fraction transmitted

$$= \cos\theta\, e^{-\mu r_1\left[\sqrt{\frac{r_2^2}{r_1^2} - \sin^2\theta} - \cos\theta\right]}\, d\theta$$

Thus

$$F' = Ff = \frac{J_2}{J_1}$$

$$= \frac{e\sigma_a + e\tau_2}{e\sigma_a + e\tau_1} \cdot \frac{S_1}{S_2} \cdot \frac{\int_0^{\frac{\pi}{2}} \cos\theta\, e^{-\mu_2' r_1\left[\sqrt{\frac{r_2^2}{r_1^2} - \sin^2\theta} - \cos\theta\right]}\, d\theta}{\int_0^{\frac{\pi}{2}} \cos\theta\, e^{-\mu_1' r_1\left[\sqrt{\frac{r_2^2}{r_1^2} - \sin^2\theta} - \cos\theta\right]}\, d\theta} \quad \ldots (10)$$

$$F'' = Ff'$$

$$= \frac{e\sigma_a + e\tau_2}{e\sigma_a + e\tau_1} \cdot \frac{S_1}{S_2} \cdot \frac{\int_0^{\frac{\pi}{2}} \cos\theta\, e^{-\mu_2 r_1\left[\sqrt{\frac{r_2^2}{r_1^2} - \sin^2\theta} - \cos\theta\right]}\, d\theta}{\int_0^{\frac{\pi}{2}} \cos\theta\, e^{-\mu_1 r_1\left[\sqrt{\frac{r_2^2}{r_1^2} - \sin^2\theta} - \cos\theta\right]}\, d\theta} \quad \ldots (11)$$

where r_2 & r_1 are the external and internal radii of the chamber.

Having established an expression for the ratio, we proceed to evaluate the theoretical ratio F of the ionizations. Then, evaluating f we determine F' taking into account the absorption in the walls of the chamber.

For this purpose, the different coefficients appearing in (9) and (10) were determined as follows:

(c) Theoretical Determination of the Effective Atomic Number of the Walls.

The atomic number of the material of the chambers is required in the evaluation of the photoelectric absorption coefficient. The effect of varying the atomic number of the chamber wall, on the ionization inside it, is also one of the problems to be investigated. Hence the need arises to determine the atomic number of the different mixtures used for constructing the chambers. A statement of "effective atomic number," $\bar{Z}$" of the pressed material replaces the atomic number Z which is used for the simple elements.

As the atomic number is one of the fundamental factors governing the absorption in a medium, its determination should be based on the consideration of the two components of the absorption coefficient namely,

(a) the scattering absorption coefficient.

and (b) the photoelectric absorption coefficient.

It is known that the scattering absorption coefficient σ is independent of the atomic number for the range of wavelengths used in this investigation; while the photoelectric absorption coefficient τ depends to a large extent on the atomic number. Therefore an expression for $\overline{Z}$ is usually derived from the relation between τ and $\overline{Z}$.

Workers in this field have given different formulae for this relation leading to different values for $\overline{Z}$. Fricke and Glasser[43] derived a formula for the effective atomic number based on the fact that the photoelectric absorption coefficient is proportional to Z^3. As the absorption coefficient is purely additive and independent of the chemical composition of the material, their formula took the form:

$$\overline{Z} = \sqrt{\frac{a_1 Z_1^4 + a_2 Z_2^4 + a_3 Z_3^4 \cdots}{a_1 Z_1 + a_2 Z_2 + a_3 Z_3 \cdots}}$$

where the a's denote the number of atoms per c.c. of each element of the compound and the Z's are the atomic numbers.

This formula is not quite accurate since τ is not exactly proportional to Z^3.

The expression we have used for calculating $\overline{Z}$ is based on Walters'[44] formula

$$\tau = 2.64\, Z^{2.94}\, \lambda^3,$$

which was found to fit the experimental data better than the previous one and it is used for calculating the absorption coefficient in this work. We have thus taken $\overline{Z}$ to be given by:

$$\overline{Z} = \sqrt[2.94]{\Sigma a_i Z_i^{2.94}}$$

where a_i is the fractional content of electrons for an element of atomic number Z, and Σ is made for all the elements present in the compound.

Substituting in the above equation the values of "a's" and "Z's" for different elements present in the following compound:

100 parts of bakelite ($C_6H_5 \cdot CH_2$)
20 parts of graphite (C)
2 parts of vanadium oxide (V_2O_5)

$\overline{Z}$ is found to be 7.64 which is the effective atomic number of air derived from the previous formula. Chambers of this mixture were manufactured [see p.(111)] and used as ~~an~~ "air-wall" chamber.

$\overline{Z}$ was calculated for another mixture of:

100 parts bakelite
20 parts graphite

Figure (17)

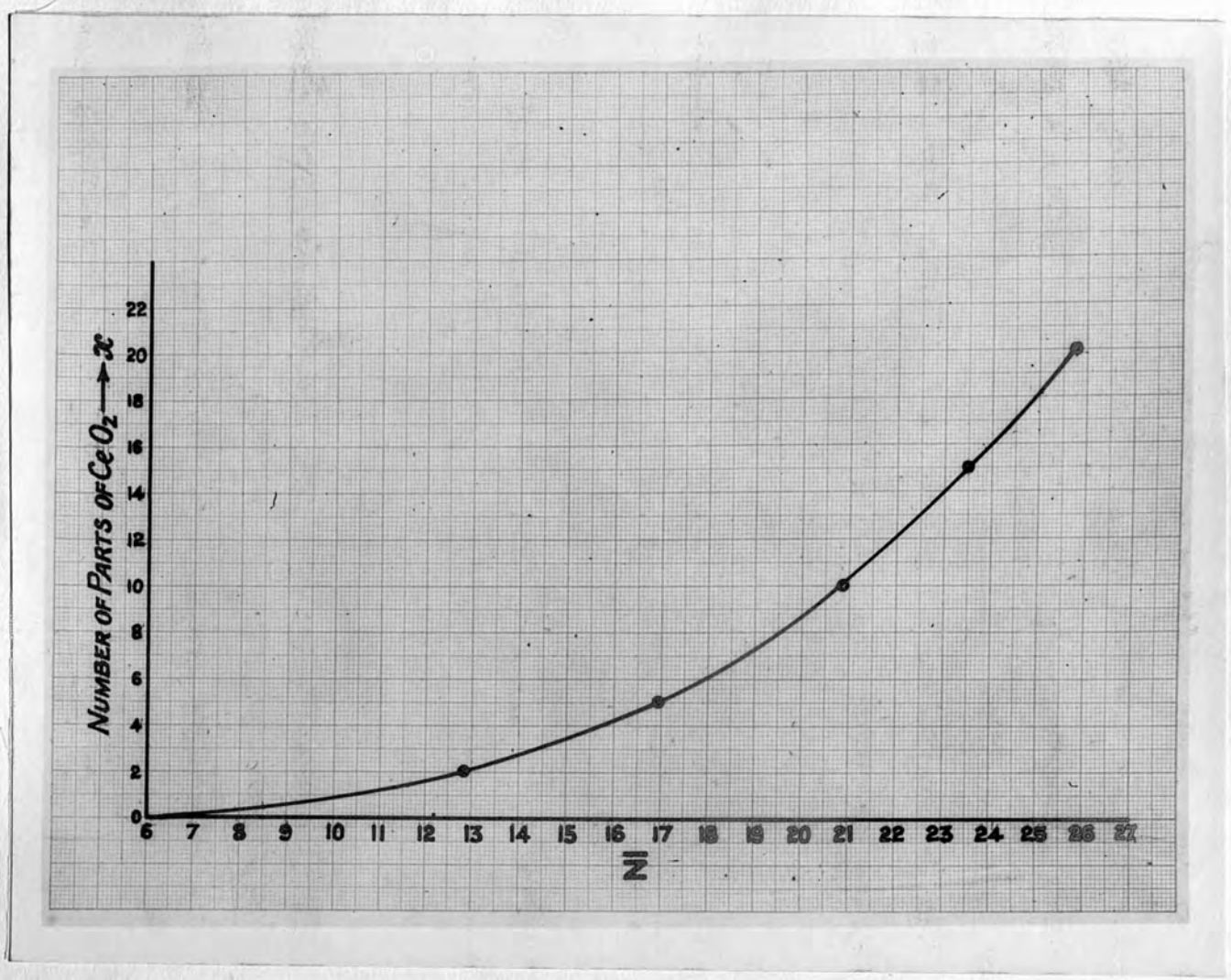
NUMBER OF PARTS OF $CeO_2 \longrightarrow x$
0
2
4
6
8
10
12
14
16
18
20
22
6 7 8 9 10 11 12 13 14 15 16 17 18 19 20 21 22 23 24 25 26 27
$\overline{Z}$

x parts cerium oxide (CeO_2)

where x may take different values.

A curve between x and Z was drawn (see fig. 17) from which the value of x required to obtain a certain $\overline{Z}$ can be interpolated.

The following table contains the calculated Z for the corresponding values of x chosen

The No. of parts of CeO_2 in the mixture	0	2	5	10	15	20
The corresponding $\overline{Z}$	6.09_5	12.8_2	16.98	20.84	23.5	25.79

(d) Calculation of the density and the Electron Density of the chamber wall material.

The electron density was determined from the formula[45]

$$n_z = N n_M \frac{\rho}{M}$$ electrons per c.c.

where N is Avogadro's number $= 6.06 \times 10^{23}$

n_M is the number of electrons in the molecule of weight M

ρ is the density in gm./c.c.

The following table includes the whole data for

calculating n_z and also the electron density corresponding to the effective numbers of the different chambers used in the investigation.

$\bar{Z}$	M	n_M	ρ	n_z /c.c
7.64	46.9	24.87	1.44	4.65×10^{23}
12.84	46.9	24.84	1.44	4.63×10^{23}
17.04	47.75	25.13	1.44_9	4.63×10^{23}
20.84	49.15	25.74	1.46	4.64×10^{23}

From the table we see that the electron density is the same for all the chambers used i.e. independent of the atomic number which is a characteristic phenomenon in the case of this kind of plastic.

The density ρ in the previous table was determined as follows:

Uniform discs were made of each mixture by the same process as that (described later) in making the chambers. The dimensions of each disc were measured accurately and t their masses were determined on a chemical balance. From these data the density of each mixture was computed.

Calculated $\bar{Z}$	diameter in cm.	Thickness in cm.	Wgt. in gm. W	ρ in gm./c.c.
7.64	1.516	.494	1.281	1.44_4
	1.516	.494	1.281	
	1.516	.492	1.287	
12.84	1.507	.525	1.359	1.44_1
	1.507	.483	1.252	
	1.516	.505	1.316	
17.04	1.512	.550	1.362	1.44_9
	1.510	.432	1.160	
20.84	1.508_6	.542	1.403	1.46_3
	1.502_3	.541	1.415	

It is seen from the last column that the density is almost constant for all the effective atomic numbers used.

(e) <u>Determination of the Absorption Coefficients for various Plastic Wall Materials.</u>

If a homogeneous beam of radiation falls on an absorber, the intensity of the beam is reduced according to the following formula:

$$I_x = I_0 \, e^{-\mu x}$$ see equation (3) p. (11)

where I_0 is the initial intensity of the beam, I_x is the final intensity of the beam after traversing a thickness x

of the absorber and μ is termed the linear absorption coefficient of its material.

μ is partly due to true absorption, partly due to absorption by scattering and partly to true scattering. Also in the case of very hard x-rays and γ-rays of more than 1 MEV one may have to take into account the coefficient of pair-production, if the atomic number of the absorber is sufficiently great. This coefficient is negligible for light materials we are considering.

Therefore the components of μ (per electron $e\mu$) are:

1. The scattering coefficient σ (per electron $e\sigma$) which is the sum of:
   (a) The scattering absorption coefficient, per electron $e\sigma_a$
   and (b) The true scattering coefficient, per electron $e\sigma_s$
2. The photoelectric absorption coefficient, per electron $e\tau$

1. <u>The evaluation of the scattering absorption coefficient per electron $e\sigma_a$</u>

The scattering absorption coefficient per electron is independent of the nature of the scatterer as shown experimentally by different observers [46, 47, 48] in the range of wavelengths and materials used in this investigation. Its

magnitude depends on the wavelength of the radiation, being predominant in the short wave length region while for long wavelengths it becomes almost negligible compared with the photoelectric coefficient.

Several formulae have been derived (Thomson, Compton, Dirac) for calculating $e\sigma$. None exactly fits the experimental observations, especially when the frequency of radiation is large.

The most satisfactory expressions are those given by the Klein and Nishina[49] quantum mechanical formulae, based on Dirac's relativistic theory of the electron, namely:

$$e\sigma = \frac{2\pi e^4}{m^2c^4}\left[\frac{2(1+\alpha)^2}{\alpha^2(1+2\alpha)} - \frac{1+\alpha}{\alpha^3}\log(1+2\alpha) + \frac{1}{2\alpha}\log(1+\alpha) - \frac{1+3\alpha}{(1+2\alpha)^2}\right]$$

and

$$e\sigma_a = \frac{2\pi e^4}{m^2c^4}\left[\frac{2(1+\alpha)^2}{\alpha^2(1+2\alpha)} - \frac{1+3\alpha}{(1+2\alpha)^2} + \frac{(1+\alpha)(1+2\alpha-2\alpha^2)}{\alpha^2(1+2\alpha)^2} - \frac{4\alpha^2}{3(1+2\alpha)^2} - \left(\frac{(1+\alpha)}{\alpha^3} - \frac{1}{2\alpha} + \frac{1}{2\alpha^3}\right)\log(1+2\alpha)\right]$$

$\alpha = \frac{h}{mc^2}$ the charge of the electron $e = 4.8025 \times 10^{-10}$ E.S.U.

$m = 9.1066 \times 10^{-28}$ gm. velocity of light 2.9977×10^{10} cm/sec.

h is planck's constant $= 6.624 \times 10^{-27}$ ergs/sec.

The following values of $e\sigma_k$ and $e\sigma_a$ at different λ's are computed from these formulae.

The scattering coefficient per electron according to Klein-Nishina formula.

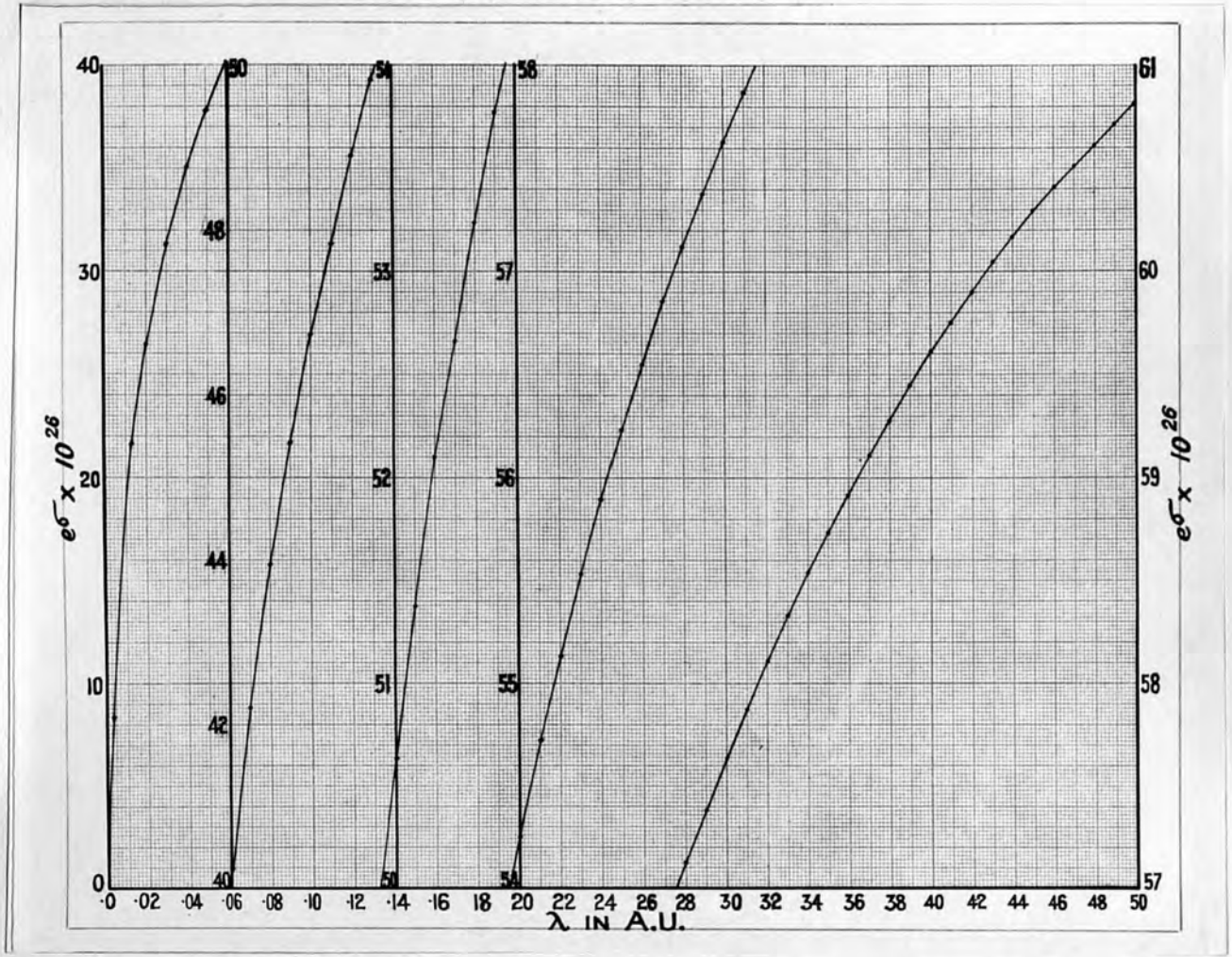

Figure (18)

The scattering absorption coefficient per electron according to Klein-Nishina formula.

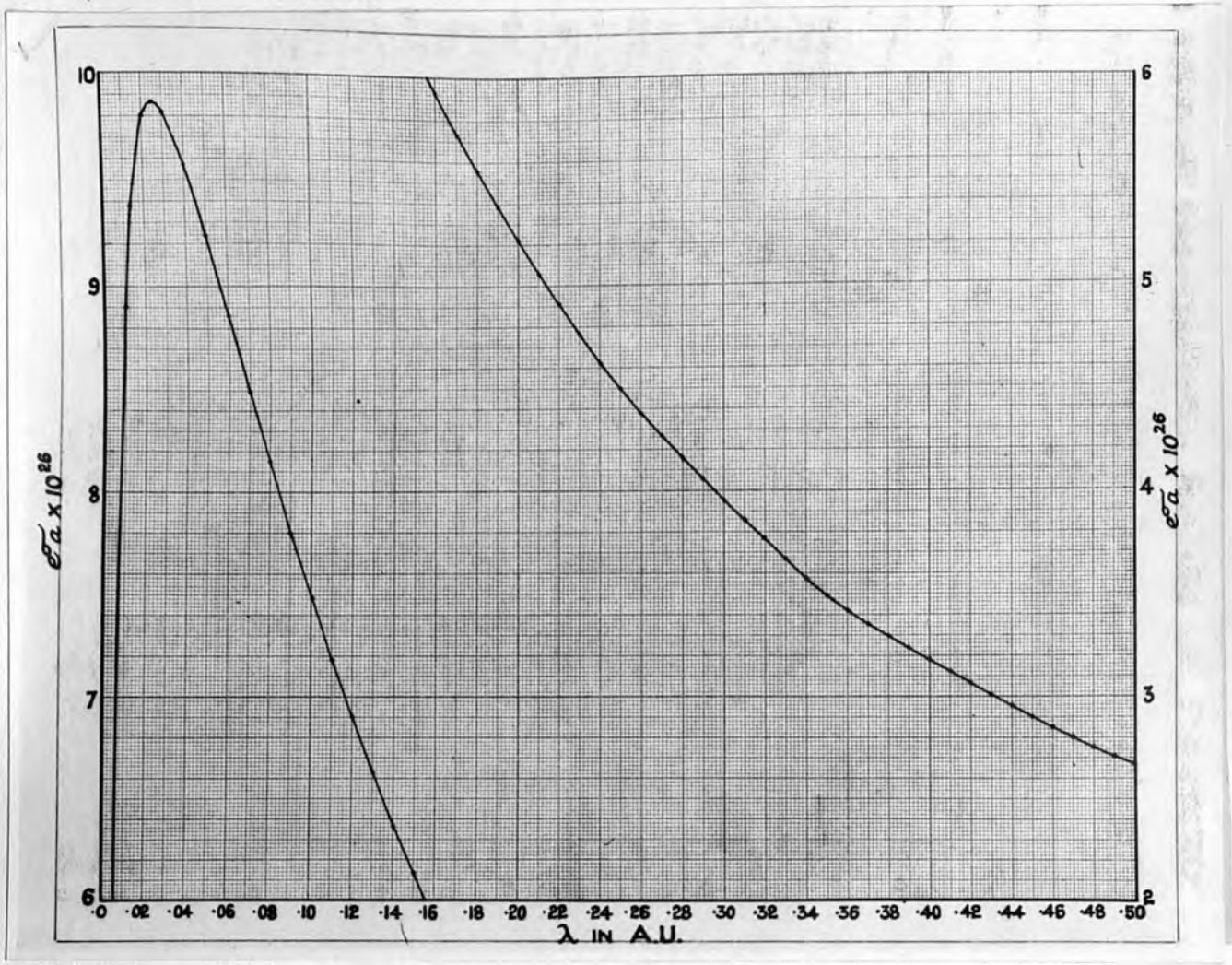

Figure (I9)

The values of $\epsilon\sigma$ and $\epsilon\sigma_a$ in this table are used throughout the present investigation whenever required. Figs (18) and(19) show these data graphically

λ in A.U.	$\epsilon\sigma \times 10^{26}$	$\epsilon\sigma_a \times 10^{26}$	λ in A.U.	$\epsilon\sigma \times 10^{26}$	$\epsilon\sigma_a \times 10^{26}$
.013	21.6	9.370	.31	57.87	3.863
.40	35.00	9.570	.32	58.11	3.775
.06	40.23	8.860	.33	58.33	3.675
.08	43.94	8.152	.34	58.54	3.575
.09	45.42	7.805	.35	58.73	3.492
.10	46.72	7.488	.36	58.92	3.425
.11	47.87	7.185	.37	59.11	3 362
.12	48.90	6.906	.38	59.28	3 300
.13	49.82	6.631	.39	49.45	3 242
.14	50.63	6.365	.40	59.61	3 187
.15	51.38	6.138	.41	59.75	3.123
.16	52.10	5.933	.42	59.90	3.065
.17	52.66	5.738	.43	60.05	3 010
.18	53.24	5.563	.44	60.17	2.956
.19	53.77	5.388	.45	60.30.	2 903
.20	54.25	5.225	.46	60.41	2.852
.21	54.72	5.065	.47	60.51	2.804
.22	55.13	4.908	.48	60.61	2 754
.23	55.53	4.763	.49	60.71	2.710
.24	55.90	4.625	.50	60.80	2.668
.25	56.23	5.500	.575	—	2.375
.26	56.55	4.382	.75	—	1.890
.27	56.85	4.271	.95	—	1.500
.28	57.12	4.160			
.29	57.38	4.060			
.30	57.63	3 950			

2. Evaluation of the photoelectric absorption coefficient per electron

The photoelectric absorption coefficient is referred to as the true absorption since the whole energy of the quantum is absorbed within the atom with the ejection of a photo-electron. Therefore it is dependent both upon the nature of the absorber and the wave length of the incident radiation.

Many empirical[50, 51, 28, 44, 52] expressions based on experimental data have been suggested for its calculation but none of them cover a relatively wide range of wave lengths or atomic numbers really well.

Walter's formula[44]

$$\tau = 2.64 Z^{2.94} \lambda^3,$$

where τ the photoelectric absorption coefficient per electron

Z = the atomic number of the absorber,

λ = the wave length of the radiation,

has been found to fit the older experimental observations fairly well. More recently Victoreen[53] reviewed all the absorption data available and came to the conclusion that the following expression

$$\frac{\tau}{\rho} = \alpha Z^2 \left(\frac{Z}{A}\right) \lambda^3 - \beta Z^5 \left(\frac{Z}{A}\right) \lambda^4$$

holds for all elements when suitable values for the constants α and β are chosen, provided the wave length of the radiation used is less than the K absorption line.

Where $(\frac{2Z}{A})$ corrects for the variation in the number of atoms/gm due to the presence of isotopes, and A is the atomic wt.

$$\alpha_K = az^2 + bz - c$$

$$\beta_K = dz^2 - ez + f$$

The values of α and β change at each critical wave length. The constants, a,b.c.d.e and f change at each critical wave length and on each side of $z = 5$.

The values of the constants used in calculating the photoelectric absorption coefficient are those corresponding to $z > 5$, since we are interested only in materials of atomic number greater than 5:

a	= 0.0000400	d	= 0.000380
b	= 0.00728	e	= 0.00152
c	= 0.0114	f	= 2.35

The values of $e\tau$ are then obtained from the following relation:

$$e\tau = \frac{\tau}{n_z} = \frac{\tau}{6.06 \times 10^{23} n_M \frac{\rho}{M}} = \frac{\tau}{\rho} \frac{M}{6.06 \times 10^{23} n_M}$$

where M is weight of the molecule

n_M is the number of electrons/molecule.

the following tables give the σ values calculated by applying Walter's and Victoreen's formulae to the material of the different chambers used.

The $\bar{Z}$ values previously calculated on p. (74) are used here.

The constants used in the calculation of σ from Victoreen's formula are included in the following table.

$\bar{Z}$	$\bar{Z}^2$	$\bar{Z}^5$	$\frac{2\bar{Z}}{A}$	α	$\beta \times 10^6$	$\alpha\bar{Z}^2\left(\frac{2\bar{Z}}{A}\right)$	$\beta\bar{Z}^5\left(\frac{2\bar{Z}}{A}\right)$
7.64	58.3	198 X 10^3	1.026	0.0466	2.361	2.78	0.479
12.84	165.0	350 X 10^3	1.025	0.0887	2.393	13.77	0.85
17.04	290.0	244 X 10^4	1.030	.1245	2.435	37.25	6.14.
20.84	435.0	394 X 10^4	1.024	.1579	2.484	70.30	10.06

The values in the following table are used in establishing the tables of the photoelectric absorption coeffic ents.

$\bar{Z}$	7.64	12.84	17.04	20.84
$\sigma \times 10^{26}$ Walter's	1052 λ^3	4800 λ^3	11000 λ^3	20380 λ^3
$\sigma \times 10^{26}$ Victoreen's	.311 $\frac{I}{\rho}$	.311 $\frac{I}{\rho}$	.313_5 $\frac{I}{\rho}$	.315 $\frac{I}{\rho}$

Figure (20)

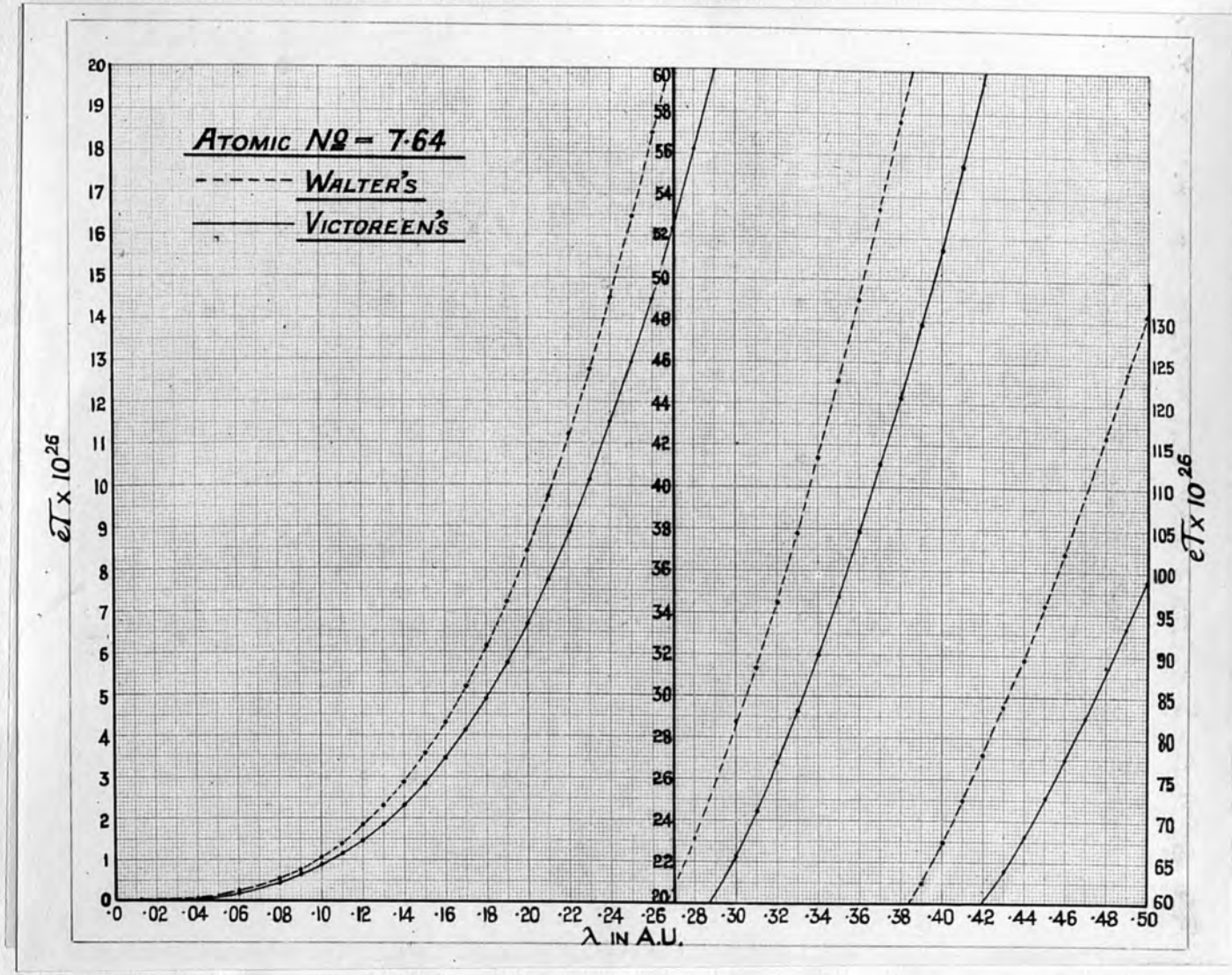
ATOMIC Nº = 7·64
WALTER'S
VICTOREEN'S
eT x 10^26
λ IN A.U.
0 ·02 ·04 ·06 ·08 ·10 ·12 ·14 ·16 ·18 ·20 ·22 ·24 ·26 ·28 ·30 ·32 ·34 ·36 ·38 ·40 ·42 ·44 ·46 ·48 ·50

The Photoelectric absorption coefficient

The material of the air wall chamber Nolii $\bar{Z} = 7.64$

Fig. (20) represents τ against λ

λ in A.U.	$\frac{I}{\rho} \times 10^4$ Viet.	$\tau \times 10^{26}$ Viet.	$\tau \times 10^{26}$ Watt.
.013	0.0611	.0019	.0023
.04	1.768	.055	.067
.06	5.948	.185	.227
.08	14.05	.4365	.539
.09	22.49	.70	.767
.10	27.35	.855	1.05
.11	36.34	1.13	1.40
.12	47.12	1.47	1.87_5
.13	59.78	1.86	2.31
.14	74.56	2.32	2.88
.15	91.48	2.84	3.55
.16	110.9	3.45	4.31
.17	132.9	4.13	5.17_5
.18	157.6	4.9	6.14
.19	184.8	5.75	7.21
.20	214.9_6	6.69	8.42
.21	248.4	7.75	9.75
.22	285.3	8.87	11.21
.23	324.9	10.1	12.80
.24	369.1	11.55	14.54
.25	416.3	12.95	16.45
.26	467.6	14.5	18.50

cont.

λ in A.U.	$E_p \times 10^4$ Viet.	$eT \times 10^{26}$ Viet.	$eT \times 10^{26}$ Watt.
.27	521.5	16.2	20.70
.28	581.6	18.09	23.10
.29	642.6	19.99	25.60
.30	713.2	22.20	28.40
.31	785.6	24.40	31.35
.32	862.2	26.80	34.50
.33	943.3	29.30	37.80
.34	1028	31.99	41.40
.35	1119	34.80	45.10
.36	1219	37.90	49.10
.37	1320	41.05	53.38
.38	1425	44.30	57.65
.39	1529	47.83	62.45
.40	1657	51.50	67.40
.41	1785	55.50	72.50
.42	1911	59.50	78 00
.43	2051	63.80	83.70
.44	2190	68.13	89.50
.45	2343	72.9	96.00
.46	2493	77.5	102.2
.47	2652	82.5	109.1
.48	2825	88.00	116.2
.49	3001	93.5	125.9
.50	3180	99.0	131.0
.575	4767	148.4	200.0
.75	10230	318	444.0
.95	19940	620	902.0

Figure (21)

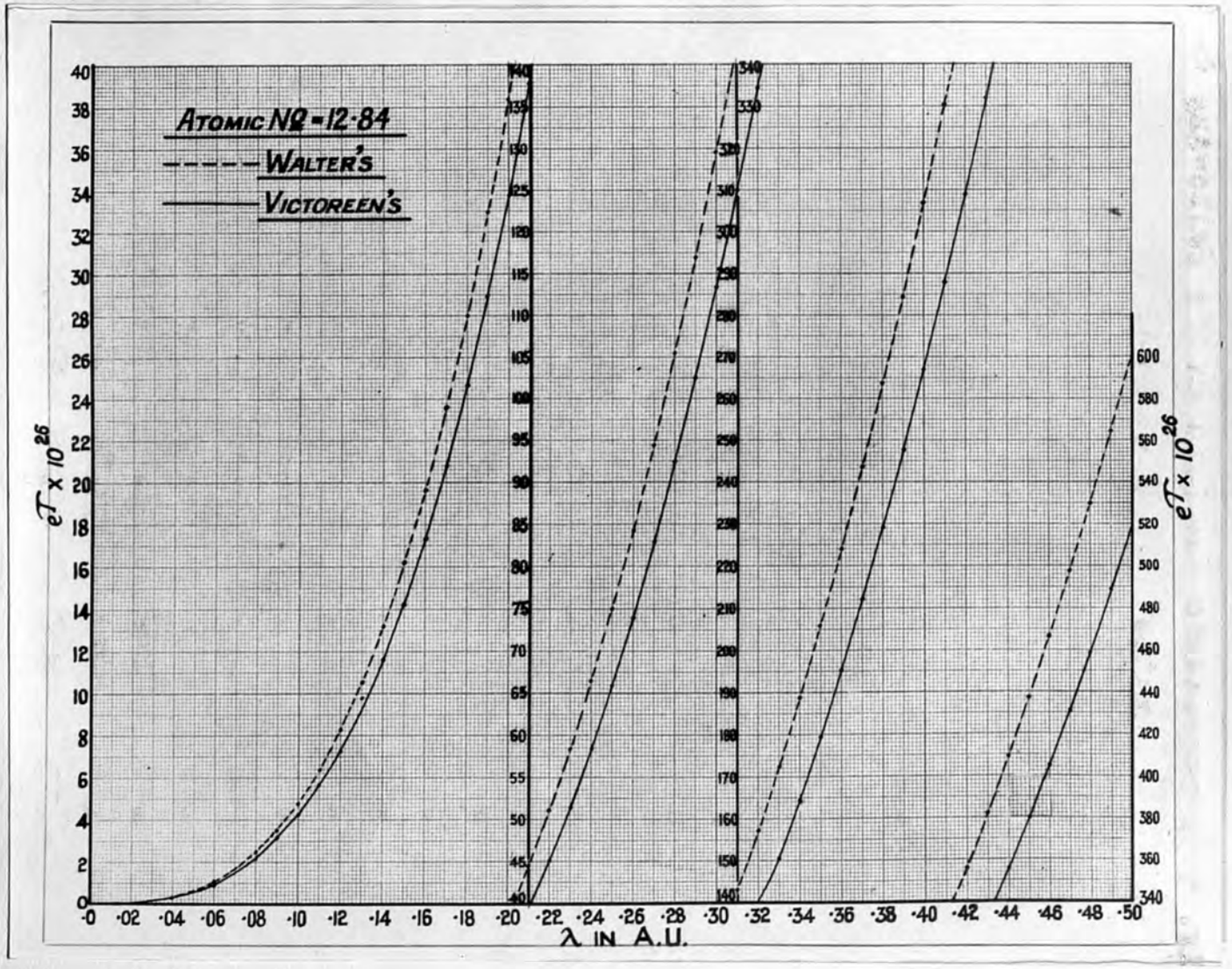

The Photoelectric absorption Coefficient

The material of the chamber No.(2) $\bar{Z} = 12.84$

Fig. (21) represents the data in the following table i.e. τ against λ graphically.

λ in A.U.	$\frac{\tau}{\rho} \times 10^4$ Wat.	$\tau \times 10^{26}$ Wat.	$\tau \times 10^{26}$ Watt.
.013	0.30	0.0093	.0105
.04	8.75	0.272	.307
.06	29.49	0.917_5	1.037
.08	70.15	2.18	2.46
.09	103.2	3.15	3.50
.10	136.9	4.25	4.80
.11	182.0	5.66	6.39
.12	234.6	7.30	8.28
.13	315.6	9.81	10.54
.14	374.7	11.64	13.20
.15	460.6	14.31	16.20
.16	558.9	17.35	19.65
.17	669.4	20.80	23.60
.18	794.1	24.68	28.00
.19	933.9	29.00	32.95
.20	1088	33.80	38.40
.21	1261	39.20	44.5
.22	1445	45.00	51.10
.23	1650	51.40	58.40
.24	1876	58.40	66.40
.25	2118	65.88	75.00
.26	2378	74.00	84.25
.27	2660	82.80	94.40

cont.

λ in A.U.	$\mathcal{F}_p \times 10^4$ Viet.	$\mathcal{F} \times 10^{26}$ Viet.	$\mathcal{F} \times 10^{26}$ Walk
.28	3148	92.50	105.5
.29	3300	102.5	117.0
.30	3646	113.3	129.6
.31	4022	125.0	143.0
.32	4416	137.3	157.3
.33	4850	150.5	172.4
.34	5297	164.8	189.0
.35	5773	179.5	206.0
.36	6282	195.4	224.0
.37	6817	212.0	243.5
.38	7373	229.2	263.7
.39	7969	247.7	284.5
.40	8603	267.2	307.0
.41	9260	288.0	330.5
.42	9941	309.0	356.0
.43	10680	332.0	382.0
.44	11420	355.4	409.0
.45	12220	380.0	437.5
.46	13030	405.0	467.0
.47	13870	431.3	497.5
.48	14760	459.0	530.0
.49	15710	489.0	564.5
.50	16670	518.8	600.0
.575	25170	782.0	912.5
.75	55310	1720.0	2022.0
.95	111100	3450.0	4112.0

Figure (22)

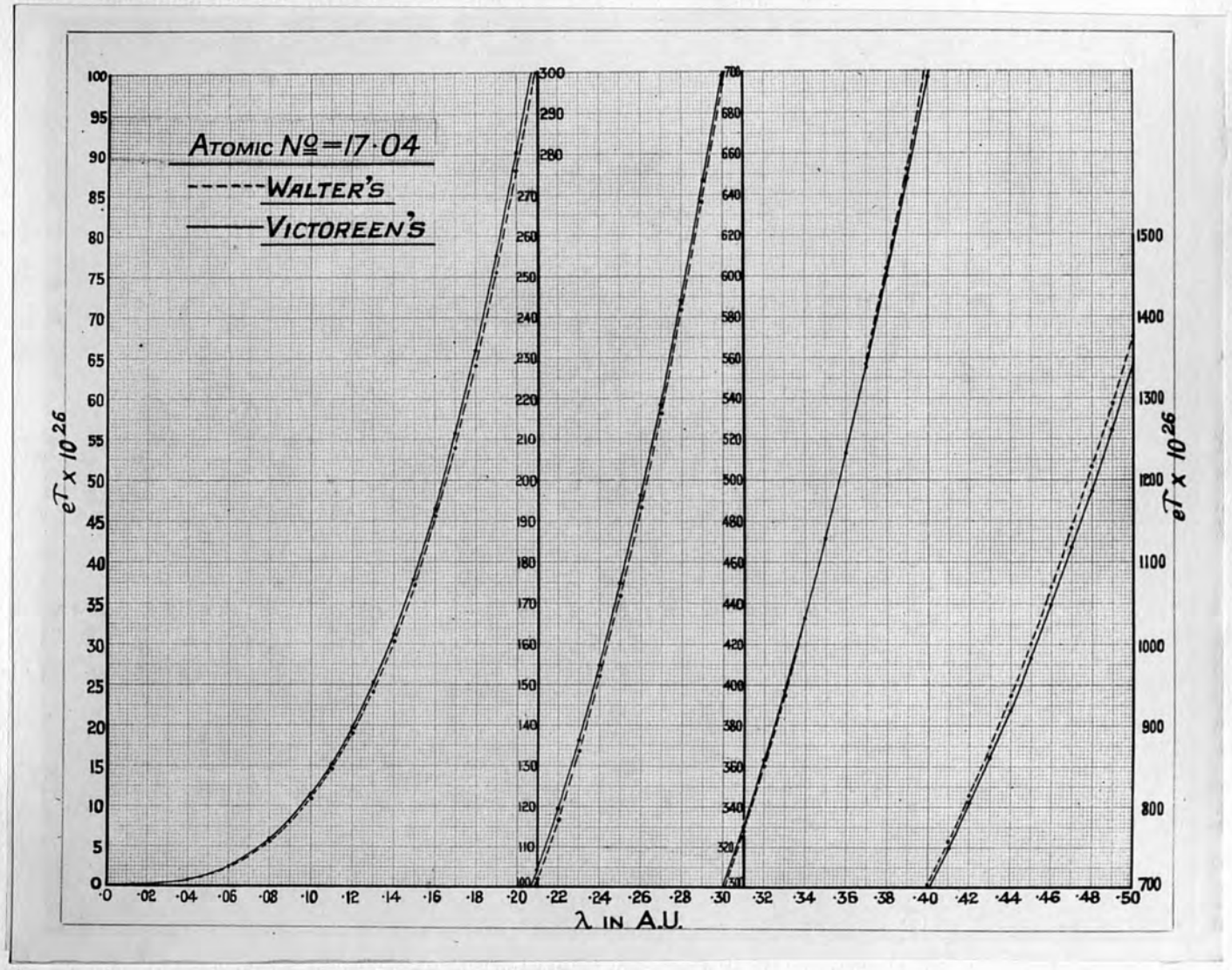

The Photoelectric Absorption Coefficient for Chamber $\bar{Z}=17.04$

Fig. (22) represents e^{τ} against λ graphically.

λ in A.U.	$\frac{\tau}{\rho} \times 10^4$ Viet.	$e^{\tau} \times 10^{26}$ Viet.	$e^{\tau} \times 10^{26}$ Walt.
.013	0.816	0.025_6	0.024
.04	23.69	0.743	.704
.06	79.72	2.50	2.38
.08	188.2	5.90	5.63
.09	267.5	8.38	8.02
.10	366.4	11.48	11.00
.11	487.0	15.26	14.64
.12	631.3	19.78	19.01
.13	801.2	25.20	24.17
.14	997.7	31.27	30.18
.15	1226	38.43	37.13
.16	1485	46.55	45.06
.17	1781	55.82	54.04
.18	2106	66.00	64.15
.19	2474	77.60	75.45
.20	2882	90.40	88.00
.21	3330	104.4	101.9
.22	3821	119.8	117.1
.23	4359	136.6	133.8
.24	4941	154.9	152.1
.25	5585	175.0	171.9
.26	6265	196.4	193.3
.27	6994	217.5	216.5
.28	7798	244.2	241.5

cont.

λ in A. U.	$\frac{I}{p} \times 10^{4}$ Vict	$eI \times 10^{26}$ Vict.	$eI \times 10^{26}$ Watt
.29	8728	273.6	268.3
.30	9553	299.2	297.0
.31	10520	330.0	328.0
.32	11560	363.5	360.5
.33	12660	397.0	395.3
.34	13800	432.5	432.3
.35	15040	471.5	471.6
.36	16350	512.5	513.2
.37	17730	556.0	557.2
.38	19130	600.0	603.6
.39	20680	648.0	652.5
.40	22260	698.0	704.0
.41	23930	750.0	758.1
.42	25680	805.0	815.0
.43	27500	862.0	874.6
.44	29380	919.0	937.0
.45	31430	984.0	1002
.46	33460	1048	1071
.47	35630	1117	1142
.48	37870	1187	1216
.49	40220	1261	1294
.50	42810	1342	1375
.575	64050	2007	2090
.75	137600	4310	4640
.95	269000	8440	9450

Figure (23)

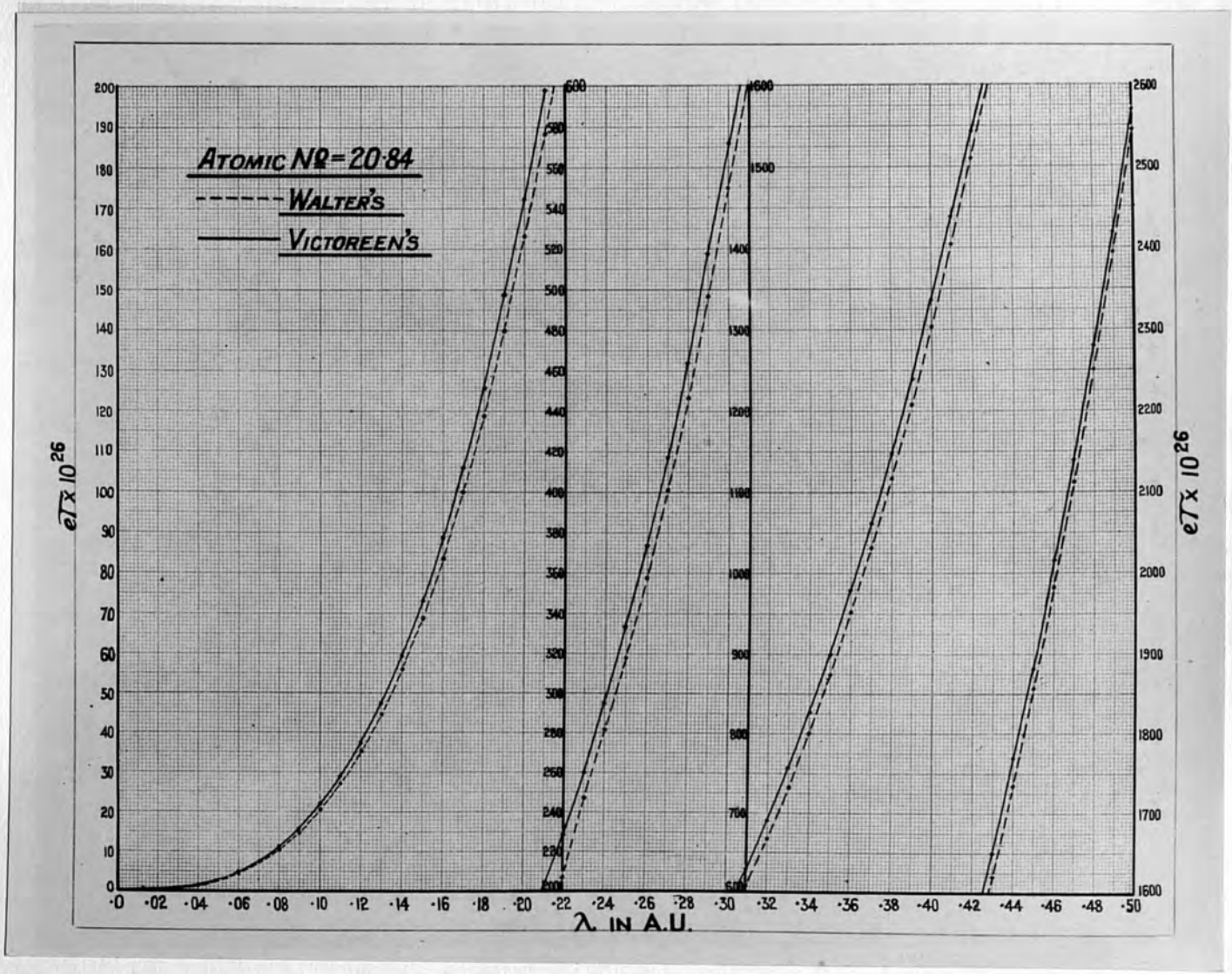

The Photoelectric Absorption Coefficient of
for chamber No. (4) $\bar{Z} = 20.84$

Fig. (23) shows the relation between τ & λ

λ in A.U.	$\frac{\tau}{\rho} \times 10^4$ Vict.	$\tau \times 10^{26}$ Vict.	$\tau \times 10^{26}$ Watt.
.013	1.54	0.048_6	0.045
.04	44.74	1.41_5	1.31
.06	150.7	4.76	4.42
.08	359.6	11.32	10.44
.09	505.4	15.90	14.85
.10	702.9	22.15	20.38
.11	921.8	29.00	27.12
.12	1193	37.55	35.19
.13	1511	47.55	44.75
.14	1891	59.50	55.90
.15	2321	73.05	68.80
.16	2824	88.90	83.50
.17	3369	106.1	100.0
.18	3994	125.9	118.8
.19	4709	148.9	139.8
.20	5463	172.2	163.0
.21	6314	199.0	188.5
.22	7251	228.8	216.8
.23	8269	260.5	247.6
.24	9386	295.5	281.5
.25	10610	334.0	318.2
.26	11890	374.0	358.0

cont.

λ in A.U.	$\mathcal{F}\times10^4$ Viet.	$\mathcal{E}\times10^{26}$ Viet.	$\mathcal{E}\times10^{26}$ Walt.
.27	13300	418.0	401.0
.28	14760	464.0	447.0
.29	16480	518.0	497.0
.30	18180	572.0	550.0
.31	20000	629.0	607.0
.32	22000	690.5	668.0
.33	24060	757.5	732.0
.34	26260	827.0	801.0
.35	28600	900.0	874.0
.36	31110	979.0	952.0
.37	33710	1062	1032
.38	36450	1148	1117.5
.39	39380	1240	1208
.40	42420	1337	1304
.41	45650	1438	1405
.42	48970	1544	1510
.43	52410	1650	1620
.44	56120	1770	1734
.45	59880	1882	1856
.46	63900	2015	1983
.47	68000	2140	2112
.48	72300	2280	2251
.49	76800	2420	2395
.50	81570	2570	2545
.575	122500	3880	3870
.75	264700	8400	8587
.95	521000	16520	17450

From the above tables and graphs we see that the values of the photoelectric absorption coefficient calculated from Victoreen's and Walter's formulae disagree considerably, especially at low atomic numbers and long wave lengths.

For $\overline{Z} = 7.64$, the value of τ given by Walter's formula is higher than that given by Victoreen's by 22.7% at .08 A.U. This deviation increases as the wavelength increases reaching 45.5% at .95 A.U.

For $\overline{Z} = 12.84$ the deviation is 12.8% at .08 A.U. increasing to 19% when we reach .95 A.U.

For $\overline{Z} = 17.04$. The value given by Walter's formula is lower than that given by Victoreen's by 5.1% at .08 A.U. This deviation decreases as the wavelength increases till they become exactly the same at .34 A.U, then the values given by Walter's begin to be more and more than Victoreen's as the wavelength increases; the deviation amounts to 12% at .95 A.U.

In the case of $\overline{Z} = 20.84$ also the value of τ by Walter's is lower by 7.8% at .08 A.U. This deviation decreases with wavelength, being .3% at .575 A.U. Then τ given by Walter exceeds that given by Victoreen. The amount of deviation is 5.6% at .95 A.U.

Figure (24)

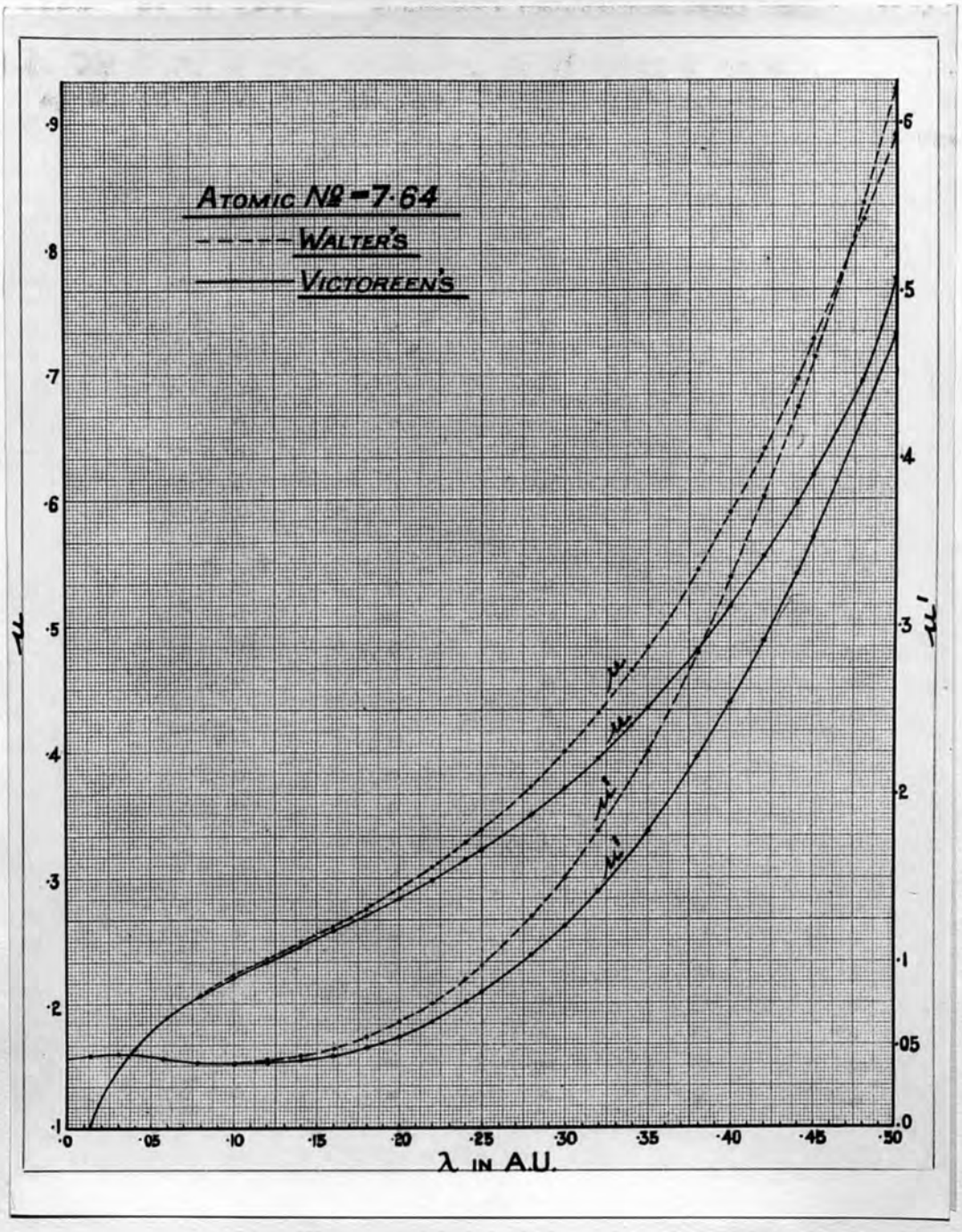
ATOMIC Nº = 7·64
WALTER'S
VICTOREEN'S
μ
μ'
λ IN A.U.
·9
·8
·7
·6
·5
·4
·3
·2
·1
·6
·5
·4
·3
·2
·1
·05
0
·05
·10
·15
·20
·25
·30
·35
·40
·45
·50

The Linear absorption coefficient for the air-wall chamber of effective atomic number 7.64.

$\mu' = (\sigma_a + \tau_c T) n_z$, n_z is the electron density 4.65×10^{23} electron /cc.

$\mu = (\sigma_a + \sigma_s + \tau_c T) n_z$ when taking into account the effect of the true scattering.

Fig.(24)

λ in A.U.	μ' Viet.	μ' Walt.	μ Viet.	μ Walt.
.013	.0436	.0436	.100	.100
.04	.0447	.0448	.163	.163
.06	.0421	.0422	.188	.188
.08	.0399	.040	.206	.207
.10	.0388	.039	.221	.223
.12	.0389	.041	.234	.236
.14	.0404	.043	.246	.249
.16	.0436	.048	.258	.262
.18	.0486	.055	.270	.276
.20	.0554	.064	.284	.292
.22	.064	.075	.298	.309
.24	.076	.089	.315	.328
.25	.081	.097	.322	.338
.28	.104	.127	.350	.373
.30	.122	.150	.371	.400
.32	.142	.178	.395	.431
.34	.165	.209	.421	.465
.35	.178	.226	.435	.483
.38	.222	.284	.481	.544
.40	.254	.328	.516	.590
.42	.291	.377	.555	.640
.44	.330	.430	.596	.695
.45	.352	.460	.620	.727
.48	.425	.552	.694	.822
.50	.473	.621	.743	.890

Figure (25)

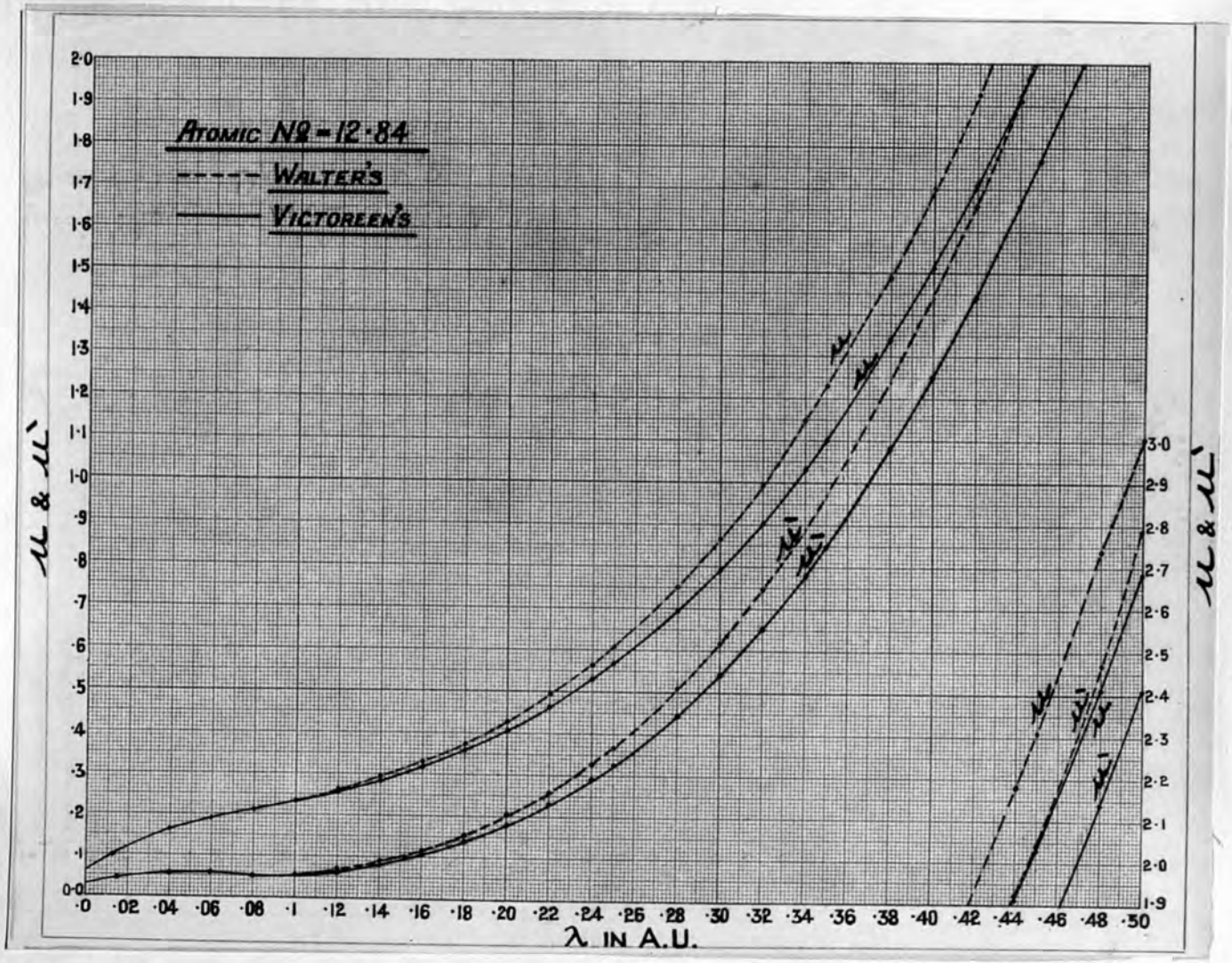
ATOMIC Nº = 12·84
WALTER'S
VICTOREEN'S
μ & μ'
λ IN A.U.
0·0 ·02 ·04 ·06 ·08 ·1 ·12 ·14 ·16 ·18 ·20 ·22 ·24 ·26 ·28 ·30 ·32 ·34 ·36 ·38 ·40 ·42 ·44 ·46 ·48 ·50
2·0 1·9 1·8 1·7 1·6 1·5 1·4 1·3 1·2 1·1 1·0 ·9 ·8 ·7 ·6 ·5 ·4 ·3 ·2 ·1 0·0
3·0 2·9 2·8 2·7 2·6 2·5 2·4 2·3 2·2 2·1 2·0 1·9

The Linear absorption coefficient for chamber No.(2) of atomic number 12.84

Fig. 25.

$\mu' = (\sigma_a + \sigma_T) n_z$, n_z where $n_z = 4.63 \times 10^{23}$ electron/cc.

$\mu = (\sigma_a + \sigma_s + \sigma_T) n_z$ Taking into account the effect of true scattering.

λ in A.U.	μ' Vict.	μ' Walt.	μ Vict.	μ Walt.
.013	.0434	.0434	.10	.10
.04	.0455	.0457	.163	.163
.06	.0453	.0458	.191	$.190_6$
.08	.048	.049	$.213_5$	$.215^6$
.10	$.054_4$	.060	$.236^5$	.239
.12	$.066^4$	.070	.260	.265
.14	.083	.091	.288	.296
.16	.108	.118	.322	.333
.18	.140	.155	.361	.376
.20	.181	.205	.407	.429
.22	.231	.260	.463	.492
.24	.292	.329	.529	.566
.25	.326	.368	.565	.609
.28	.446	.508	.626	.753
.30	.544	.618	.791	.867
.32	.654	.745	.905	.996
.34	.780	.890	1.03_3	1.15
.35	.846	.970	1.10^3	1.23
.38	1.08	1.24	1.33_7	1.49_8
.40	1.25	1.44	1.51^7	1.70^8
.42	1.44_5	1.66	1.71	1.92_5
.44	1.66^5	1.91	1.92_5	2.18^5
.45	1.77	2.04	2.04^5	2.31
.48	2.14	2.47	2.41	2.74
.50	2.41	2.79	2.68	3.06

Figure (26)

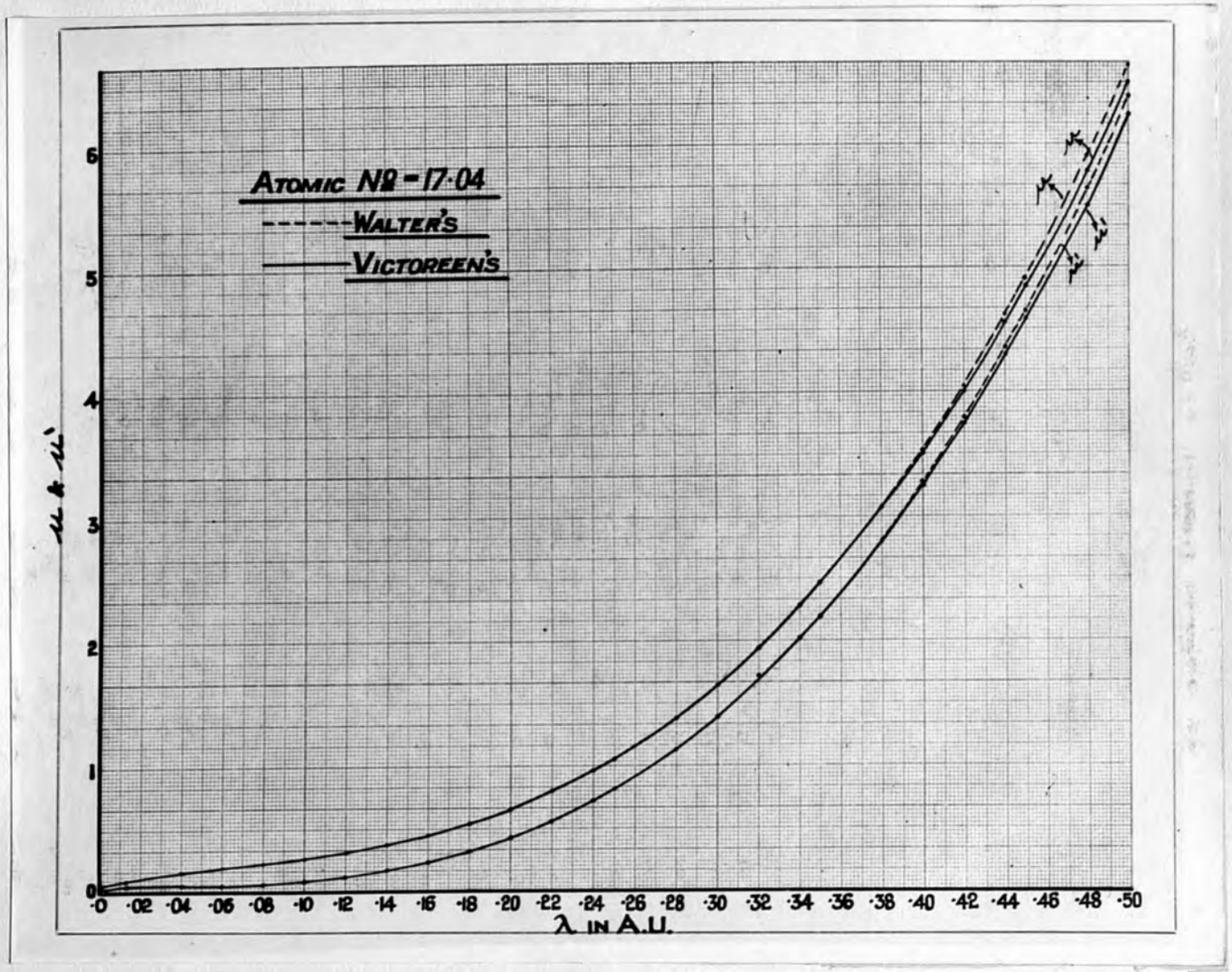
ATOMIC Nº - 17·04
WALTER'S
VICTOREEN'S
μ & μ'
0
1
2
3
4
5
6
·0 ·02 ·04 ·06 ·08 ·10 ·12 ·14 ·16 ·18 ·20 ·22 ·24 ·26 ·28 ·30 ·32 ·34 ·36 ·38 ·40 ·42 ·44 ·46 ·48 ·50
λ IN A.U.

The Linear absorption coefficient for chamber No. (3) of Atomic Number 17.04

Fig. (26)

$\mu' = (\sigma_a + \sigma_T) n_z$ where $n_z = 4.63 \times 10^{23}$ electrons/c.c.

$\mu = (\sigma_a + \sigma_s + \sigma_T) n_z$ Taking into account the effect of true scattering.

λ in A.U.	μ' Viet.	μ' Walt.	μ Viet.	μ Walt.
.013	.0425	.0425	.098	.098
.04	.0467	.0465	.1619	.1616
.06	.0514	.0508	.1935	.1936
.08	.065	.0637	.2315	.230
.10	.088	.0855	.269	.2678
.12	.124	.120	.318	.315
.14	.174	.169	.380	.374
.16	.243	.236	.457	.450
.18	.332	.323	.552	.544
.20	.444	.432	.670	.660
.22	.576	.565	.810	.799
.24	.738	.725	.977	.964
.25	.834	.816	1.07	1.058
.28	1.15	1.14	1.396	1.383
.30	1.403	1.39	1.656	1.643
.32	1.708	1.687	1.96	1.94
.34	2.02	2.027	2.28	2.27
.35	2.20	2.20	2.46	2.46
.38	2.79	2.81	3.06	3.07
.40	3.25	3.28	3.51	3.53
.42	3.74	3.79	4.0	4.05
.44	4.28	4.35	4.55	4.62
.45	4.58	4.65	4.85	4.92
.48	5.50	5.64	5.77	5.91
.50	6.23	6.38	6.50	6.65

Figure(27)

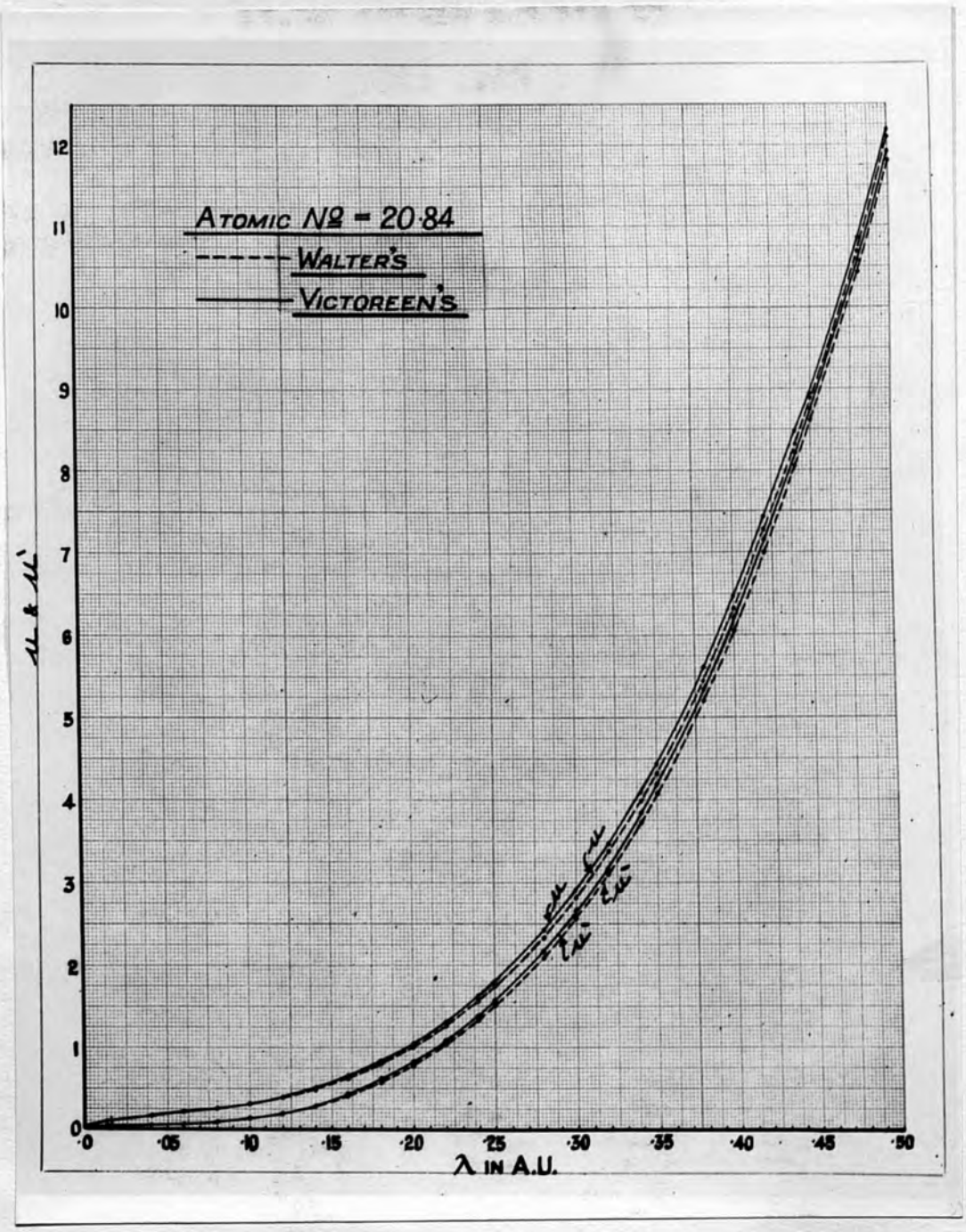
ATOMIC Nº = 20·84
WALTER'S
VICTOREEN'S
12
11
10
9
8
7
6
5
4
3
2
1
0
·0
·05
·10
·15
·20
·25
·30
·35
·40
·45
·50
λ IN A.U.

The linear absorption coefficient for chamber No. (4) of atomic number 20.84

Fig. (27)

$\mu' = (e\sigma_a + e^2)\, n_z$ $\qquad n_z = 4.64 \times 10^{23}$ electrons/cc.

$\mu = (e\sigma_a + e\sigma_s + e^2)\, n_z$ Taking into account the effect of true scattering.

λ in A.U.	μ' Vict.	μ' Walt.	μ Vict.	μ Walt.
.013	.0436	.0436	.100	.100
.04	.0508	.0504	.168$_7$	.168
.06	.0631	.0615	.208$_5$	.207
.08	.091	.086	.256	.252
.10	.137$_6$	.129	.319	.311
.12	.206^6	.195	.401	.390
.14	.306	.288	.510	.494
.16	.440	.414	.654	.628
.18	.609	.576	.830	.798
.20	.822	.780	1.05	1.007
.22	1.084	1.028	1.315	1.26
.24	1.39	1.327	1.63	1.56$_3$
.25	1.57	1.51$_5$	1.81	1.73^6
.28	2.17	2.09^5	2.42	2.34^6
.30	2.67	2.57	2.92	2.82
.32	3.17	3.11	3.47	3.37
.34	3.85	3.73	4.10	3.99
.35	4.19	4.066	4.44	4.32
.38	5.34	5.20	5.60	5.45
.40	6.21	6.05	6.48	6.32
.42	7.16	7.00	7.44	7.28
.44	8.22	8.05	8.48	8.31
.45	8.75	8.61	8.94	8.88
.48	10.59	10.44	10.85	10.70
.50	11.91	11.80	12.20	12.08

(f) The Stopping power per electron " S."

This question has been investigated by many authors and seems to present pracitcal difficulties. From Madgwick's [54] measurements the relative stopping power S, is found to be independent of the atomic number. From Z = 13 to Z = 79, S showed little tendency to decrease as Z increased. Gray [4] studied this question experimentally and came to the conclusion that the stopping powers of any two media are independent of the speed of the particles. It is also independent of the wave length of the radiation whatever the nature of the wall material may be. Gray also found a change of about 9% from Z = 6 to Z = 13 and another 8% between Z = 13 and Z = 29. His results are in good agreement with Bethe's [55] theoretical values.

The following values of the ratio of the stopping powers for various atomic numbers are calculated from Gray's[4] values for S.

$$\frac{S\ (7.64)}{S\ (12.84)} = .95\ ,\quad \frac{S\ (7.64)}{S\ (17.04)} = .923\ \&\quad \frac{S\ (7.64)}{S\ (20.84)} = .91$$

(9) Calculation of the Ratio of Ionization "F"

These values of the ratio of the stopping powers together with the values of the quantities σ_a & τ calculated in the previous tables (pp. (79, 83 ... 90) were used for the determination of the theoretical ratio of the ionization currents F from equation (7) p(68)). which should be obtained if the theory is a full explanation of the facts. F_V is determined by inserting the value of τ from Victoreen's formula while F_W is the value of the ratio when using Walter's value for τ . σ_a is the same for both since it is independent on Z (see p. (77).

The following tables together with the accompnaying graphs fig. (28,29 and 30) represent the ratio of the ionization for the chambers used in the investigation calculated on the basis of Gray's theory for the ionization in small chambers.

Figure (28)

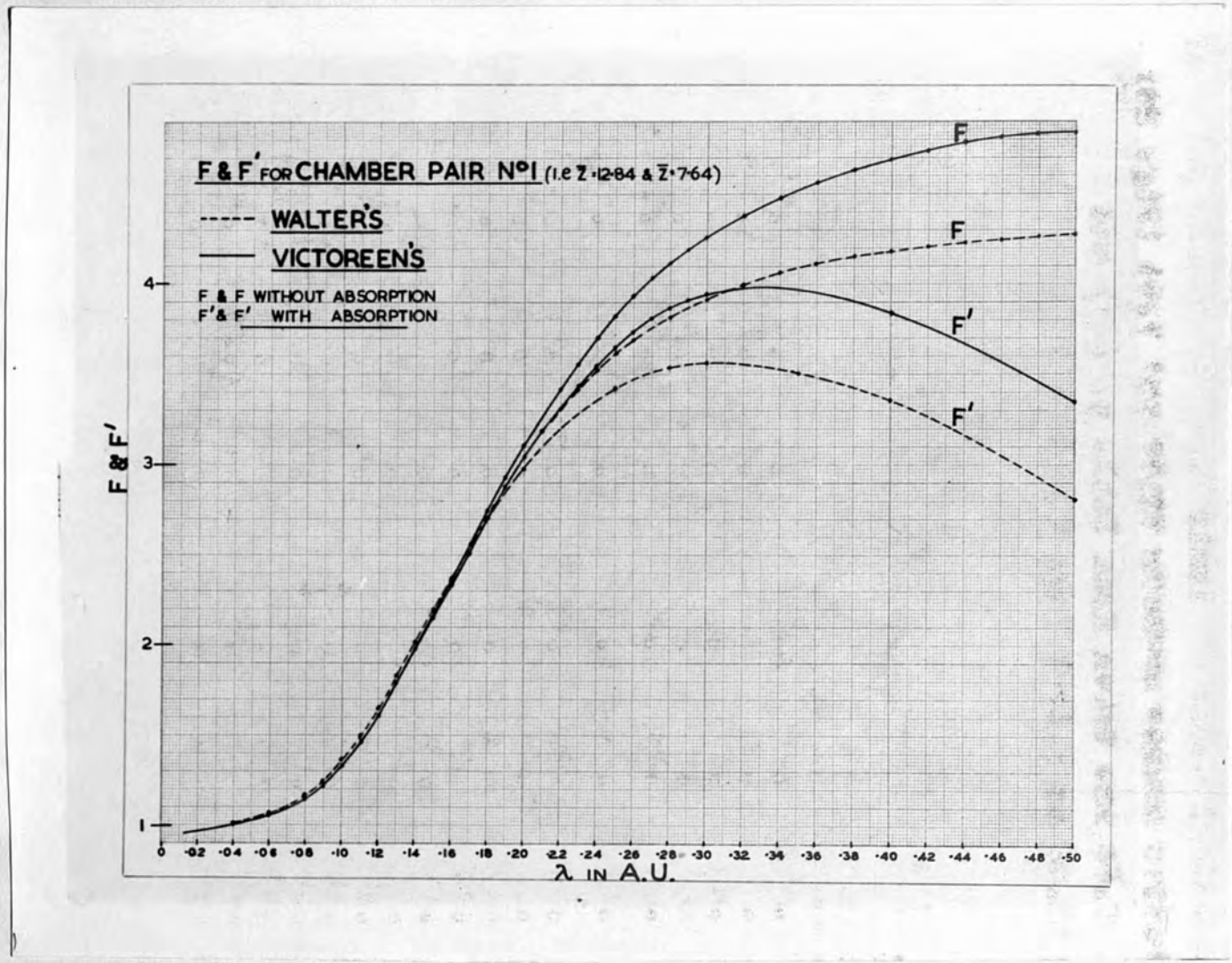
F & F' FOR CHAMBER PAIR N°1 (i.e $\bar{Z}$ ·12·84 & $\bar{Z}$ ·7·64)
----- WALTER'S
—— VICTOREEN'S
F & F WITHOUT ABSORPTION
F' & F' WITH ABSORPTION
F
F
F'
F'
F & F'
1
2
3
4
0 ·02 ·04 ·06 ·08 ·10 ·12 ·14 ·16 ·18 ·20 ·22 ·24 ·26 ·28 ·30 ·32 ·34 ·36 ·38 ·40 ·42 ·44 ·46 ·48 ·50
λ IN A.U.

Theoretical ratio of ionization in chamber pairs of effective atomic numbers 12.84 and 7.64 (Fig. 28) e^{T} for $\overline{Z} = 7.64$ are taken from Table p. (83) and e^{T} for 12.84 on p.(85) from Table (79).

λ in A.U.	F_W	F_V	λ in A.U.	F_W	F_V
.013	0.95	0.95	.23	3.42_5	3.57
.04	1.01	1.01	.24	3.53^5	3.695
.06	1.065	1.06	.25	3.61	3.82
.08	1.16	1.14	.26	3.69	3.94
.09	1.25_4	1.23	.27	3.76	4.03
.10	1.36_7	1.34	.28	3.81	4.11_5
.11	1.50	1.47	.29	3.87	4.20
.12	1.64	1.61	.30	3.91_5	4.26
.13	1.82_5	1.84	.32	4.00^5	4.38
.14	2.01^5	1.97	.34	4.07	4.69
.15	2.19	2.16	.36	4.11	4.57_5
.16	2.37	2.35_5	.38	4.15_6	4.63^5
.17	2.55	2.55^2	.40	4.17^6	4.68_6
.18	2.72_5	2.74^5	.42	4.20_7	4.73^6
.19	2.89^3	2.92^3	.44	4.22^7	4.78_2
.20	3.068	3.11	.46	4.24^5	4.81^2
.21	3.18	3.276	.48	4.25_5	4.83
.22	3.30	3.42	.50	4.28^5	4.86

Figure(29)

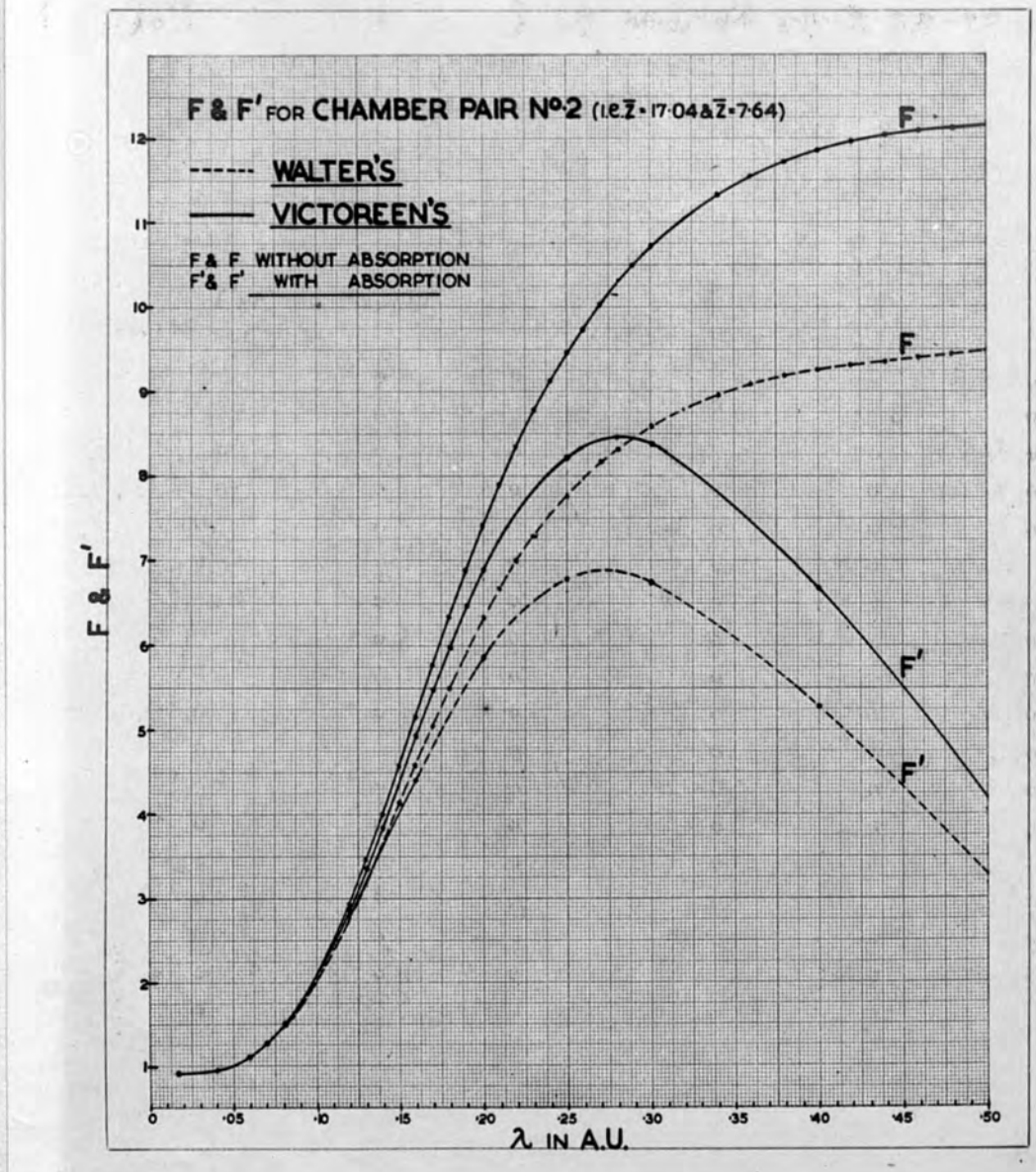
F & F' FOR CHAMBER PAIR No.2 (i.e. $\bar{z}$ = 17·04 & $\bar{z}$ = 7·64)
WALTER'S
VICTOREEN'S
F & F WITHOUT ABSORPTION
F' & F' WITH ABSORPTION
F
F
F'
F'
F & F'
λ IN A.U.
0
·05
·10
·15
·20
·25
·30
·35
·40
·45
·50
1
2
3
4
5
6
7
8
9
10
11
12

Theoretical ratio of ionization in chamber pairs of effective atomic numbers 17.04 and 7.64 (Fig. 29)
$\mathcal{T}$'s are taken from Tables p. (87 483) & con P.(79).

λ in A.U.	F_W	F_V.	λ in A.U.	F_W	F_V
.013	.923	.926	.23	7.28	8.78
.04	.960	.968	.24	7.55	9.11
.06	1.05	1.07	.25	7.77	9.45
.08	1.46	1.51	.26	7.97	9.75
.09	1.68	1.76	.27	8.16	10.02
.10	2.00	2.10	.28	8.30	10.31
.11	2.38	2.49	.29	8.48	10.50
.12	2.76	2.94	.30	8.58	10.70
.13	3.18	3.46	.32	8.78	11.03
.14	3.65	4.01	.34	8.95	11.34
.15	4.13	4.58	.36	9.08	11.55
.16	4.59	5.17	.38	9.20	11.71
.17	5.05	5.76	.40	9.25	11.86
.18	5.51	6.33	.42	9.32	11.96
.19	5.93	6.88	.44	9.36	12.03
.20	6.32	7.42	.46	9.42	12.08
.21	6.65	7.88	.48	9.45	12.12
.22	6.98	8.35	.50	9.50	12.16

Figure (30)

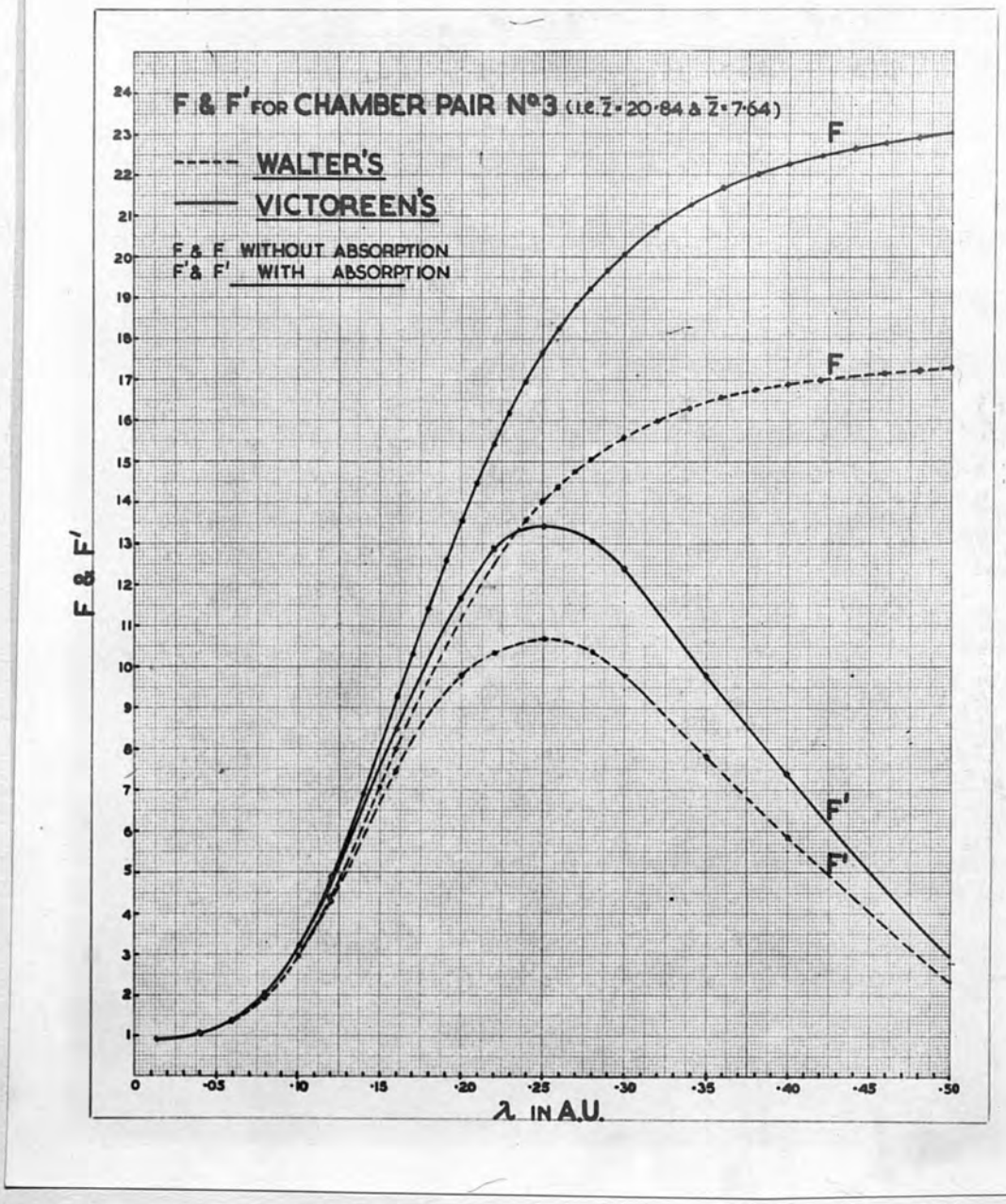
F & F' FOR CHAMBER PAIR No 3 (i.e. $\bar{Z}$ = 20·84 & $\bar{Z}$ = 7·64)
WALTER'S
VICTOREEN'S
F & F WITHOUT ABSORPTION
F' & F' WITH ABSORPTION
F
F
F'
F'
F & F'
λ IN A.U.
0
·05
·10
·15
·20
·25
·30
·35
·40
·45
·50

Theoretical ratio of ionization in chamber pairs of effective atomic numbers 20.84 and 7.64 (Fig. 30). $\sigma\tau$'s are taken from Tables on p. (89, 83) and σ_a from Table on p. (79).

λ in A.U.	F_W	F_V	λ in A.U.	F_W	F_V.
.013	.914	.915	.23	13.10	16.24
.04	1.03	1.04	.24	13.60	16.95
.06	1.33	1.37	.25	14.04	17.65
.08	1.95	2.06	.26	14.40	18.26
.09	2.41	2.53	.27	14.80	18.85
.10	2.98	3.24	.28	15.07	19.16
.11	3.64	3.96	.29	15.40	19.70
.12	4.37	4.83	.30	15.60	20.07
.13	5.23	5.80	.32	15.97	20.68
.14	6,12	6.90	.34	16.30	21.30
.15	7.04	8.03	.36	16.55	21.67
.16	7.94	9.20	.38	16.75	22.00
.17	8.90	10.30	.40	16.85	22.29
.18	9.67	11.44	.42	16.99	22.45
.19	10.50	12.60	.44	17.10	22.62
.20	11.24	13.54	.46	17.16	22.80
.21	11.88	14.50	.48	17.24	22.90
.22	12.48	15.44	.50	17.35	23.00

So far the ratio of the ionization currents has been determined without absorption in the walls of the chambers. Equation (10) p. (70) gives the ratio taking into account the absorption in the walls when $\cos\theta$ is neglected*, and (11) when it is put into the coefficient μ. It was found that the two equations gave the same value for F for a certain wavelength and a certain pair of chambers.

We proceed now by evaluating the factor f responsible for the absorption in the walls:

$$f = \frac{\int_0^{\frac{\pi}{2}} \cos\theta \, e^{-\mu_1' r_1 \left[\sqrt{\frac{r_2^2}{r_1^2} - \sin^2\theta} - \cos\theta\right]} \, d\theta}{\int_0^{\frac{\pi}{2}} \cos\theta \, e^{-\mu_1' r_1 \left[\sqrt{\frac{r_2^2}{r_1^2} - \sin^2\theta} - \cos\theta\right]} \, d\theta}$$

This expression was determined graphically for each λ in the Tables pp. (104, 105, 106).

The following example illustrates the procedure followed for calculating "f."

Evaluation of the factor "f", for $\lambda = 0.5$ A.U. for chamber pairs of $\overline{Z}$ (12.84 and 7.64):

1 – Evaluation of $r_1\left[\sqrt{\frac{r_2^2}{r_1^2} - \sin^2\theta} - \cos\theta\right]$

$r_1 = 1.00$ cm. $\qquad r_2 = 1.15$cm.

$r_2^2/r_1^2 = 1.322$

* Ideally it might be desirable to neglect $\cos\theta$ in the absorption coefficient since this type of scattered radiation would presumably contribute to the production of ionization.

θ	$\sin\theta$	$\sin^2\theta$	$\cos\theta$	$\frac{r_2^2}{r_1^2}-\sin^2\theta$	$\sqrt{\frac{r_2^2}{r_1^2}-\sin^2\theta}$	$r_1\left[\sqrt{\frac{r_2^2}{r_1^2}-\sin^2\theta}-\cos\theta\right]$
0	0	0	1	1.322	1.15	0.150
10	0.1736	0.0301	0.985	1.292	1.136	0.151
20	0.3420	0.1170	0.940	1.205	1.098	0.158
30	0.5000	0.250	0.866	1.072	1.035	0.169
40	0.6428	0.413	0.766	0.909	0.953	0.187
50	0.7660	0.587	0.643	0.735	0.856	0.213
60	0.8668	0.750	0.500	0.572	0.756	0.256
70	0.9397	0.883	0.342	0.439	0.662	0.320
80	0.9848	0.970	0.174	0.353	0.593	0.419
90	1.00	1.00	0	0.322	0.567	0.567

2- Evaluation of the integrals envolved in the factor "f"

$\mu_1' = 0.621$ from table on p. (92)

$\mu_2' = 2.79$ from table on p. (93)

θ	$\mu_1' r_1\left[\sqrt{\frac{r_2^2}{r_1^2}-\sin^2\theta}-\cos\theta\right]$	$e^{-\mu_1' r_1\left[\sqrt{\frac{r_2^2}{r_1^2}}\right.}$	$e^{-\mu_1' r_1[\ ]\cos\theta}$	$e^{\mu_2' r_1[\ ]}$	$e^{-\mu_2' r_1[\ ]}$	$e^{-\mu_2' r_1[\ ]\cos\theta}$
0	0.0932	0.911	0.911	0.418	0.659	0.659
10	0.938	0.911	0.896	0.422	0.656	0.646
20	0.982	0.906	0.852	0.441	0.643	0.605
30	0.105	0.901	0.780	0.471	0.624	0.540
40	0.116	0.891	0.682	0.521	0.594	0.455
50	0.132	0.876	0.564	0.594	0.552	0.355
60	0.159	0.853	0.426	0.714	0.490	0.245
70	0.199	0.819	0.280	0.893	0.409	0.140
80	0.260	0.771	0.134	1.169	0.311	0.054

The values of $e^{-\mu_1 r_1\left[\sqrt{\frac{r_2^2}{r_1^2}-\sin^2\theta}-\cos\theta\right]}\cos\theta$ is plotted against θ and the area A_1 under the curve is determined graphically. Similarly for the area A_2 corresponding to putting the μ_2' in place of μ_1' in the above expression

$$f = 0.663$$

$$\therefore F' = 0.663 \times 4.28 = 2.81$$

Theoretical values for the ratio F_w' & F_v' given by equation (10) p. (70) for chamber pairs of effective atomic numbers 12.84 and 7.64 (Fig. 28).

The values of μ_1' are tablulated on pp.(92) and μ_2' on pp. (93). F_w and F_v are taken from tables on p.(98).

f_w and f_v are obtained by inserting σT from Walter's and Victoreen's equations respectively in the expression of "f" on p. (101).

λ in A.U.	F_w	$F_w' = f_w F_w$	f_v	$F_v' = f_v F_v$
.013	1	0.95	1	0.95
.04	1	1.01	1	1.01
.06	1	1.065	1	1.06
.08	1	1.16	1	1.144
.12	1	1.64	.998	1.61
.16	.984	2.33	.985	2.32
.20	.974	2.98	.974	3.03
.25	.974	3.42	.956	3.65
.28	.928	3.54	.941	3.87
.30	.910	3.56	.925	3.94
.40	.805	3.36	.820	3.84
.50	.663	2.81	.693	3.35

Theoretical values for F_w' & F_v' (Equation 10, p. (70) for chamber pairs of effective atomic numbers 17.04 and 7.64 (Fig. 29).

The values of μ_1' and μ_2' are taken from the tables on pp. (92) and (94) respectively.

F_w & F_v are taken from table of p(99).

λ in A.U.	f_w	$F_w' = f_w F_w$	f_v	$F_v = f_v F_v$
.013	1	.923	1	.926
.040	1	.960	1	.968
.060	1	1.05	1	1.07
.08	.999	1.46	.997	1.505
.12	.998	2.75	.980	2.88
.16	.960	4.41	.960	4.96
.20	.93	5.88	.927	6.87
.25	.871	6.78	.870	8.21
.30	.786	6.75	.784	8.38
.40	.572	5.29	.565	6.70
.50	.346	3.27	.345	4.19

Theoretical values for F_W' & F_V' (Equation 10 P. (70) for chamber pairs of effective atomic numbers 20.84 and 7.64 (Fig. 30).

The values of μ_1' and μ_2' are taken from the tables on pp. (92) and (95) respectively. The values F_W & F_V are taken from table on p(100).

λ in A.U.	f_W	$F_W' = f_W F_W$	f_V	$F_V' = f_V F_V$
.013	1	.914	1	.915
.04	1	1.026	1	1.039
.06	.999	1.328	.997	1.366
.08	.990	1.93	.989	2.037
.12	.971	4.24	.960	4.64
.16	.927	7.41	.923	8.49
.20	.871	9.80	.863	11.70
.22	.828	10.32	.832	12.86
.25	.760	10.68	.761	13.44
.28	.686	10.34	.680	13.05
.30	.628	9.80	.618	12.40
.35	.475	7.43	.457	9.80
.40	.346	5.86	.332	7.38
.50	.135	2.33	.129	2.97

(h) Comparison between F corresponding to the complete distribution curve and that corresponding to H.V.L.

It was thought that a point of interest might be to determine the ionization ratio from the complete distribution curve and to compare it with the ratio taken from the ratio-wavelength curves fig. (28,29,30) to see how far they agree with each other.

The F-ratio corresponding to the complete distribution curve.

For this purpose the effective $\overline{(e\sigma_a + e\tau)}$ was calculated from the spectral distribution curve.

$$\overline{(e\sigma_a + e\tau)} = \frac{\sum (e\sigma_a + e\tau)_{\lambda_1} A_1}{\sum A_1}$$

where $(e\sigma_a + e\tau)_{\lambda_1}$ is the value corresponding to the mean wavelength of a vertical strip on the graph of area A fig. (2) and the summation covers the whole area under the curve.

The values of $(e\sigma_a + e\tau)_{\lambda_1}$, $(e\sigma_a + e\tau)_{\lambda_2}$ .... etc. were taken from fig. (19,20,21,22,23) for $e\sigma_a$ and $e\tau$ respectively. The total areas under the curves were taken from Tables on pp. (32, 35 & 38).

The following example shows the evaluation of $\overline{(e\sigma_a + e\tau)}$ for a distribution curve of 150 kVp and H.V.L. 5mm.Al. for chamber pairs of 20.84 and 7.64.

λ mean in A.U.	$(\sigma_a+\tau_W)_{7.64}$ $\times 10^{26}$	$(\sigma_a+\tau_W)_{7.64} A_1$ $\times 10^{26}$	$(\sigma_a+\tau_V)_{7.64}$ $\times 10^{26}$	$(\sigma_a+\tau_W)_{20.84}$ $\times 10^{26}$	$(\sigma_a+\tau_W)_{20.84}$ $\times 10^{26}$	$(\sigma_a+\tau_W)_{20.84}$ $10^{26} \times A_1$	$(\sigma_a+\tau_V)_{20.84}$ $\times 10^{26}$	$(\sigma_a+\tau_V)_{20.84}$ $\times 10^{26} \times A_1$
.115	8.5	.0213	8.25	.0206	37.00	.0925	40.00	0.10
.1375	9.0	.348	8.80	.3408	59.50	2.308	62.6	2.43
.1625	10.2	.810	9.30	.738	94.00	7.45	99.00	7.855
.1875	12.1	1.235	11.00	1.122	140.0	14.28	148.5	15.10
.2125	15.1	1.64	13.00	1.425	202.0	22.17	210.0	22.00
.2375	18.8	2.03	15.60	1.685	280.0	30.25	292.0	30.40
.270	24.97	3.78	20.47	3.10	407.0	61.70	422.3	64.00
.315	36.8	5.38	29.30	4.285	642.0	94.00	660.0	96.50
.370	56.74	6.80	44.41	5.325	1042	125.0	1065.0	127.9
.450	98.9	9.40	75.8	7.20	1870	177.7	1870.0	177.6
.575	202.4	7.59	150.8	5.65	36814	145.8	3828.0	143.7
.750	445.9	2.23	320.4	1.61	86419	43.2	8402.0	42.01

$\Sigma(\overline{\sigma_a+\tau_W})A_1$ $\Sigma(\sigma_a+\tau_V)A_1$ $\Sigma(\sigma_a+\tau_W)A_1$ $\Sigma(\sigma_a+\tau_V)A_1$

$= 41.26$ $= 32.50$ $= 723.95$ $= 729.6$

$A = .9955$ taken from p (35)

Thus $\overline{(\sigma_a+\tau_W)}_{7.64} = 41.5 \times 10^{-26}$ & $(\overline{\sigma_a+\tau_V})_{7.64} = 32.7 \times 10^{-26}$

& $(\sigma_a+\tau_W)_{20.84} = 727 \times 10^{-26}$ & $(\sigma_a+\tau_V)_{20.84} = 733$ 10

where τ_W & τ_V are the photoelectric absorption coefficients from Walter's & Victoreen's formulae respect.

The values of $(\overline{e\sigma_a + e\tau})$ used for calculating F in the following table were determined in the same manner for all the Z used and all the kVp stated in the table.

Column (1) gives the kVp applied to the X-ray tube.

" (2) gives the effective wavelength determined from the complete spectral distribution energy.

" (3) gives the effective wavelength corresponding to the H.V.L.

" (4) gives the effective atomic number of each pair of chambers used.

" (5) contains the ratio F calculated by Gray's theory using the $(\overline{e\sigma_a + e\tau})$ evaluated from the spectral distribution.

" (6) is the ratio taken from figs. (28,29,30) which corresponds to λ_e of the H.V.L. of the beam.

" (7) the ratio taken from figs. (28,29,30) for λ_e from the energy distribution curve.

(1)	(2)	(3)	(4)	(5)		(6)		(7)	
KVp	λ_e Distribution Curve	λ_e From H.V.L.	$\bar{Z}$	From $\overline{(\sigma_a + \sigma_T)}$		From λ_e of the H.V.L.		From curves ratio corresponding to λ from Distribution Curves.	
				F(W)	F(V)	F(W)	F(V)	F(W)	F(V)
90	.417	.405	(12.84 & 7.64)	4.25	4.88	4.19	4.7	4.21	4.73
			(17.04 & 7.64)	9.41	12.03	9.27	11.89	9.31	11.95
			(20.84 & 7.64)	17.25	22.9	16.9	22.3	16.98	22.42
150	.287	.288	(12.84 & 7.64)	3.98	4.38	38.60	4.18	38.60	4.18
			(17.04 & 7.64)	8.73	10.97	8.43	10.91	8.44	10.91
			(20.84 & 7.64)	15.94	20.40	15.30	19.58	15.30	19.58
170	.256	.269$_6$	(12.84 & 7.64)	3.87	4.81	3.76	4.03	3.67	4.01
			(17.04 & 7.64)	7.67	9.19	8.15	9.98	7.87	9.59
			(20.84 & 7.64)	15.40	19.6	14.8	18.85	14.30	18.10

IV.

EXPERIMENTAL DETERMINATION OF THE RATIO "F"

(a) The processing of the chambers

The bakelite synthetic resin was obtained from Messrs. "Bakelite Ltd.", the cerium oxide (CeO_2) and vanadium (V_2O_5) from Messrs. Griffin and Tatlock and the graphite from Messrs. Cromile and Piercy. The latter was guaranteed very pure.

Chambers were made from the mixtures given in the following table:

No.	Composition	z by calculation
1.	50 gram of bakelite 10 gram of graphite 1 gram of V_2O_5	7.64
2.	50 gram of bakelite 10 gram of graphite 1 gram of CeO_2	12.84
3.	50 gram of bakelite 10 gram of graphite 2.55 gram of CeO_2	17.04
4.	50 gram of bakelite 10 gram of graphite 5 gram of CeO_2	20.84

Figure(3I)

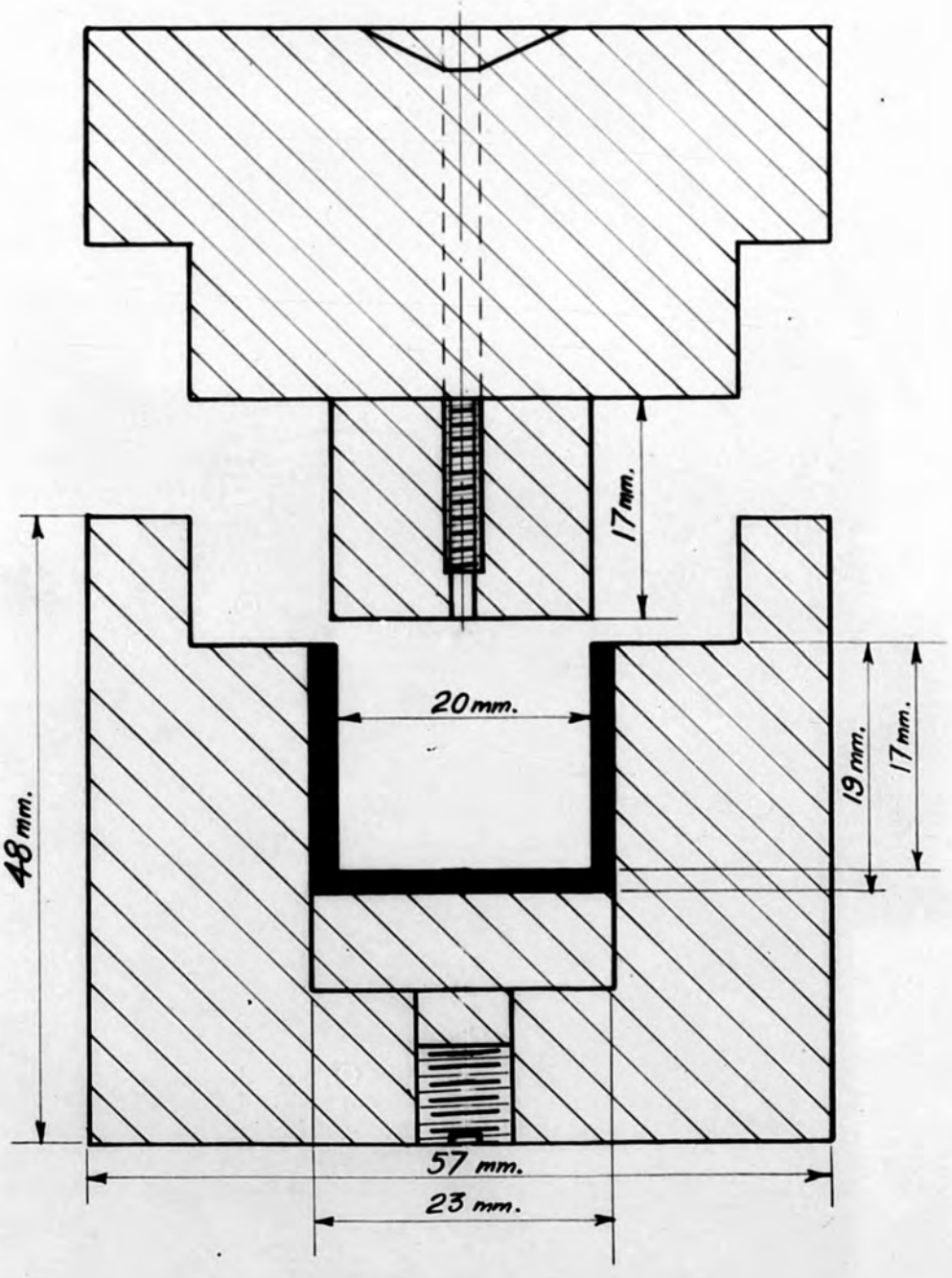

— THE CHAMBER MOULD —

Figure(32)

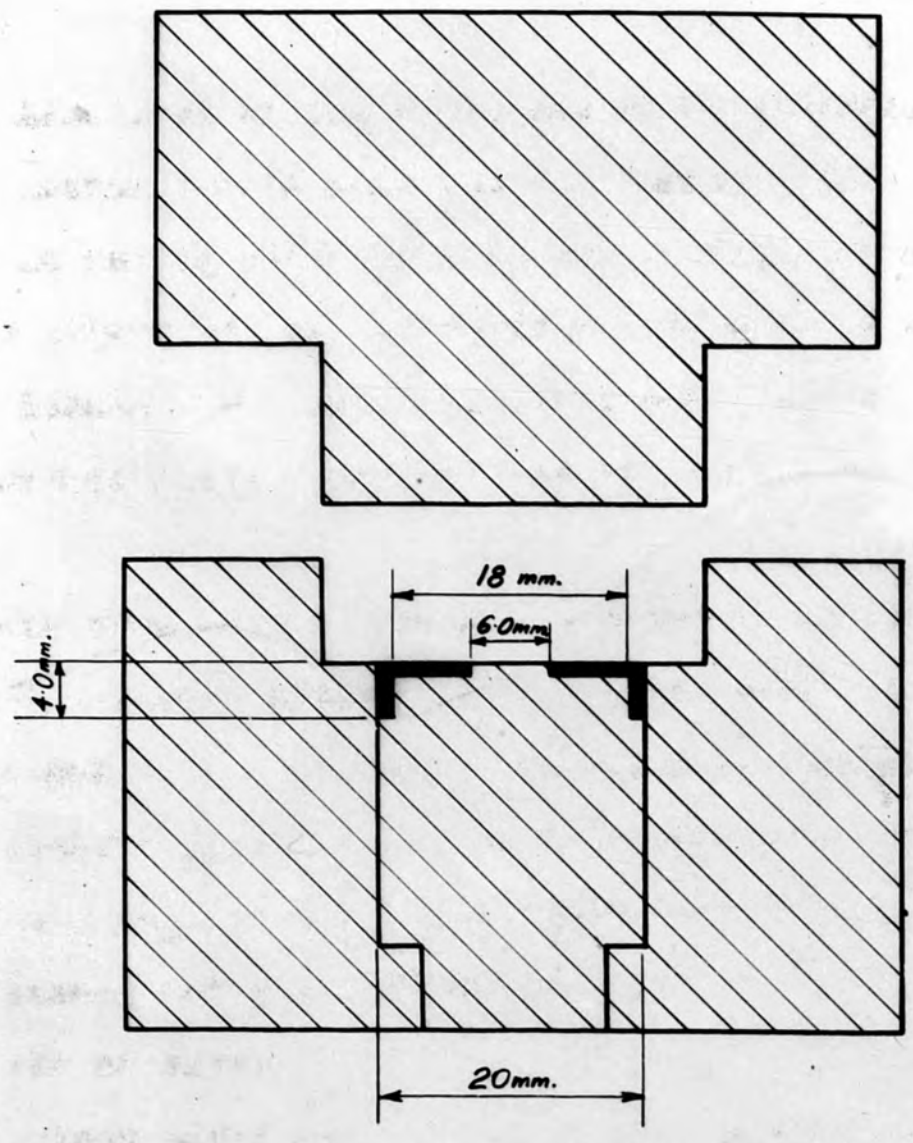

— GUARD RING MOULD —

The bakelite resin was first ground in a ball mill, for about eight hours. It was then sieved through a mesh 60 to the inch. The fine bakelite powder so obtained was mixed with the graphite and the proper amount of V_2O_5 or CeO_2. The complete mixture was placed in the ball mill and ground for another eight hours to ensure good mixing.

The moulds in which the chamber parts were moulded figs. (31.32) were made of high tensile steel. The mould was first warmed on a Bunsen flame and lubricated with paraffin wax after which it was filled with powder. It was then put in a suitable hydraulic press and heated by a gas ring up to 270°C. Simultaneously the pressure was raised gradually up to about 2000 pounds to the square inch. Under these conditions the synthetic resin polymerises, passes into a state of flux and takes up the shape of the mould. After this it was kept in the mould until it became a hard solid material. The time required for the polymerization process was about five minutes.

After "cooking", the chamber parts may be removed from the mould. The method of construction thus enables the chambers and auxiliary parts to be made exactly to one pattern. All these mixtures were found easy to manufacture.

Figure(33)

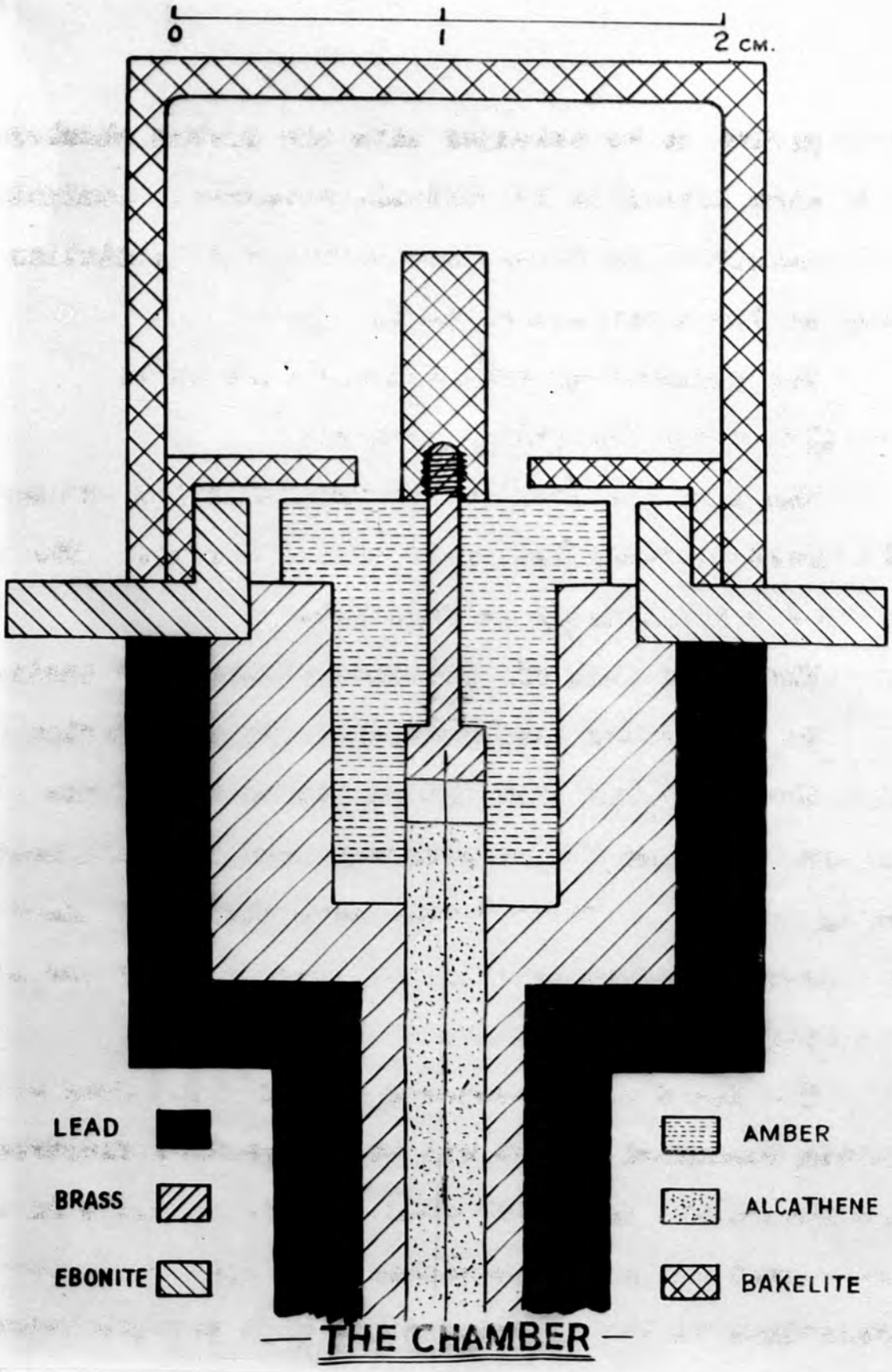
0
1
2 CM.
LEAD
BRASS
EBONITE
AMBER
ALCATHENE
BAKELITE
THE CHAMBER

They proved to be stronger than the carbon chambers. They also proved to be reliable electrical conductors and consistant in their interaction with radiation as seen in the experimental data.

Two chambers of each mixture were made.

b Details of the Ionization chambers

The chambers used in the investigation are made in the moulds already described (figs. 31.32). The essential parts are illustrated in fig. (33).

The guard ring was provided so that the ionization will be due to the one material. By this device we ensure that the electrons from the walls, which produce the ionization, come almost entirely from the wall material being studied. Those coming from the amber insulator are prevented from contributing very much to the ionization.

c- The Leads:

The leads are telcothene cables about four metres in length connected at one end to the central electrode and the chamber. The other ends connect to plugs in the instrument via amber insulation and make the necessary connection to the condensers and high tension terminals.

The cables are screened and protected by metallic

Figure (34)

—THE ELECTRICAL CIRCUIT—

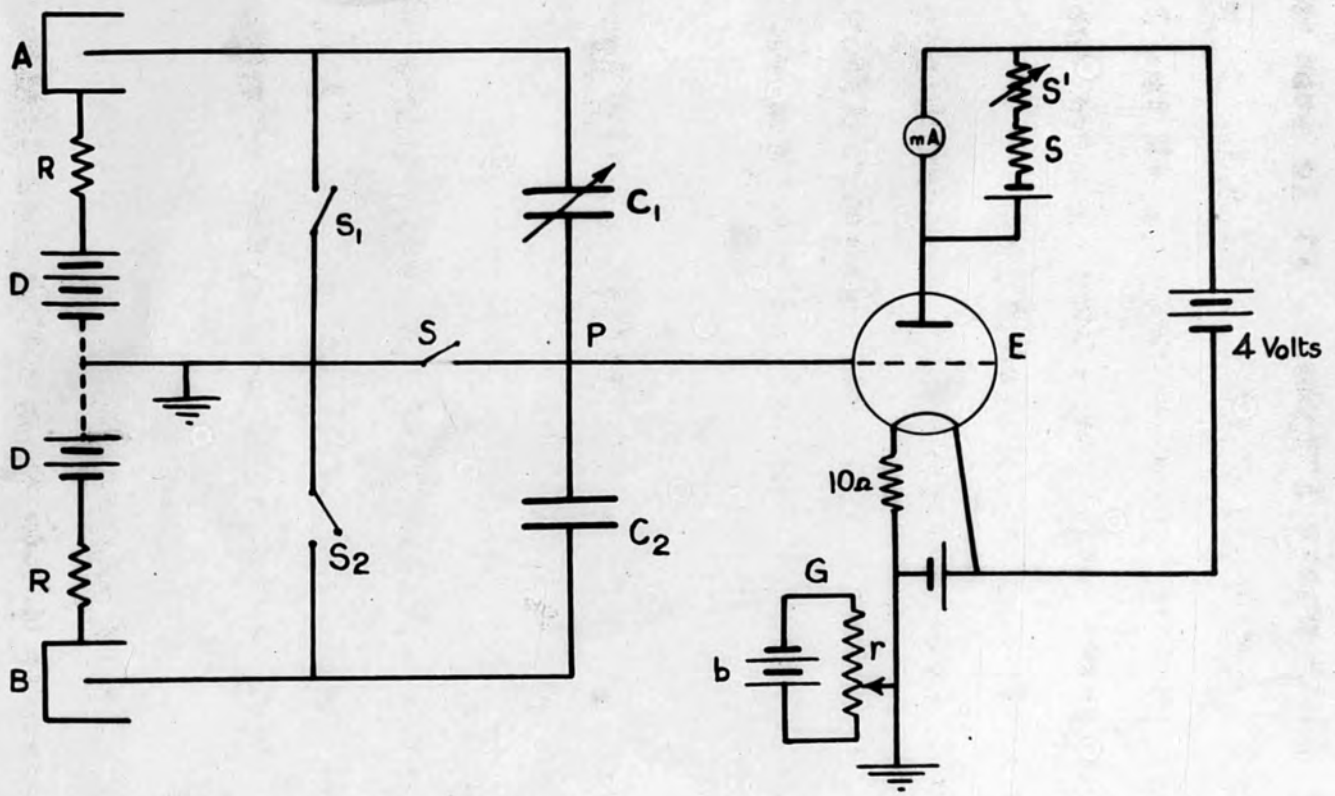

A & B Ionization Chambers

R & R High Resistances 1 MΩ

D & D Dry Batteries of 228 volts each

$S_1 S_2$ & S Switches

C_1 & C_2 Condensers of capacity about 120 μμF each.

E The electrometer triode valve

mA The microameter

S Fixed resistance 1000Ω

S' Two variable resistances in series, one coarse 20,000Ω & one fine 40Ω.

G Grid Bias potentiometer arrangement
r – 40,000Ω b – 4 volts

tubing covering their whole length. It is assumed in the theory of the instrument used (p.114) that C' and C'' (which are almost entirely the capacities of the leads) are equal. Thus great care was taken to make the cables equal in length to fulfil this condition.

In our experiments, however, it was never necessary to interchange the leads and if any slight difference in the capacity exists it will be included in the calibration of the apparatus.

(b) Apparatus for measuring the ratios of the ionization currents in pairs of chambers.

(i) The electrical circuit

The electrical circuit used is essentially that described by Kemp(56) and is shown in fig. (34). The theory of its action, which has been given by Kemp(8) is as follows.

(ii) The Theory of the Apparatus

The two chambers A and B in which the ionization currents are to be compared are connected in such a way that, when they are irradiated, the central electrode of one of them, say A, accumulates a positive charge while that of the other accumulates a negative charge. Let the

potential difference of the collecting system of A be V_1 and its capacity C' and that of B be V_2 and its capacity C''

Thus
$$V_1 = \frac{Q_1}{C_1 + C'} \quad \ldots\ldots \quad (1)$$

and
$$V_2 = \frac{-Q_2}{C_2 + C''}, \quad \ldots\ldots \quad (2)$$

where Q_1 and Q_2 are the charges collected on the electrodes in a certain time.

Thus
$$\left| \frac{V_2}{V_1} \right| = \frac{Q_2}{Q_1} \cdot \frac{C_1 + C'}{C_2 + C''}, \quad \ldots\ldots \quad (3)$$

If the point P between C_1 and C_2 is at earth potential, then V_1 and V_2 will be the potential differences across the capacities C_1 and C_2 and hence

$$\left| \frac{V_2}{V_1} \right| = \frac{C_1}{C_2} \quad \ldots\ldots \quad (4)$$

From (3) and (4) we get:

$$\frac{Q_2}{Q_1} = \frac{C_1}{C_2} \cdot \frac{C_2 + C''}{C_1 + C'} \quad \ldots (5)$$

C' and C'' are almost entirely the capacities of the

leads. They can be made practically equal and much greater than C_1 or C_2 for all possible values of C_1 and C_2. If, however, any slight difference between the values of C' and C'' exists it will be included in the calibration of the instrument and therefore will not affect the observations. Hence (5) can be written:

$$F = \frac{Q_2}{Q_1} \simeq \frac{C_1}{C_2} \qquad \ldots\ldots \quad (6)$$

Therefore the setting of the capacity potential divider which keeps P at earth potential after opening the switches S_1, S_2 and S is a measure of the ratio $\frac{Q_2}{Q_1}$ i.e. the ratio F of the ionization currents in the two chambers.

The microammeter in the anode circuit of the valve provides a fine means for detecting the proper setting for the balance.

(iii) Practical Construction for the Circuit:

C_1 and C_2 are two ordinary wireless air condensers. The capacity of each is approximately 120 $\mu\mu$F. They were modified to suit the purpose to which they are put by taking out some of the plates to reduce the capacity.

The insulation is of amber throughout. One of the condensers is kept fixed nearly at its full capacity while the capacity of the other can be varied. The latter is joined through amber insulation to a dial control. Both condensers are provided with amber insulated leads to the rest of the apparatus. These two condensers constitute the capacity potential divider.

An electrometer triode valve was used to indicate balance. Its essential characteristic is the extremely low value of grid current when operated under certain conditions. This is very useful for measuring small currents such as the ionization currents produced in the chambers by radiation. It provides an alternative to the more usual forms of electrometers which may be very delicate and need elaborate precautions and adjustment. The valve is mounted on a rubber base to prevent vibrations affecting the filament which result in a change of filament current. In our experiments the valve was used as a sensitive means for detecting the correct setting of the capacity potential divider and therefore the observations are independent of its characteristics. A micoram-meter, reading 50 μA , is connected in the anode circuit

of the valve to provide a sensitive indication of the correct setting.

(iv) Other parts of the circuit

The grid bias consists of a potentiometer arrangement. Two accumulators are used with a rheostat of the order of 40,000 Ω. This arrangement is found useful for it prevents the anode current from drifting when the grid is disconnected from the earth. The grid potential is kept at a voltage slightly less than -2 volts.

A resistance of 10 ohms is included in the filament circuit to adjust the current to the required value.

Two high resistances R and R connect the terminals of the chambers to the high tension battery to prevent any possibility of short circuit.

Two accumulators each of two volts are used for the anode potential.

The arrangement for backing off the current consists of two variable resistances S and S', one for coarse and the other for fine adjustment, connected to the anode in the manner shown in fig. (34).

(v) The switches

The switches constitute a very important part of

Figure(35)

— DIFFERENT VIEWS OF THE SWITCHES —

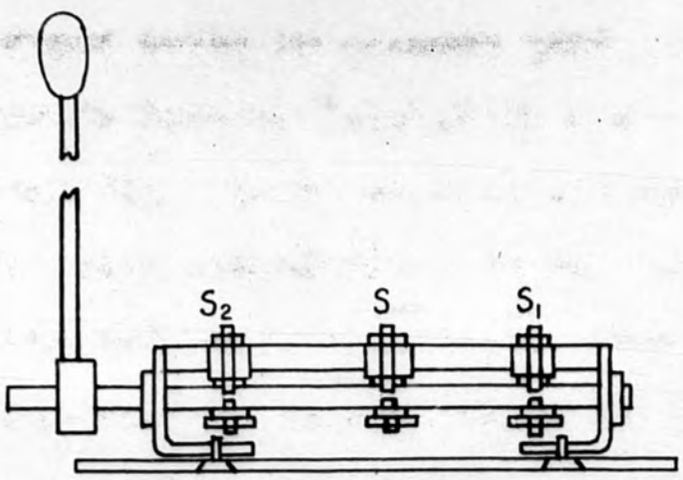

FRONT ELEVATION

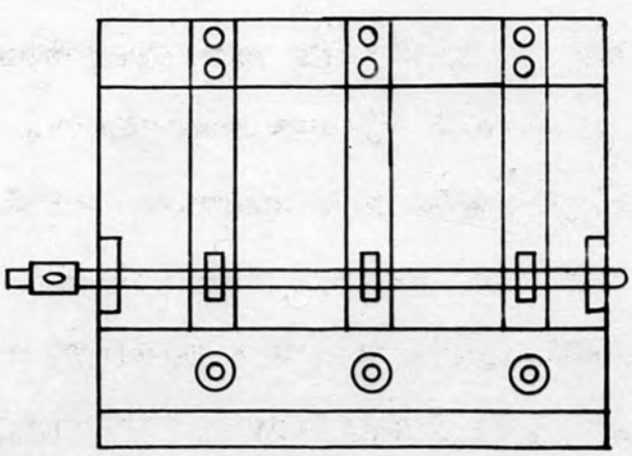

PLAN

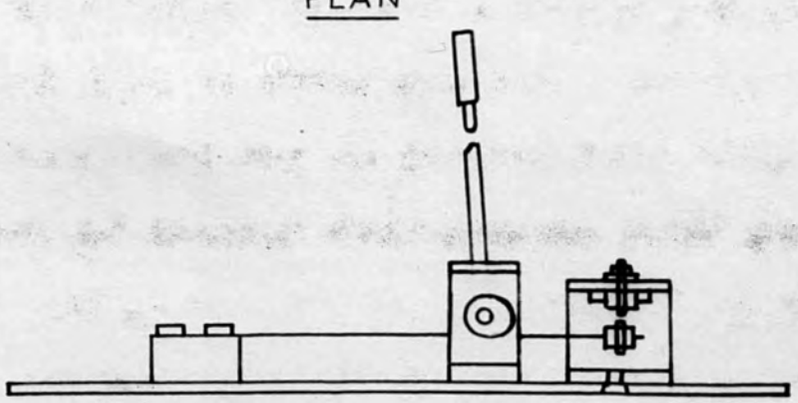

SIDE ELEVATION

the circuit. They consist of three light strips of spring (60 mm. x 7 mm. x 24 S.W.G.) mounted at one end on a block of brass and each carrying a platinum contact at its free end. These contacts are held against similar platinum contacts mounted in amber insulators set in a brass block. The three sets of contacts are separated to break the circuit by three cams which are mounted on a shaft and press on to the steel spring so as to deflect them when rotated. The cams are operated together by a lever which is attached to the cam shaft. The three amber insulated contacts are provided with leads which connect them with the rest of the circuit while the contacts on the steel springs are connected throughout the frame to earth. The brass block carrying the earth and the insulated contacts are both mounted on to a base plate of brass. The cam shaft is held in position by two brackets also mounted on the base plate. The time of opening each contact with respect to the others is arranged by the setting of its cam on the cam shaft. Fig. (35) shows different views of the switches. Figs. (36,37) show photographs of the apparatus and chambers.

Interior of the Apparatus showing valve, capacity potential divider, switches, etc.

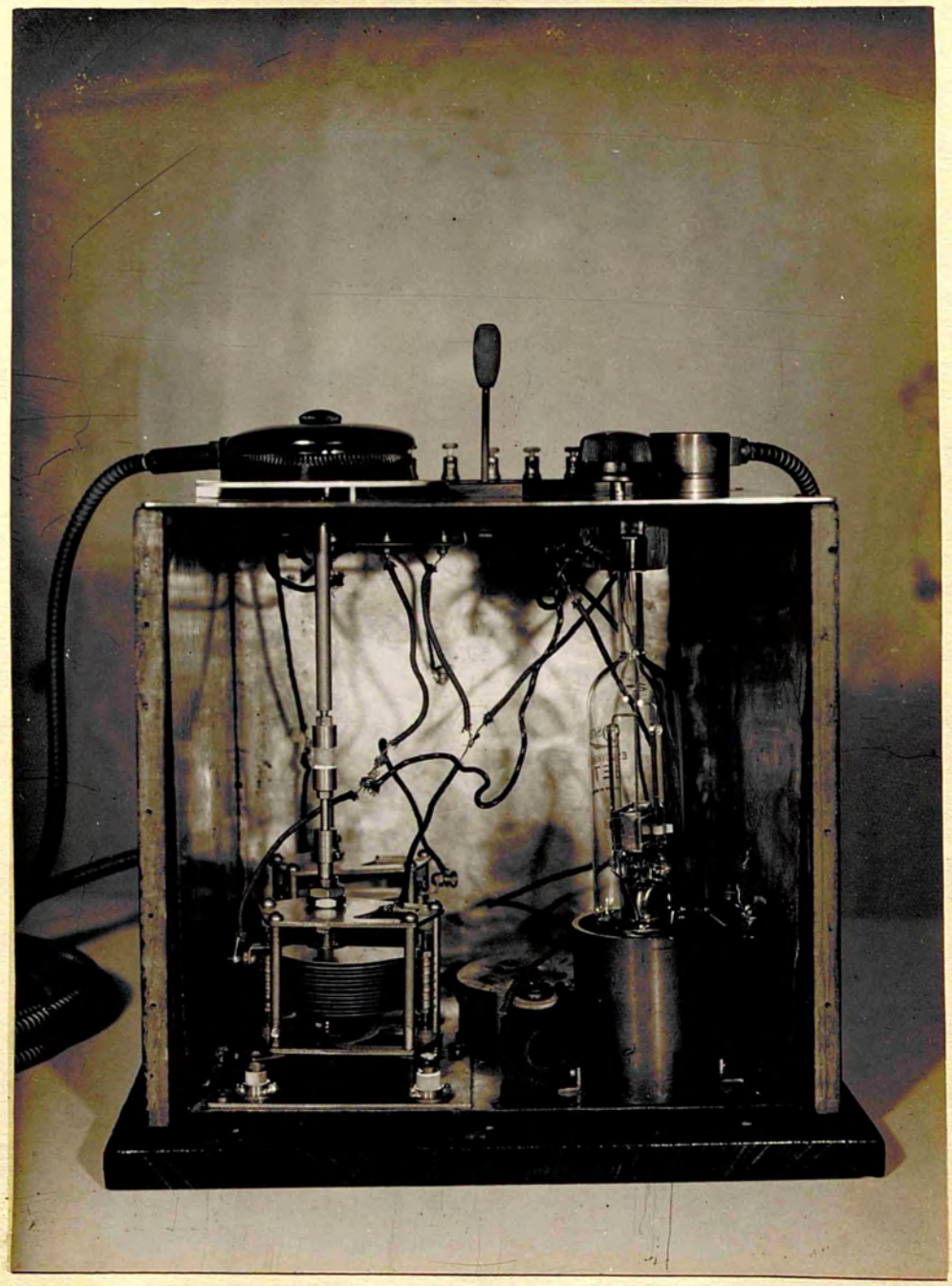

Figure (36)

The Apparatus, Chambers and Leads

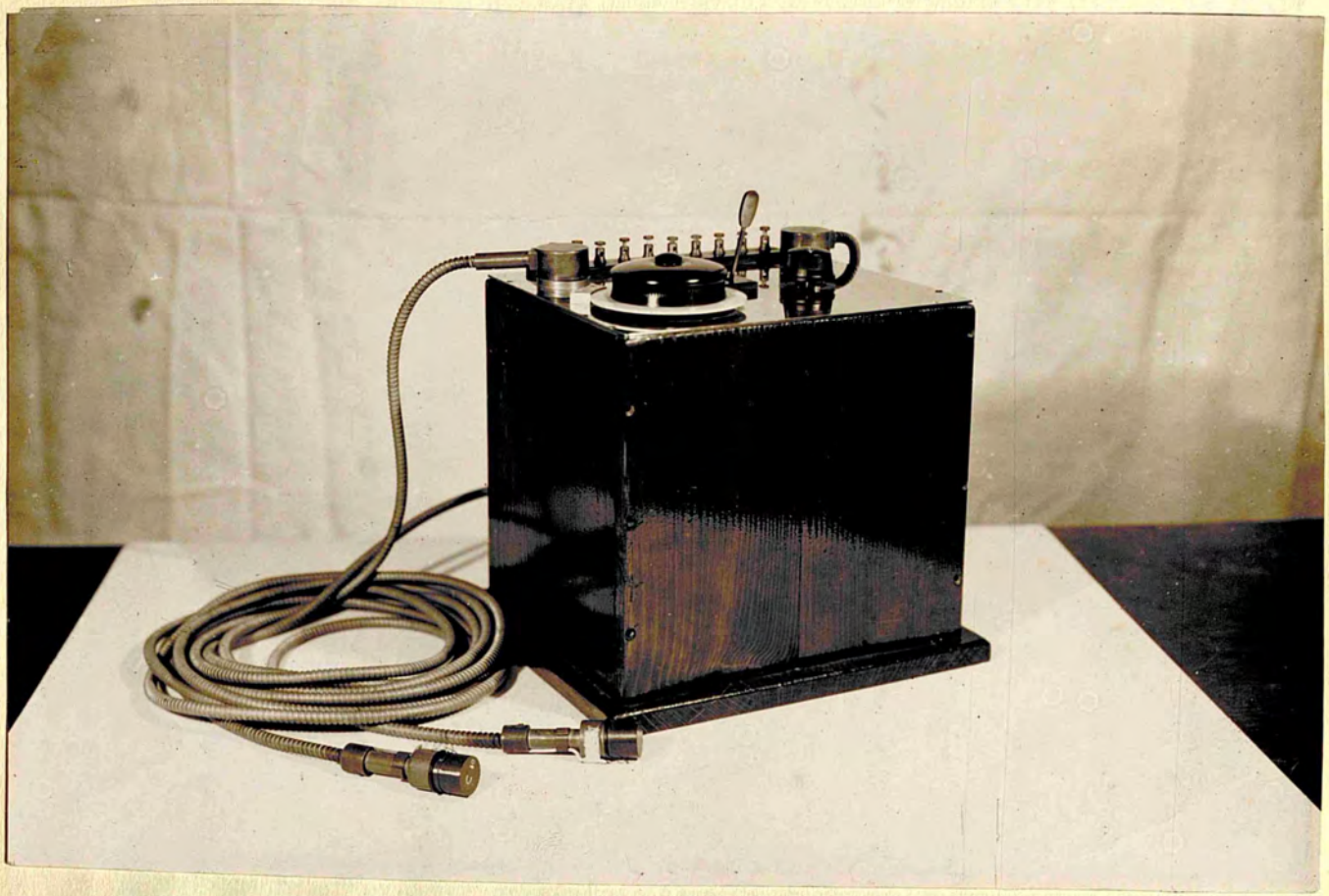

Figure (37)

(vi) Adjustment of the order of opening the switches.

A circuit such as that shown in fig. (38) may be used for adjusting the order of opening of the switches. In our experiments the switch S which is connected to the grid of the electrometer valve should open first in all cases as seen from the theory of the apparatus. S_1 and S_2 are adjusted by their screws so that they open almost at the same time after S. The movement of the needles of the galvanometers G_1 and G_2 indicates the order of opening the switches.

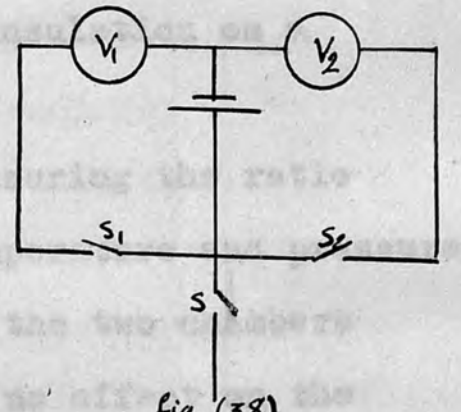

Fig. (38)

(vii) Precautions and procedure

The insulating parts in the apparatus must be absolutely clean. The cleaning is done by washing them with alcohol, drying carefully, polishing them with amber powder and blowing them vigorously with a blower. All the other parts of the apparatus must also be cleaned and dried thoroughly and then a large quantity of a drying agent (magnesium perchlorate) must be enclosed in the apparatus. It is very important that the apparatus should

be kept dry and clean for any slight dirt or moisture may give rise to a drift in the microammeter needle and make it difficult to get a steady null point. All the insulating parts were tested for good insulation on a Wulf electrometer.

In the method adopted here for measuring the ratio F, it was found unnecessary to make temperature and pressure corrections for the two factors affect the two chambers simultaneously and therefore will have no effect on the ratio.

The circuit is connected and left for about 20 minutes to settle down i.e. until the needle of the microammeter indicates no motion. The backing-off device may be used if necessary. The grid potential is adjusted until with the grid isolated there is no drift of the needle. The grid bias is checked every now and then to ensure that there is no drift of the needle when the grid is disconnected from the earth and that conditions are, therefore, as they were originally.

The whole apparatus is tested after connecting the chambers with the high tension to ensure that there is no

leakage in any part of the apparatus, leads or chamber insulation. This is done by opening the switches and observing the needle of the microammeter. If no current flows in the microammeter, then the insulation is good and the apparatus is ready for taking readings.

The chambers were put in the beam so as to fulfil the requirements of the different experiments to be carried out. In each case the setting of the variable condenser C_1 is found which maintains the needle of the microammeter in the same position both before and after opening the switches. This indicates that the correct ratio $\frac{C1}{C2}$ has been obtained which maintains the point P at earth potential after disconnecting the switches from earth, the condition required by the theory.

The reading of the scale connected to the capacity C_1 is noted and from the calibration curve Fig. (40) the corresponding ratio of the ionization currents in the two chambers is obtained.

(viii) Calibration of the apparatus.

The calibration of the instrument was made in two steps:

1. An investigation of the inverse square law for a specific x-ray beam.
2. Determination of the variation of the scale reading with charge ratio.

1. An investigation of the inverse square law.

The calibration may be carried out most readily by making use of the inverse square law[8] It was therefore necessary to determine the range of distances along the beam axis within which the law is obeyed.

A Siemen's tube was used together with a Siemen's and Victoreen dosemeter.

The beam was directed horizontally away from any scattering material. The exciting voltage of the beam was 103.5 kVp. The added filter was 2 mm. Al., so that the H.V.L. of the beam was between 3.5 and 4 mm. Al. A cylindrical applicator of diameter 8 cm. was used to collimate the beam. The Siemen's ionization chamber was put at the side of the applicator to serve as a monitor, while the Victoreen ionization chamber was moved along the axis of the beam.

The dose received by the Victoreen chamber in the

Relation between $I/\sqrt{dose}$ & the distance d in cm.

from the filter to the chamber.

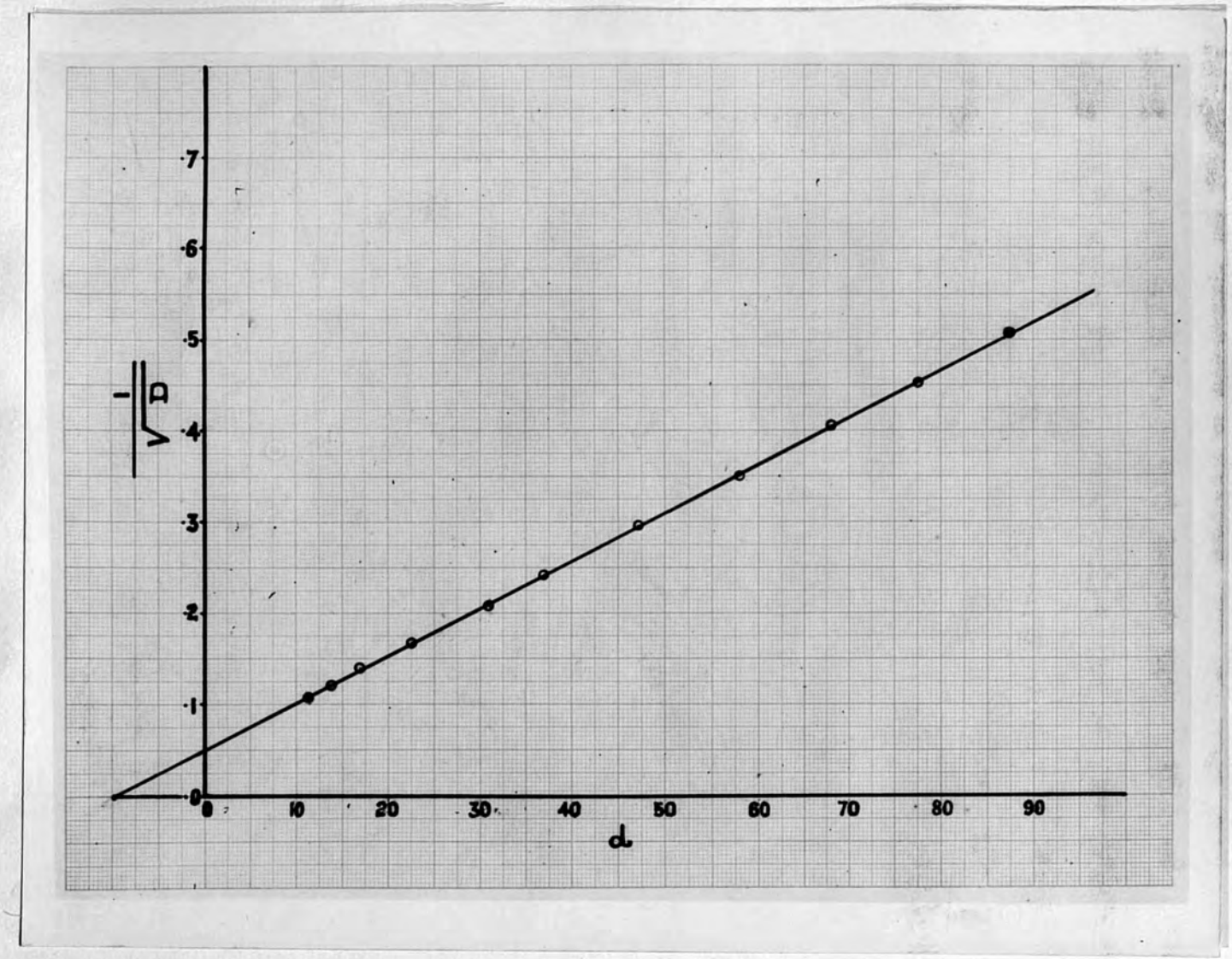

Figure (39)

time required by the Siemen's chamber to integrate from 20 r to 120 r was found for each distance. Each reading was taken twice and a good agreement was found between the dose obtained in each case.

The results are shown in the following table and graphicelly in Fig. (39)

Distance from filter to the far side of the chamber d cm.	Mean Dose D in r on Victoreen's	$\frac{1}{\sqrt{D}}$
11.25	89.5	0.106
13.85	68.7	0.121
16.95	52.0	0.139
22.50	35.0	0.167
30.10	23.4	0.207
30.20	23.8	0.205
36.90	17.0	0.243
37.0	16.6	0.246
47.3	11.4	0.296
58.2	8.1	0.351
68.3	6.1	0.405
77.5	4.9	0.452
87.6.	3.85	0.510

Fig (39) represents the relation between d and $1/D$ which is a straight line, showing that the inverse square law is obeyed within the range of distances shown in the above table.

Using the results of this investigation we could calibrate the instrument with the same beam using points within the experimental distances shown above.

2 - The variation of the scale reading with the ratio

The same conditions as in the above experiment being used, two of the air wall chambers (No.1) were mounted on the instrument fig. (34). They were symmetrically disposed with respect to the axis of the beam. One of them was kept fixed and the other was moved in small steps along the beam.

At each position of the moving chamber, the null point reading of the scale was observed. This was carried on until a set of readings covering the whole scale of the instrument had been obtained.

The following table gives the observations taken on three different days. It shows also the consistency and the reproducibility of the readings of the scale.

Figure(40)

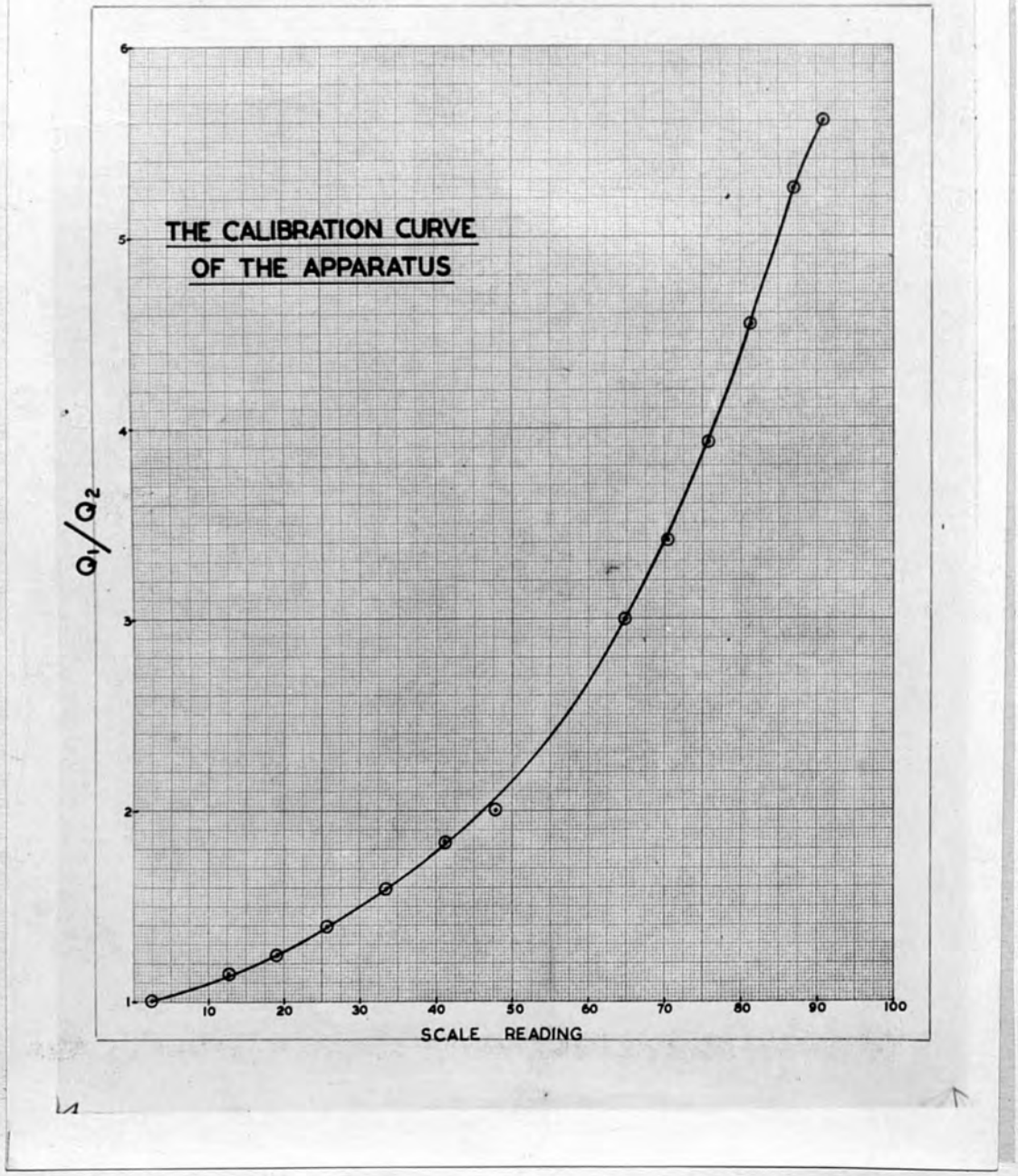
THE CALIBRATION CURVE
OF THE APPARATUS
Q_1/Q_2
1
2
3
4
5
6
10
20
30
40
50
60
70
80
90
100
SCALE READING

The distance between the centre of the fixed chamber and the target = 28.89 cm.

Distance from centre of chamber to target in cms x	Scale reading (1)	Scale reading (2)	Scale reading (3)	Mean scale Reading	$\frac{Q_2}{Q_1}=\frac{x^2}{(28.89)^2}$
28.89	3.1	1.3	3.1	2.5	1.00
30.94	12.9	12.6	12.8	12.7	1.14
32.44	19.3	19.1	19.6	19.3	1.26
34.14	25.6	25.5	25.6	25.6	1.40
36.54	34.0	33.4	34.0	33.7	1.60
39.14	41.1	41.2	41.1	41.1	1.83
41.34	48.4	47.1	48.0	47.8	2.00
43.94	53.3	52.9	53.3	53.2	2.30
47.04	59.7	59.3	59.7	59.6	2.65
49.94	65.0	64.6	65.0	64.9	3.00
53.34	70.9	70.0	70.5	70.4	3.41
57.34	75.8	—	75.8	75.8	3.93
61.49	81.4	81.1	81.4	81.3	4.54
65.76	86.9	—	—	86.9	5.18
68.34	91.1	90.2	91.1	90.8	5.60
71.34	96.2	—	96.2	96.2	6.12

Fig (40) represents the relation between the scale reading and $\frac{Q_2}{Q_1}$

(ix) Investigation in the Saturation Voltage of the Chambers.

To determine the saturation voltage for the chambers the following experiments were carried out:

One of the "air wall" chambers (No. I) and chamber (No.4) p. (111) were mounted on the instrument. They were put symmetrically with respect to the axis of an x-ray beam (effective wave length 0.150Å) at a point where the dose-rate was of the order of 8r/min.

1. The following table shows the variation of the voltage applied to the chamber (No. (1)), with the ratio of the charges collected by the two central electrodes of the chambers, keeping the voltage of the chamber (No. 4) constant.

Fig. (41a)

Voltage for air wall chamber No(1)	48	60	72	108	120	156	168	180	216	288	300	
Ratio	3.97	3.68	3.54	3.37	3.35	3.3	3.29	3.27	3.25	3.25	3.25	

Saturation Curves

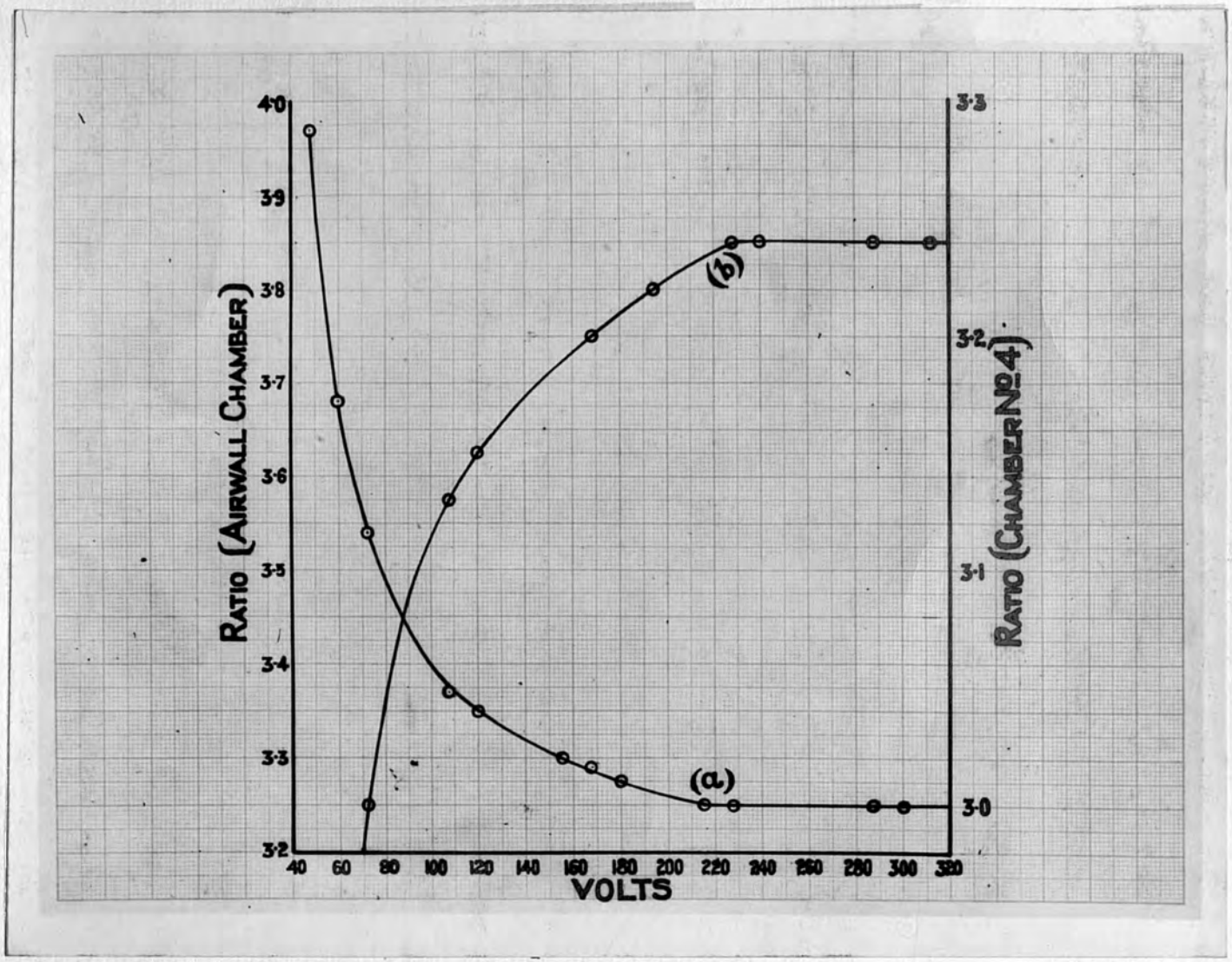

Figure (41)

2. The following table contains the observations of the ratio with varying voltages applied to chamber (No. 4) keeping the voltage applied (No.1) constant at 228.

Fig. (41b)

Voltage of chamber No.(4)	72	108	120	168	192	228	240	288	312
Ratio	3.0	3.13	3.15	3.2	3.22	3.24	3.24	3.24	3.24

As a result of the above investigation the working conditions for the Westinghouse set were as follows:

1. The minimum voltage applied to the chambers for attaining saturation was 228 volts.
2. The chambers were put at a point where the dose was of the order of 8r/min.

In the case where the Victor Maximar and the million volt set were used the chambers were put at a distance from the target where the dose-rate was about the same as mentioned above.

Since the greatest ionization current was anticipated in the chamber (No. 4) of atomic No. 20.84 it was safe to

use this voltage for the other chambers of lower atomic number in which the ionization current was expected to be less.

(x) Wavelength Independence of the Ratio given by two Identical Air Wall Chambers

The air wall chambers described elsewhere, which were manufactured from bakelite graphite - vanadium oxide mixture were tested for similarity at different wavelengths with the same apparatus. Fig. (34)

Using qualities of radiations chosen to cover nearly the whole range needed for the investigation, a pair of the chambers was examined, i.e. the ratio of their ionization currents was measured.

The following table contains the results.

KVp.	added filter	λe A.U.	Ratio
60	0	.63	.98
90	2 mm. Al.	.402	.99
106.8	4 mm. Al.	.322	.98
120	0.11 mm.Cu. + 1 Al. mm.	.236	1.01
180	0.214 mm.Cu + 1 mm.Al	.177	1.00
200	0.5 mm.Cu. + 1 mm.Al.	.150	1.00
220	.5 mm.Cu + .274 mm.Sn + 1 mm.Al.	.086	1.05

The last column shows approximate constancy of the ratio with the variation of quality of the beam. This gives evidence of the characteristic property of the similarity of the chambers.

e. Experimental results:

The procedure described on p. (120) was used when measuring the ratio of the ionization currents in each pair of chambers with the equivalent atomic number recorded in the following tables. The effective wave lengths for which the ratios are required are taken from the tables on pp. (53 & 63). The conditions under which the X-ray tube was operated are also stated in the same tables pp. (53 & 63).

Two of the chambers (the air wall and another having atomic number as stated in the tables) were mounted on the apparatus Fig. (34). They were put symmetrically with respect to the axis of the beam at a point where the dose-rate was of the order of 8r/min. For this order of dose-rate it was found by experiment p. (127) that a chamber potential of the order of 228 volts was suffeicient for saturation even for the greater ionization currents

produced in the chambers with walls of the highest effective atomic number. Dry batteries were used to provide the chamber potential. The following tables give the results obtained.

The ratios recorded in these tables were taken from the calibration curve fig. (40). They correspond to the scale readings observed in the experiments.

Variation of experimental F with

Wavelength.

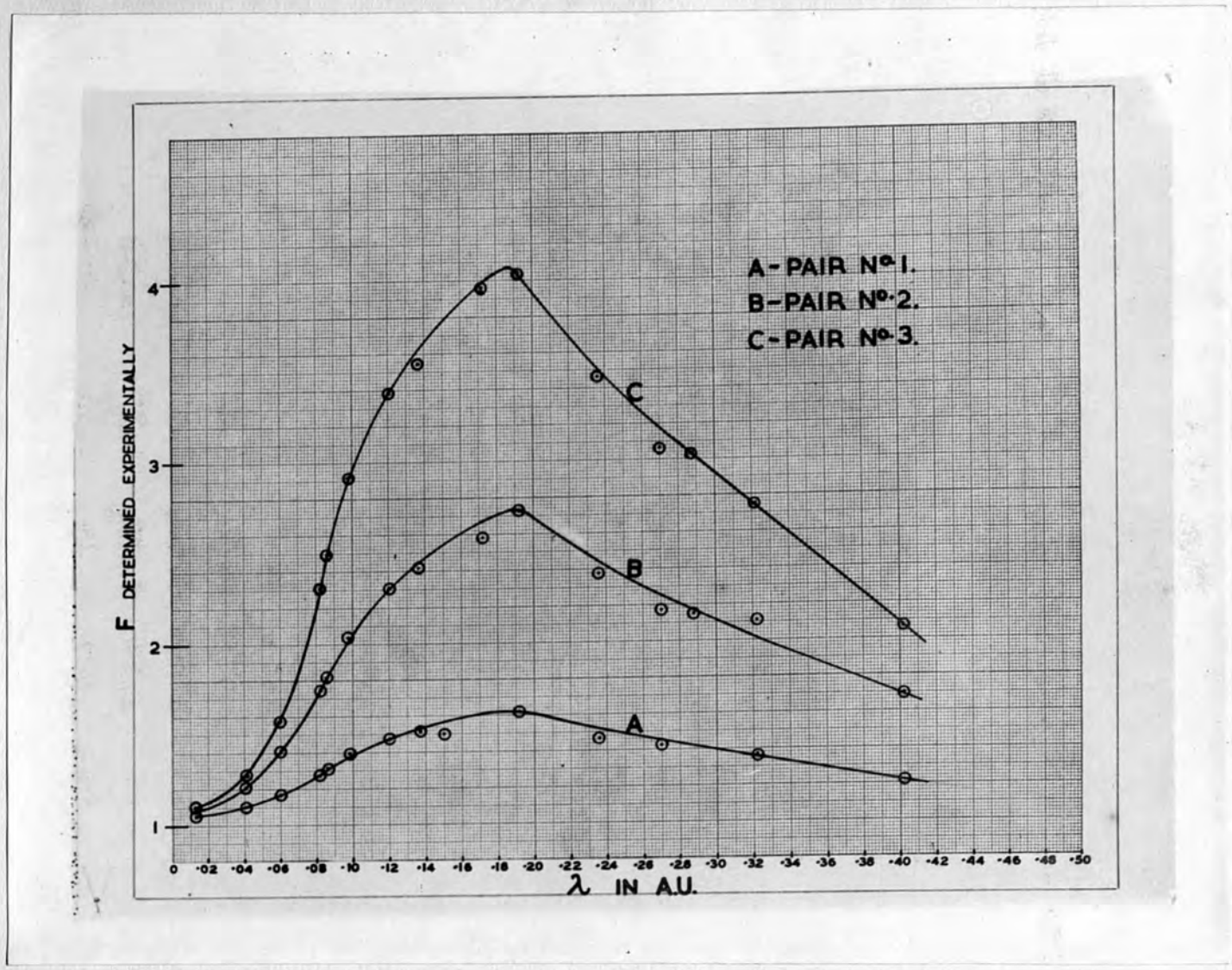

Figure (42)

Experimental Data I

Fig. 42 A.

Air wall chamber (A) $\overline{Z} = 7.64$ and Chambers A & B, $\overline{Z} = 12.84$

No	λ_e in A.U.	ratio A_V &A	ratio A_V &B	mean ratio
1	.013	1.07	1.045	1.057_5
2	.041	1.0	1.0	1.0
3	.06	1.06	1.06_5	1.063
4	.082	1.28	1.28	1.28
5	.086	1.315	1.31_4	1.314_5
6	.098	1.40	1.39_7	1.398_5
7	.120	1.52	1.415	1.467_5
8	.137	1.566	1.47	1.518
9	.172	1.62	1.52	1.57
10	.192	1.66	1.57	1.61_5
11	.236	1.45_5	1.47	1.462_5
12	.270	1.44_5	1.41	1.427
13	.288	1.42_5	1.40_1	1.413
14	.322	1.38_6	1.35	1.368
15	.402	1.23_5	1.19_5	1.215

Experimental data II

Fig. 42 B.

Air wall chamber A_v, $\overline{Z}$ = 7.64 and chambers A & B, $\overline{Z}$ = 17.04

No.	λ_e A.U.	ratio A_v &A	ratio A_v &B	Mean ratio
1	.013	1.08	1.08	1.08
2	.041	1.1	1.11	1.105
3	.06	1.27_5	1.27_5	1.275
4	.082	1.75	1.75	1.75
5	.086	1.804	1.81	1.807
6	.098	2.033	2.048	2.040_5
7	.120	2.29	2.32	2.30_5
8	.137	2.413	2.42	2.416_5
9	.172	2.525	2.636	2.580_5
10	.192	2.66	2.795	2.727_5
11	.236	2.36	2.39	2.37_5
12	.270	2.09	2.25	2.17
13	.288	2.075	2.22	2.147
14	.322	2.12	2.10	2.11
15	.402	1.70	1.696	1.70

Experimental Data III

Fig. 42 C.

Air wall chamber $A_v \bar{Z} = 7.64$ and chambers A & B $\bar{Z} = 20.84$

No	λ_e A.U.	ratio A_v &A	ratio A_v &B	mean ratio
1	.013	1.104	1.104	1.104
2	.041	1.26_6	1.26_5	1.26_6
3	.060	1.59	1.56_8	1.57_8
4	.082	2.31	2.31	2.31
5	.086	2.51	2.465	2.487_5
6	.098	2.935	2.90	2.917_5
7	.120	3.39	3.38	3.385
8	.137	3.57	3.52	3.545
9	.172	3.78	3.79	3.78_5
10	.192	3.96	4.11	4.035
11	.236	3.41	3.505	3.547_5
12	.270	3.018	3.10	3.059
13	.288	3.0	3.075	3.037_5
14	.322	2.71	2.79	2.75
15	.402	2.01	2.115	2.06

V

COMPARISON BETWEEN THEORETICAL AND EXPERIMENTAL DATA

In equations (10) and (11) p. (70), for short wave lengths, the scattering absorption coefficient is predominant while the photoelectric absorption coefficient is negligible.

Thus $F' \longrightarrow 1$ for short wave-lengths

For intermediate wavelengths the important factor is σ. As this coefficient is proportional to $\overline{Z}^{2.94}$ (in the case of Walter's formula), we have,

$$F' \longrightarrow \frac{\overline{Z}_2^{2.94}}{\overline{Z}_1^{2.94}}$$

where $\overline{Z}_1$ and $\overline{Z}_2$ are the effective atomic numbers of the air wall and heavier material respectively.

Therefore F' increases chiefly according to this relation. The amount of increase depends on the values of $\overline{Z}_2$ and $\overline{Z}_1$, being greater for greater $\overline{Z}_2$.

For longer wavelengths the factor governing the ratio is the absorption in the walls i.e. the factor "f." This factor decreases and becomes very small since the absorption coefficient μ_1 becomes greater and greater as the wavelength increases. This has the effect of causing F' to

decrease after it has reached a certain maximal value. The amount of diminution depends on the linear absorption coefficient of the heavier wall material.

Therefore, we should expect a maximum in the intermediate region of wavelengths. This maximum depends on the material of the chamber which is compared with the air wall chamber, being greater for greater $\overline{Z}_2$.

Also we should expect the rate of decrease in F', over the long wavelengths, to depend on $\overline{Z}_2$, this rate is less for $\overline{Z}_2$ nearer to $\overline{Z}_a$ of air, while for $\overline{Z}_2 \gg \overline{Z}_a$ it is considerable.

The following tables contain experimental values of the ratio (taken from the smooth curves fig. (42)) together with theoretical values at different qualities, for the different pairs of chambers used.

The theoretical and experimental values were made to coincide at 0.013 A.U. and hence all the theoretical Values were multiplied by the required factor to agree with this alteration. This wavelength was chosen because one would anticipate that the theory would be most accurate at this point and indeed, it might be expected to be a precise statement of the ionizations produced (Gray 1936).

Also σ is practically negligible at this wavelength so that ambiguities about the values of this quantity are of little consequence.

The final columns give the ratio of the theoretical to the experimental ratios.

I

$\overline{Z}$ (12.84 and 7.64)

λ_e in A.U.	F'_w (cal.)	F'_v (cal.)	F (exp.)	F'_v ↗	F'_w ↗	$\frac{F'_w \text{ (cal.)}}{F \text{(exp.)}}$	$\frac{F'_v \text{ (cal.)}}{F \text{ exp.}}$
0.013	0.95	0.95	1.058	1.05_6	1.06	1	1
0.04	1.00	1.01	1.10_2	1.114	1.12_6	1.01	1.02
.06	1.06_5	1.06	1.17	1.186	1.18	1.013	1.01
0.08	1.16	1.14	1.27_5	1.291	1.27	1.012	.995
0.12	1.64	1.61	1.467	1.827	1.79_3	1.246	1.22_4
0.15	2.185	2.15	1.56_5	2.43	2.40	1.55	1.53
0.18	2.70	2.70	1.61	3.01	3.01	1.87	1.87
0.19	2.845	2.87	1.61_6	3.16_5	3.20	1.96	1.98
0.20	2.98_5	3.05	1.606	3.32	3.40	2.07	2.12
0.22	3.20	3.31_5	1.55_7	3.56_5	3.69	2.29	2.37
0.24	3.36	3.55	1.508	3.74	3.96	2.48_5	2.62_5
0.28	3.54	3.87	1.428	3.95_5	4.31	2.77	3.02
0.32	3.55_4	3.98	1.357	3.96	4.43	2.92	3.26_6
0.38	3.42_5	3.90_5	1.252	3.82	4.35	3.05	3.47
0.42	3.27	3.76	1.18_8	3.64_5	4.19	3.07	3.53
0.46	3.055	3.57	1.12_3	3.40	3.98	3.03	3.54

II

$\overline{Z}$ (17.04 and 7.64)

λ in A.U.	F'_w (cal.)	F'_v (cal.)	F (exp.)	F'_w ↗	F'_v ↗	$\frac{F'_w \text{ (cal.)}}{F \text{ (exp.)}}$	$\frac{F_v \text{ (cal.)}}{F \text{ (exp.)}}$
0.013	.926	.926	1.08	1.08	1.08	1	1
0.04	.96	.96	1.21	1.12	1.12	.925	.925
0.06	1.10	1.10	1.41	1.28_3	1.28_3	.91	.91
0.08	1.46	1.50	1.71	1.69	1.75	.996	1.02
0.10	2.00	2.10	2.06	2.33	2.45	1.13	1.19
0.12	2.76	2.88	2.305	3.22	3.36	1.39_5	1.46
0.16	4.42	4.96	2.61	5.15	5.79	1.97_5	2.18
0.18	5.19	5.97	2.71	6.05	6.96	2.25_4	2.57
0.20	5.88	6.87	2.69	6.85	8.01	2.55	2.98
0.22	6.35	7.56	2.55	7.41	8.83	2.90	3.46
0.24	6.67	8.04	2.41_5	7.77	9.38	3.22	3.89
0.26	6.86	8.34	2.305	8.01_5	9.74	3.48	4.22
0.28	6.87	8.45	2.206	8.00	9.86	3.63	4.47
0.32	6.50	8.12	2.02	7.58	9.46	3.75	4.69
0.36	5.95	7.47	1.86	6.94	8.7	3.73	4.68
0.40	5.28	6.68	1.70	6.15	7.79	3.62	4.55

III

$\overline{Z}$ (20.84 and 7.64)

λ in A.U	F_w' (cal.)	F_v' (cal.)	F (exp.)	$F_w'\nearrow$	$F_v'\nearrow$	$\frac{F_w'(cal.)}{F(exp.)}$	$\frac{F_v'(cal.)}{F(exp.)}$
0.013	.915	.915	1.104	1.104	1.048	1	1
0.04	1.03	1.03	1.27	1.24_3	1.24_3	.980	.980
0.06	1.33	1.37	1.58	1.60_5	1.65_3	1.016	1.047
0.08	1.93	2.037	2.2	2.33	2.46	1.06	1.12
0.10	2.98	3.22	2.96	2.59_5	3.88	1.21_4	1.31
0.12	4.24	4.64	3.38	5.11	5.6	1.51	1.65_5
0.15	6.61	7.55	2.78_5	7.97	9.11	9.11	2.41
0.19	9.34	11.00	4.05	11.26	13.28	2.78	3.27
0.22	10.32	12.86	3.69	12.47	15.3	3.38	4.14
0.25	10.68	13.44	3.37	12.9	16.22	3.83	4.82
0.28	10.34	13.05	3.10	12.48	15.75	4.03	5.08
0.32	9.01	11.34	2.76	10.89	13.7	7.94	4.95
0.38	6.61	8.35	2.26	7.97	10.08	3.53	4.45
0.44	4.4	5.47	1.76	5.31	6.6	3.02	3.75
0.48	2.99	3.71	1.44_6	3.61	4.48	2.5	3.1

Relation between $F_{cal.}/F_{exp.}$ & wavelength.

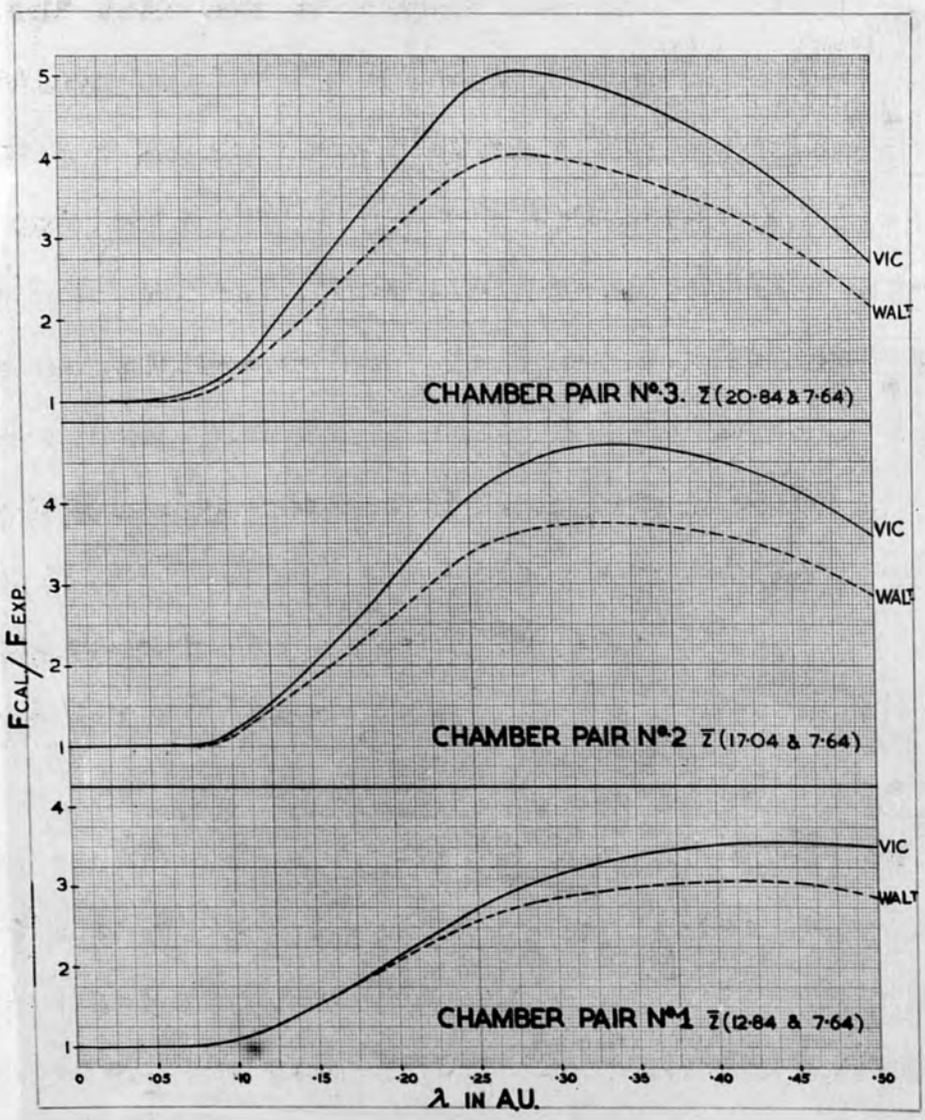

Figure (43)

From the tables and graphs we see that the experimental results agree with the theoretical values qualitatively; the experimental ratio being nearly unity for short wavelengths, then increases rapidly till it attains a maximum at about 0.19 A.U., then decreases as the wavelength increases. It is also noticed (Fig. 42), as was predicted by the theory, that the values of the maxima vary with the nature of the material to be compared with the air wall chamber. The greatest maximum value of F' is for $\overline{Z} = 20.84$ and least for $\overline{Z} = 12.84$. It may also be seen that the right hand side branch of the curves is flattest for $\overline{Z} = 12.84$, but the decrease is more rapid as $\overline{Z}$ increases.

Therefore the general qualitative features of the experimental curves agree with the theory fairly well.

Quantitatively we find considerable differences between the experimental and the theoretical curves especially for the longer wavelengths. They seem to agree in all the chamber pairs used, up to .08 A.U., then begin to deviate considerably, the theoretical in one case being more than four times the experimental as seen in Fig. (43).

When Victoreen's formula is used in the calculation of the e^{τ}, the ratios deviate more from the experimental ones

than in the case when Walter's formula is used for calculating $\mathcal{T}$. It seems that Walter's formula fits experimental observations of this kind better than Victoreen's.

VI

DISCUSSION AND CONCLUSIONS

1. In the calculation of the value of F corresponding to the complete spectral distribution of energy in the x-ray beam, it is in most cases sufficiently accurate to regard the beam as having the effective wavelength which corresponds to its half value layer in copper. This is illustrated by the calculations in which we obtained the ratio corresponding to the effective wavelength of the H.V.L. of the beam.

From the tables on p. (110) it is clear that the ratio calculated from the effective wavelength corresponding to the H.V.L. of the beam agrees fairly well with the ratio calculated from the complete spectral distribution curve. The difference between the ratios does not exceed 4% (approximately) in all the cases shown in the table except one (170 kVp) where it amounts to about 7%. In the latter case the difference can be attributed to the fact that the effective wavelengths differ among themselves by about 5%. It may be stated that the difference between the two ratios increases as the voltage across the tube increases. This is, perhaps, because the theories adopted in determining the

the spectral distribution of energy do not completely fulfil the requirements for hard radiation. In support of this opinion it was observed in some cases that we were unable to get a straight line for ($\frac{x}{y}$, y) see p. (22) even if we allow for the characteristic radiation. This suggests that factors other than the characteristic radiation should be accounted for in order that Jones-Silberstein formula should fit the absorption data for hard radiation. Therefore it was taken as being sufficiently accurate and more convenient to use the effective wavelength corresponding to the H.V.L. of the beam, in establishing the ratio wavelength curves. The measurements of the H.V.L.'s were carried out by an instrument (fig. 34) which provided a good means for measurements of such nature. The ratio of the intensities of the beam before and after it passes through a filter were obtained directly and independently of any fluctuations which may occur in the voltage across the X-ray tube and result in error in the measurement of the H.V.L. if the latter is taken by one chamber.

2. Chambers which were moulded from mixtures of bakelite, vanadium or cerium oxide with 20 parts of graphite were found to behave remarkably well as regards their electrical conductivity and their consistent interaction with the radiations used in the investigations.

As shown in the table of p.(129) individual "air-wall" chambers (no.1) pressed from bakelite graphite with 2 parts added of V_2O_5 were found to be practically identical in their behaviour over the range of wavelengths examined. The ratio of the ionization currents in a pair of these chambers was practically constant and equal to unity over a wide wavelength range (from 0.63 to 0.086 A).

From the data in the tables on pp. (132, 132 & 134) it may be seen that where one of the chambers is of a higher effective atomic number, individual chambers do not necessarily give exactly the same ratio but the variations are relatively small: it would seem that chambers having specific "wall characteristics" can be pressed fairly reliably. This point may be of some interest and value in relation to the production of pressed chambers having specific "wall characteristics" for the investigation of X-rays or the measurement of neutrons. The maximum difference in ratio of ionization

recorded by two samples of the same atomic number did not exceed 5%. In the case of the chambers made of a mixture of $\overline{Z}$ = 12.84, the maximum variation in ratio of ionization amounted to about 6%.

In all cases the variations of the ratio from sample to sample show themselves most markedly as the long wavelengths are approached. The maximum variations are always in the intermediate region of wavelengths i.e. when the ratio attains its maximal value (see pp. 132, 133, 134). They are almost non-existent in the short wavelength region. This may be attributed to the fact that ionization in this region is chiefly due to Compton recoil electrons which are independent of the wall material, the photo-electrons forming a very small fraction of the total electronic emission from the walls.

That the observations are reproducable from day to day can be easily seen from the results on p.(126). The values in this table were taken on different days; all of them are practically the same within experimental errors.

3. Previous measurements of the ratio of ionization currents produced in small chambers with walls of different atomic numbers by high voltage radiation were found[3, 1, 57, 5] to give results considerably smaller than those calculated from the theory; and in general the differences between theory and experiment increased with increase in wavelength of the raiation. One of the causes of this disagreement is perhaps because it is not yet fully realised how small the chamber must be to fulfil the theoretical requirements; indeed it may be impossible to fulfil those requirements in practice. Gray[42] suggested the following approximate limits to the linear dimensions of the chamber at which the theory and experiment might be expected to agree in the case of air-wall chambers:

(1) a few mm. for X-rays.

(2) 0.1 mm. for hard X-rays (200 KV constant potential filtered with 1.5 mm. Cu)

(3) still less for softer X-rays.

It is possible that other factors may also be present when the chambers are not air-walled.

Chambers of dimensions of these magnitudes are difficult to manufacture. Also the ionization currents in such chambers are very small and difficult to measure. Any slight

error in measurement will lead to considerable error in the final results. If valve amplification is used to increase the degree of sensitivity, the accuracy of measurement of these ionization currents may be considerably affected by the variations which may occur due to the degree of amplification and to the complexity of the resulting circuit. While many[58,59,60] observers using chambers of varying sizes, ranging from the above orders of dimensions upwards, failed to confirm Gray's theory experimentally, other[43,61,62,63] experimental results agreed with the theory. Fricke and Glasser[43] showed experimentally that the ionization per unit volume is independent of the size of the chambers up to a volume of about 4.7.c.c. in carbon or aluminium chambers irradiated with x-rays of the qualities used in deep therapy which at the time were of the order 0.1 to 0.2 A.U. It thus seems that the question of the volume of the chambers is not the only important one when the ratio is concerned.

The deviation in the case of large chambers of high atomic number has been attributed to the fact that the ranges of the electrons become smaller as the wavelength increases until they only ionize a small layer of air near the walls. A small part of this deviation has been attributed[3,6] to

characteristic radiation from the walls.

On the other hand it is to be expected[42] that if we use chambers of material of low atomic number, with volumes considerably larger than that required by the theory, the ionization will be the same as in small chambers i.e. being equal to the theoretical value. This is because the decrease in the emission from the walls should be counterbalanced by the electrons generated in the air itself. The volume of the chambers used was about 4 c.c. which is within the limits stated by Fricke and Glasser[43] required to fulfil the theoretical conditions for chambers of Z similar to those used in the experiment.

It was thought that a point of interest in this connexion might be the determination of the mean ranges in air of the secondary electrons emitted from the walls of the different chambers used, since they might conceivably be related to the results obtained.

Therefore in the following tables the ranges in air have been calculated using Wilson's formula:

$$R = \frac{E^2}{440} \text{ cm.}$$

where R is the range in cm. and E has been taken as the mean energy in eKV of the recoil electrons and the photo-electrons from the chamber walls.

We have followed Lea's method[64] of calculating the mean energy of the recoil and photoelectrons and the following table contains the mean ranges of the secondary electrons originating from the air wall material of the chambers together with the data used in the calculation.

Column (1) gives the wavelength in A.U.

" (2) gives the quantum energy h i.e. the photo-electron energy Ep taken from Lea's table[64].

" (3) gives the mean energy E_r of the recoil electron[64]

" (4) gives $e\sigma_a$ taken from the tables on p. (79).

" (5) gives $e\tau$ taken from the tables on pp.(83 & 84) and the values of $e\tau$ for other chambers are taken from tables on pp. (85 ..... 90).

" (6), (7) give the proportion of total energy A which appears as recoil electrons and B as photo electrons where

$$A = \frac{\frac{e\sigma_a}{e\sigma_a + e\tau}}{E_r}$$

$$B = \frac{\frac{e\tau}{e\sigma_a + e\tau}}{Ep}$$

Column (10) gives the range of the recoil electron

$$R_r = \frac{E_r^2}{440} \text{ cm.}$$

" (11) gives the range of photo electrons

$$R_p = \frac{E_p^2}{440} \text{ cm.}$$

" (12) gives the mean energy Rm of the recoil and photo electrons

$$Rm = R_rC + R_pD$$

TABLE I

Ranges of the electrons originated in the wall of the chamber of $\bar{z} = 7.64$

(1)	(2)	(3)	(4)	(5)	(6)	(7)	(8)	(9)	(10)	(11)	(12)
λ in A.U.	E_p	E_r	$\sigma_a \times 10^{26}$	$\sigma_T \times 10^{26}$	A	B	C	D	R_r in cm.	R_p in cm.	R_m in cm.
.015	826.6	331.0	9.5	.002	1	0	1	0	249	1550.0	249.0
.033	413.3	130.4	9.82	.030	.995	.005	1	0	38.7	388.0	38.7
.06	206.7	46.0	8.86	.185	.975	.025	1	0	4.8	97.0	4.8
.08	155.0	28.22	8.15	.437	.938	.062	.989	.011	1.81	54.6	2.39
.10	124.0	19.7	7.49	.855	.878	.122	.978	.022	.882	35.0	1.60
.13	95.39	12.38	6.63	1.86	.742	.258	.957	.043	.348	20.7	1.22
.15	79.40	9.3	6.14	3.55	.634	.366	.938	.062	.197	14.3	1.02
.16	73.5	8.20	5.93	4.31	.58	.420	.925	.075	.153	12.3	1.06
.17	69.1	7.33	5.74	5.18	.526	.474	.913	.087	.1221	10.9	1.06
.18	65.6	6.70	5.56	6.14	.476	.524	.90	.100	.101	9.8	1.07
.19	63.4	6.20	5.39	7.21	.428	.572	.885	.115	.0873	9.13	1.15
.20	62.00	5.90	5.23	6.69	.383	.617	.867	.134	.079	8.73	1.24
.30	41.33	2.81	3.95	22.20	.122	.878	.672	.329	.018	3.88	1.26
.40	31.00	1.64	3.19	51.50	.045	.955	.473	.528	0061	2.18	1.15
.50	24.8	1.12	2.67	99.00	.02	.98	.312	.688	.0028	1.4	.97

The ranges in this table are calculated in the same manner described in the previous table for chambers of $\overline{Z}$ as stated.

λ in A.U.	R_m in cm. for $\overline{Z} = 7.64$	R_m in cm. for $\overline{Z} = 12.84$	R_m in cm. for $\overline{Z} = 17.04$	R_m in cm. for $\overline{Z} = 20.84$
.015	249	249	249	250
.03	38.7	40.46	43.25	47.76
.06	4.8	7.12	9.87	14.02
.08	2.39	4.45	7.61	11.85
.10	1.60	4.05	7.33	11.22
.13	1.22	3.83	6.90	9.84
.15	1.02	3.51	6.05	8.19
.16	1.065	3.43	5.74	7.59
.17	1.06	3.40	5.51	7.12
.18	1.07	3.38	5.34	6.73
.19	1.16	3.485	5.33	6.62
.20	1.24	3.65	5.38	6.56
.30	1.27	2.70	3.30	3.51
.40	1.16	1.82	2.01	2.09
.50	0.97	1.32	1.34	1.37

If the differences between the theoretical and experimental results are to be attributed to the ranges of the electrons, being small compared with the dimensions of the chambers, it might be suggested that up to a range of 2.39 cm. (the range at 0.08 A.U.) the ionization due to the electrons originating in the air inside the chamber is negligible compared with the ionization originating in the chamber walls, since the theoretical and experimental ratios agree fairly well up to the above mentioned wavelength, 0.08 A.U.

We notice that at the wavelength 0.08 A.U. where the theory and experiment seem to begin to disagree the electron ranges in the air wall chamber are just of the order of the chamber dimensions. This may be related to the observations and further similar experiments with much smaller chambers might be of interest in order to see whether there is any real foundation for this point of view.

---

(4) The calculations (table 98, 99 & 100 fig. 28,29, 30) show that no matter what effective atomic number be used for the wall material of the chamber of high atomic number, (at least up to $\overline{Z}$ = 20.84), this method will not allow us reliably to relate the ratio calculated with the quality above 0.30 A.U. although it can be used for shorter wave lengths. The reason is evident from the curvesof fig. (28,29,30) where it is seen that the rate of change of the ratio with wave length is very small above 0.30 A.U.

When a correction is made for absorption in the wall of the chamber the limit is still further reduced and we conclude that the method is unsuitable for wave lengths beyond 0.2 A.U.

The experimental observations show that the chamber pair method may, in practice, suffer even more severe limitations. The point of inflection in the ratio wave-length curve occurs in all cases at a wavelength of about 0.19 A.U. (fig.42) so that quality measurements could not be made for wavelengths longer than this; it would not be possible to say whether the reading was of the shorter or longer wavelength corresponding to the ratio.

This method therefore, is ruled out as unsuitable for the examination of the quality of the scattered radiations generated in a light atom medium by 200 KV x-rays or other softer X-rays. In these cases the secondary radiations may be expected to contain wavelengths which are much longer than 0.19 A.U. (Wilson)[43]. It is apparent that for the study of this particular problem some other method is needed. The method would seem to have its uses however, for the examination of the quality of the radiations scattered by harder beams of X-rays generated at say between 400 and 1000 KV.

If we assume that the theory and experiment agree at very short wavelengths of x-rays, our experiments show that the ratios predicted by Gray's theory agree with the experimental observations up to a wavelength of about 0.08A.U. (see fig. 43) for the ionization chambers used in these experiments. Clarkson and Mayneord[2] did not find such agreement between theory and experiment even for wavelengths down to 0.04 A.U. when they used chambers of graphite and copper. It should therefore be sufficient for investigations of this type by this means, using primary radiations

the secondary of which are not greater than 0.08 A.U. in wavelength to use calculated ratio values so that the need for direct calibration of the chamber-pairs would be obviated. In order to obtain the greatest rate of change of ratio with wavelength it is preferable of the chamber pairs we have studied, to use pair No.(3).

ACKNOWLEDGMENT

In conclusion the author wishes to express her thanks:- to Professor H.T.Flint for his continuous guidance and advice, to Dr. C.W.Wilson of the Physics Department Westminster Hospital (in whose laboratory the work was done) for suggesting the field of research, for the research facilities he made available and his assistance and interest throughout the work. Also to Mr. N.H.Pierce and his staff for their assistance in the construction of the apparatus, and finally to Mr. G.S.Innes for making available the St. Bartholomew's Hospital Million Volt tube for the measurement in the short wavelength region.

GENERAL REFERENCES

(1) Compton, A.H. and Allison, S.K. "X-Rays in Theory and Experiment" D.Van Nostrand Company inc, New York (1935)

(2) Wilson, C.W. "Radium Therapy, its Physical aspects", Chapman and Hall Ltd., London (1945)

(3) Rasetti, F. "Elements of Nuclear Physics" Blackie and Son Ltd., London and Glasgow (1937)

(4) Rutherford E , Chadwick, J and Ellis C.D. , "Radiation from Radioactive Substances". Cambridge University Press (1930)

(5) Plastes, "Plastics in Industry " second edition revised. Chapman and Hall Ltd. London (1942)

(6) Glasser, O. Edited by, "Medical Physics". Published by the Year book Publisher (1944).

REFERENCES

(1) Mayneord, W.V. Proc.Roy.Soc.A., Vol.CXXX p.63. 1930

(2) Clarkson, J.R. & Mayneord, W.V. Brit.Journ.Rad. Vol.XII, No.135, p. 168 (1939).

(3) Bragg, W.H. 'Studies in Radioactivity' London: Macmillan. 1912.

(4) Gray, L.H. Proc.Roy.Soc.A., Vol.CLVI, p.578,(1936)

(5) Wilson, C.W. Brit.Journ.Rad., Vol.XII No.136, p.231 (1939)

(6) Clarkson, J.R. Phil.Mag.ser.7,Vol.XXXI, p.437 (1941)

(7) British Empire Cancer Campaign, 23rd. Annual Report, p.59 (1946)

(8) Kemp,L.A.W. Brit.Journ.Rad. Vol.XIX,No.222, p.233 (1946)

(9) Flint, H.T., and Wilson, C.W. Brit.Journ.Rad.,Vol.XI, p.112 (1938).

(10) Phillips,R. & Innes G.S., 'Supervoltage X-ray Therapy'. H.K.Lewis & Co. Ltd., London 1944.

(11) Benoist, L. Arch. d'electric. med., 10, 129-134,(1902).

(12) Villard,M.P. Arch. d'electric med., 16,236.(1908).

(13) Christen, T. Forts chr.a.d. Geb.d.Rontgen stahlen, 21, 1-22, (1914).

(14) Szilard, B. Arch. Roentg.Ray, 19, 3-20, (1914-1915)

(15) Shearer, J.S. United States Army x-ray Manual. Paul B.Hoeber, New York, (1918)

(16) Seeman, H. Strahlen therapie, 7, 69-112. (1924)

(17) Mayneord, W.V. & Robert, J.E. Brit.Journ.Rad. VIII, 341, (1935)

(18) Holthusen, H. & Golwitzer, H. strahlentherapy XXVI, 101, (1927)

(19) Pohle, E.A. & Barnes, J.M. Radiology X, 300, (1928)

(20) Mayer, W.H., Am.Journ.Roentg. and Rad. Therapy XVI, 26, (1926)

(21) Thoreos, R. Acta Radiologica Supplementum XV, (1932)

(22) Müller, W. Strahlentherapie 49, 132, (1934).

(23) Herrmann, H. & Jaeger, R. Zeit. f. Tech.Rhys. 11, 461, (1930).

(24) Nitka. H. Phys. Zeits. 35, 801, (1934).

(25) Grebe, C. & Nitzge K. Tabellen zur Dosierung der Röntgenstrahlen. Sonderband zur Strahlentherapie XIV.

(26) Daune, W. Am.J.Roentg. 9, 167, (1922).

(27) Daune, W., Hudson J.C. & Sterling, H.N. Am.J.Roentg. 20, 241, (1928)

(28) Richtmayer, F.K. Phys.Rev., XVIII 13, (1921).
Richtmayer, F.K. & Warburton F.W. Phys. Rev. VI, 539, (1923).

(29) Taylor, L. Radiology 16, 302, (1931).

(30) Mutscheller, A. Radiology XII April 283, (1929)

(31) Taylor, L. Bureau Stand.J.Research 12 April 401,(1934)

(32) Taylor L. Singer
B.S.Journ.Research 11 (RP-592) 293, (1933)

(33) Silberstein, L. Phil.Mag. I,XII series VII 375, (1933).

(34) Bell G.E. Brit.Journ.Rad. IX, 680, (1936)

(35) Jones,D.E.A. Brit.Journ.Rad. XIII, No. 147, March 1940.

(36) Greening, J.R. Brit.Journ.Rad. XX No. 230, 71 (1947).

(37) Eddy, C.E., Brit.Journ.Rad. XIII, 130, (1940)

(38) Lamarton's Unpublished work.

(39) Williams, J.H. Phys.Rev., XLIV, 144 (1933).

(40) Duane, W. & Sterstrom, W. Proc.Nat.Acad.Sci. VI, 477, (1920).

(41) Gray, L.H. Roy.Soc.Proc A. Vol. 122 p. 647 (1928-1929).

(42) Gray, L.H. Brit.Journ.Rad. Vol.X No. 116 p.601 (1937).

(43) Fricke, Glasser Amer.Jour.Roent 138,453 (1925)

(44) Walter, B., Forts. a.d.Geb. d. Roentgen 35, 929, 1308 (1927).

(45) Wilson, C.W. Brit.Journ.Rad. Vol XVIII No. 215, 344, (1945).

(46) Chao C.Y. Nat.Acad.Sci. 16, 431 (1930); Phys.Rev. 36, 1519 (1930).

(47) Read, J. & Lauristen, C. Phys.Rev. 45, 433, (1934).

(48) Cukendall, J.R. Phys.Rev, 1 , 105 (1936).

(49) Klein & Nishina Zeit. Phys. 52, 852 (1928)

(50) Siegbahn M. Physik Zeits. 15, 735, (1914).

(51) Hull, A.W. & Rice, M. Phys.Rev 8, 326 (1916).

(52) Dershem, E. & Skein, M. Phys.Rev. 37, 1238 (1931).

(53) Victoreen, J.A. Jour.App.Phys. 14, No.2, 95 (1943)

(54) Madgwick Phil.Mag., Vol 30,p. 627 (1915).

(55) Bethe Ann.Physik, Vol.5, p.325 (1930).

(56) Kemp,L.A.W. Brit.Journ.Rad. Vol.XVIII No.208, 1075 (1945).

(57) Mayneord,W.V. Brit.Journ.Rad. Vol. 4, p.369 (1931)

(58) Niehnickel & Rejewsky. Strahlen therapie. Vol. 50, p.499 (1944).

(59) Meyer, H. Strahlentherapie, Vol. 41, p.309 (1931).

(60) Niehnickel Ann.der Phys. Vol. 20, p.737 (1934).

(61) Braun & Küstner. Strahlentherapie. Vol. 33, p.273 (1939).

(62) Friedrich & Schulze. Strahlentherapie. Vol. 54, p. 553 (1935).

(63) Owen & Jones. Brit.Journ.Rad. Vol 4, p.309 (1931).

(64) Lea D.E 'Action of radiation on living cells' p.11. Cambridge University Press (1946).